

Aus der Kinderklinik und Kinderpoliklinik im Dr. von
Haunerschen Kinderspital der
Ludwig-Maximilians-Universität München

Direktor: Prof. Dr. Dr. med. Christoph Klein

**Translation of angiotensin converting enzyme 2 (ACE2) upon
liver and lung targeted delivery of optimized chemically
modified mRNA**

Dissertation
zum Erwerb des Doktorgrades der Naturwissenschaften
an der Medizinischen Fakultät
der Ludwig-Maximilians-Universität München

vorgelegt von
Eva Schrom

aus
Ried im Innkreis

2017

**Mit Genehmigung der Medizinischen Fakultät
der Universität München**

Betreuer: PD. Dr. Carsten Rudolph

Zweitgutachter: Prof. Dr. Alexander Dietrich

Dekan: Prof. Dr. med. dent. Reinhard HICKEL

Tag der mündlichen Prüfung: 16.10.2017

Eidesstattlicher Versicherung

Schrom, Eva

Ich erkläre hiermit an Eides statt,
dass ich die vorliegende Dissertation mit dem Thema

Translation of angiotensin converting enzyme 2 (ACE2) upon liver and lung targeted delivery
of optimized chemically modified mRNA

selbständig verfasst, mich außer der angegebenen keiner weiteren Hilfsmittel bedient und alle Erkenntnisse, die aus dem Schrifttum ganz oder annähernd übernommen sind, als solche kenntlich gemacht und nach ihrer Herkunft unter Bezeichnung der Fundstelle einzeln nachgewiesen habe.

Ich erkläre des Weiteren, dass die hier vorgelegte Dissertation nicht in gleicher oder in ähnlicher Form bei einer anderen Stelle zur Erlangung eines akademischen Grades eingereicht wurde.

München, 03.05.2017

To my parents

SUMMARY

Changes in lifestyle and environmental conditions give rise to increasing prevalence of liver and lung fibrosis, both having poor prognosis. Investigations about the underlying mechanisms of fibrosis revealed a dysbalance of the local renin angiotensin system (RAS) actively contributing to inflammation and fibrosis¹. The carboxypeptidase angiotensin converting enzyme 2 (ACE2) is a family member of the RAS showing high potential to reestablish RAS balance leading to resolution of inflammation and fibrosis². So far, first promising results in experimental liver and lung fibrosis have been reported upon administration of recombinant ACE2 protein or ACE2 gene therapy³⁻⁹. However, recombinant protein and gene therapy struggle with hurdles such as organ-targeted delivery, limited or challenging control of protein expression and immunogenicity among others¹⁰⁻¹². These obstacles may be overcome with latest advances in RNA transcript therapy (RTT)¹³⁻¹⁹.

The goal of this project was to establish strong and sustained ACE2 protein expression selectively in healthy and fibrotic liver and lung tissues. Special attention was paid on the protein being stably integrated into the cell membrane, a prerequisite for local enzymatic activity. For this purpose, *in vitro* transcribed chemically modified ACE2 mRNA (cmRNA) was designed and profound *in vitro* cmRNA transfection efficiency, protein expression and activity was shown. With the aim of organ targeted ACE2 protein expression, close investigations about protein maturation were performed indicating full glycosylation and correct folding of protein leading to trafficking and correct protein integration in the cell membrane. In parallel, several ACE2 cmRNA sequences were screened for strong and sustained protein expression in liver and lung cells and the best performing sequence was used for the following *in vivo* studies.

For organ targeted delivery, the optimal combination of carrier and application route was determined by application of reporter protein cmRNA and evaluation of resulting protein expression. For liver targeted cmRNA delivery, systemic application of lipidoid based formulations led to selective protein expression in the liver. For lung targeted cmRNA expression, polymer and lipidoid based formulations were investigated for nebulization, intratracheal microspray or systemic application. In the context of ACE2 expression in fibrotic lungs and based on the results achieved by intravenous administration, systemic application was identified as the optimal administration route. In a next step, both liver and lung specific delivery agents were formulated with ACE2 cmRNA and intravenously applied leading to liver

or lung targeted translation of significant amounts of ACE2 protein. Finally, these formulations were applied in two experimental models of liver and lung fibrosis and could show successful delivery of ACE2 cmRNA to liver or lung respectively. In addition, first data about protein kinetics as well as requirements for dosing and carrier selection in future preclinical studies could be collected.

In summary, an optimized ACE2 cmRNA sequence for liver and lung targeted ACE2 expression could be identified in this thesis. *In vivo* application in liver and lung targeted formulations led to strong protein expression in these organs, providing evidence that RTT is a promising approach for ACE2 based treatment of liver and lung fibrosis to be further explored in fibrotic disease models.

ZUSAMMENFASSUNG

Ungesunder Lebensstil und Umwelteinflüsse führen zu kontinuierlich steigender Prävalenz von Leber- und Lungenfibrose, beide mit schlechten bis nicht vorhandenen Heilungsaussichten für die Patienten. Untersuchungen über die zugrunde liegenden Mechanismen fibrotischer Krankheiten zeigten ein deutliches Ungleichgewicht im lokalen Renin-Angiotensin-Systems (RAS) der betroffenen Organe, was erheblich zu Entzündungsreaktionen und daraus resultierender Fibrose beiträgt¹. In diesem Kontext nimmt ACE2 (Angiotensin Converting Enzyme 2) – eine Carboxypeptidase innerhalb des RAS - eine spezielle Rolle ein, da sie durch ihre Funktionalität über großes Potential zur Auflösung von Entzündung und Fibrose verfügt. Dies wurde durch erste vielversprechende Daten in experimentellen Leber- und Lungenfibrosemodellen nach Behandlung mit rekombinantem ACE2 Protein oder ACE2 Gentherapie belegt³⁻⁹. Für beide Therapieformen gibt es jedoch eine Reihe ungelöster Problemstellungen, wie organspezifische Verabreichung, Kontrollierbarkeit der Proteinexpression und Immunogenität¹⁰⁻¹². Durch die aktuellen Entwicklungen in der RNA Transkripttherapie (RTT) erschließen sich dafür nun neue Lösungsansätze¹³⁻¹⁹.

Zielsetzung dieser Arbeit war die Etablierung von profunder und selektiver ACE2 Proteinexpression sowohl in gesundem als auch fibrotischem Leber- und Lungengewebe. Dabei wurde besonderes Augenmerk auf korrekte Proteinintegration in die Zellmembran gelegt, da es sich dabei um eine unabdingbare Voraussetzung für die lokale Enzymaktivität handelt. Zu diesem Zweck wurde im ersten Schritt *in vitro* transkribierte chemisch modifizierte ACE2 mRNA (cmRNA) entwickelt und einer umfassenden *in vitro* Analyse bestehend aus Evaluation der Transfektionseffizienz, Proteinexpression und Proteinaktivität unterzogen. Um eine organspezifische lokale ACE2 Proteinexpression zu garantieren wurden weiterführende Analysen der Proteinreifung durchgeführt. Damit konnte sowohl die vollständige Glycosylierung als auch korrekte Faltung des Proteins bestätigt werden, was zur korrekten Proteinintegration in die Zellmembrane führte. Gleichzeitig wurden mehrere ACE2 cmRNA Sequenzen einem Screening zur Bestimmung von Proteinexpressionsstärke und -dauer unterzogen und daraus die optimale Sequenz für weiterführende *in vivo* Analysen identifiziert. Im nächsten Schritt wurde mittels Reporterprotein cmRNA und daraus resultierender Proteinexpression die optimale Kombination von Carrier und Applikationsroute für die organspezifische Proteinexpression ermittelt. In der Leber konnte selektive und organspezifische Proteinexpression durch systemischer Applikation lipidoidbasierter

Formulierungen erzielt werden. Für lungenspezifische Proteinexpression wurden polymer- und lipidoidbasierte Formulierungen für Nebulisierung, intratrachealer Mikrosprayapplikation oder systemischer Applikation untersucht. Dabei wurde basierend auf diesen Ergebnissen und im Kontext der ACE2 Expression in fibrotischen Lungen die systemischen Applikation als optimale Route identifiziert. Im nächsten Schritt wurde in den Formulierungen die Reporterprotein cmRNA mit ACE2 cmRNA ersetzt, womit nach intravenöser Verabreichung sowohl in der Leber als auch der Lunge starke ACE2 Proteinexpression nachweisbar war. Diese Formulierungen wurden anschließend in zwei experimentellen Modellen der Leber- und Lungenfibrose angewandt, wobei die erfolgreiche Anreicherung von ACE2 cmRNA in Leber beziehungsweise Lunge nachgewiesen werden konnte. Zusätzlich konnten erste Daten zur Proteinkinetik als auch cmRNA Dosierung und Carrierauswahl für zukünftige präklinische Studien erhoben werden.

Zusammenfassend konnte in der vorliegenden Arbeit eine optimierte ACE2 cmRNA Sequenz zur leber- und lungenspezifischen ACE2 Expression etabliert werden. Leber- und lungenspezifischer Formulierungen und anschließende *in vivo* Applikation dieser cmRNA führten zu signifikanter Proteinexpression in den Zielorganen. Damit erweist sich die RTT als vielversprechender Ansatz für die ACE2 basierte Behandlung von Leber- und Lungenfibrose, was es nun in fibrotischen Krankheitsmodellen weiter zu entwickeln gilt.

TABLE OF CONTENTS

1	INTRODUCTION	1
1.1	Fibrotic Diseases	1
1.1.1	Liver Fibrosis	2
1.1.2	Lung Fibrosis	4
1.2	Angiotensin Converting Enzyme 2 (ACE2)	6
1.2.1	Structure and Function of ACE2	6
1.2.2	ACE2 in Liver Fibrosis	9
1.2.3	ACE2 in Lung Fibrosis	10
1.3	mRNA Transcript Therapy	11
1.3.1	mRNA	11
1.3.2	mRNA Transcript Therapy	12
1.3.3	Current Technologies in Transcript Therapy and mRNA Delivery Systems	13
1.3.4	Aim of the Study	15
2	MATERIALS and METHODS	16
2.1	Materials	16
2.1.1	ACE2 cmRNA Sequences	16
2.1.2	Cell Lines	16
2.1.3	Cell Culture Media and Supplements	16
2.1.4	Transfection Reagents	17
2.1.5	Kits	17
2.1.6	Primers	17
2.1.7	Antibodies and Dyes	18
2.1.8	Chemicals	18
2.1.9	Consumables	21
2.1.10	Technical Equipment	22
2.1.11	Software	23
2.2	Methods	24
2.2.1	cmRNA and Lipoplex Preparation	24
2.2.1.1	cmRNA Preparation	24
2.2.1.2	cmRNA Lipoplex Formation and Application	25
2.2.2	Cell Culture	26
2.2.2.1	Primary Murine Liver Cells	26
2.2.2.2	Primary Murine Lung Cells	26
2.2.2.3	Human Cell Lines	27
2.2.3	Animal Studies	27
2.2.3.1	Mice	27
2.2.3.2	Rats	28
2.2.4	cmRNA Quantification and Relative Gene Expression Analysis	28
2.2.5	Protein Analysis	29
2.2.5.1	Hydroxyproline Assay	29
2.2.5.2	Flow Cytometry Analysis	29
2.2.5.3	Protein Quantification by Western Blot	30
2.2.5.4	ACE2 Activity Assay	31

2.2.5.5	Firefly Luciferase Activity Measurements	32
2.2.5.6	Cytokine Measurements	32
2.2.6	Immunocyto- and Immunohistochemistry	34
2.2.6.1	Immunocytochemistry	34
2.2.6.2	Immunohistochemistry	34
2.2.6.3	Sirius red Staining	35
2.2.6.4	In situ Hybridisation	35
2.2.7	Statistical Analysis	36
3	RESULTS	37
3.1	Proof of Concept for ACE2 Delivery <i>in vitro</i>	37
3.1.1	ACE2 cmRNA Transfection and Translation <i>in vitro</i>	37
3.1.2	ACE2 Posttranslational Modifications	39
3.1.3	Optimization of ACE2 cmRNA for <i>in vivo</i> Application	42
3.2	Proof of Concept for ACE2 Transcript Therapy in the Liver	45
3.2.1	Liver Targeted cmRNA Delivery	45
3.2.2	Liver Targeted ACE2 cmRNA Delivery	47
3.2.3	ACE2 cmRNA Application in a Model of Non Alcoholic Steatohepatitis	49
3.3	Proof of Concept of ACE2 Transcript Therapy in the Lung	56
3.3.1	Nebulization of cmRNA	56
3.3.2	Intratracheal Application of cmRNA	59
3.3.2.1	Polymer versus Lipidoid Formulation of cmRNA	59
3.3.2.2	Intratracheal Delivery of ACE2 cmRNA in Lipidoid Formulation	60
3.3.3	Intravenous Application of cmRNA	63
3.3.3.1	Pulmonary Lipid Formulation of cmRNA	63
3.3.3.2	ACE2 cmRNA Application in a Model of Idiopathic Pulmonary Fibrosis	66
4	DISCUSSION	72
4.1	<i>In vitro</i> Analysis	72
4.2	<i>In vivo</i> Analysis	73
4.2.1	Liver	73
4.2.2	Lung	76
4.2.3	Conclusion and Outlook	81
5	ABBREVIATIONS	83
6	ACKNOWLEDGEMENTS	86
7	ASSOCIATED PUBLICATION AND THESIS	88
8	REFERENCES	89
9	APPENDIX	96
9.1	Cell Authentication	96
9.2	Angiotensin Converting Enzyme 2 Open Reading Frames	98
9.2.1	Open Reading Frame non Codon Optimized	98
9.2.2	Open Reading Frame Codon Optimized	98

LIST OF FIGURES

Figure 1: Nonalcoholic fatty liver disease pathogenesis _____	2
Figure 2: Histopathology of pulmonary fibrosis _____	4
Figure 3: Hypothesis for pathophysiological mechanisms of idiopathic pulmonary fibrosis development _____	5
Figure 4: Schematic representation of the RAS system _____	7
Figure 5: Structure of ACE2 protein _____	8
Figure 6: Structure of human mRNA _____	12
Figure 7: Structural modifications for tuning mRNA pharmacokinetics _____	14
Figure 8: Principle of the cytokine measurement _____	33
Figure 9: Levels of endogenous ACE2 mRNA _____	37
Figure 10: Detection of cmRNA and encoded protein 24 h after transfection in different cell types _____	38
Figure 11: Posttranslational processing of ACE2 protein _____	41
Figure 12: Immunofluorescent staining for ACE2 _____	42
Figure 13: Screening of ACE2 cmRNA sequences _____	43
Figure 14: Liver targeted delivery of firefly luciferase cmRNA _____	46
Figure 15: Liver targeted delivery of ACE2 cmRNA _____	48
Figure 16: Establishment of STAM model and study outline _____	49
Figure 17: Weight and serum parameters after ACE2 cmRNA treatment _____	51
Figure 18: Deposition of ACE2 cmRNA and effect on hydroxyproline content of ACE2 cmRNA treatment _____	52
Figure 19: Effects of ACE2 cmRNA treatment on fibrosis _____	53
Figure 20: NAFLD scoring _____	55
Figure 21: Study outline and nebulization apparatus _____	57
Figure 22: Luciferase activity _____	58
Figure 23: Luciferase translation post intratracheal cmRNA application _____	60
Figure 24: Reporter protein translation and ACE2 cmRNA abundance post i.t. application of ACE2 cmRNA _____	61
Figure 25: ACE2 protein translation post i.t. application and inflammatory reaction _____	62
Figure 26: Intravenous application of ACE2 cmRNA _____	65
Figure 27: Reporter protein translation and ACE2 cmRNA abundance post i.v. application of ACE2 cmRNA _____	68
Figure 28: Cytokine analysis _____	69
Figure 29: Representative hematoxylin-eosin stainings of ACE2 treatment lungs _____	70

LIST OF TABLES

Table 1: UTR sequences used in this study _____	16
Table 2: Cell lines used _____	16
Table 3: Cell culture media and supplements used _____	16
Table 4: Transfection reagents used _____	17
Table 5: Assay kits used _____	17
Table 6: Primers used for qPCR _____	17
Table 7: Antibodies and dyes used for Western Blot and FACS _____	18
Table 8: Chemicals used for cell culture _____	18
Table 9: Chemicals used for in vitro transcription _____	19
Table 10: Other chemicals _____	20
Table 11: Consumables used in this work _____	21
Table 12: List of technical equipment used in this work _____	22
Table 13: Software used for measurements and analysis _____	23
Table 14: Settings for real-time qPCR measurement _____	28
Table 15: Group allocation for NASH model _____	50
Table 16: NAFLD scoring system _____	54
Table 17: Group allocation for IPF model _____	66
Table 18: Fibrosis and Inflammation scores _____	71

1 INTRODUCTION

1.1 Fibrotic Diseases

Fibrotic diseases are one of the major causes of mortality and morbidity worldwide leading to serious economic burden and challenge for health services. It is estimated that 45 % of mortality can be attributed to fibrotic diseases in Western developed countries with likely higher numbers in developing countries. Fibrosis is defined as excessive connective tissue formation in response to severe or repetitive injury or dysregulated wound-healing which is a common pathologic manifestation of many chronic inflammatory diseases. It can affect nearly every organ with liver and lung showing rising prevalence due to changes in lifestyle or unfavorable environmental conditions²⁰⁻²². The underlying mechanisms are very heterogeneous, however all fibrotic diseases share a common set of pathogenic features leading to disruption of normal tissue architecture causing organ dysfunction and ultimately organ failure or death^{1,23}.

On a cellular level, fibroblasts play a major role in fibrogenesis. In normal conditions, they are in a quiescent state supporting organ form and function. Upon injury, they are activated and differentiate into myofibroblasts. In addition, the pool of myofibroblasts is also fueled by circulating fibrocytes and local epithelial or endothelial cells undergoing epithelial to mesenchymal transition. Myofibroblasts are contractile cells, producing increased amounts of collagens, while reducing expression of extracellular matrix (ECM) degrading enzymes. In the normal wound healing process, myofibroblasts undergo apoptosis after completed wound healing. If this process becomes aberrant, these cells survive and secrete mediators attracting even more myofibroblasts triggering a vicious circle ultimately leading to fibrosis^{1,23}.

Currently many treatment options targeting myofibroblast recruitment and activation are under investigation. Transforming growth factor beta (TGF β) is among the most studied cytokines for myofibroblasts activation, but also Wnt signaling, Hedgehog signaling, Notch signaling and a range of immunomodulatory cytokines are in focus²³. In addition, the immune system was shown to play an important role in both, stimulating as well as resolving the fibrotic process^{1,23}. Overall, therapeutic success of these attempts was so far limited²⁴⁻²⁶, and the discovery of the involvement of the renin-angiotensin-system (RAS) in fibrotic diseases raised new hope for therapeutic progress. It was shown that the organ-specific RAS is dysregulated in fibrotic diseases triggering excessive pro-inflammatory and pro-fibrotic signaling¹. Therefore, reestablishing RAS hemostasis will be the underlying driver for this work.

1.1.1 Liver Fibrosis

Liver fibrosis and subsequently liver cirrhosis are chronic liver diseases characterized by degeneration and necrosis of hepatocytes, and as a result replacement of liver parenchyma with fibrotic tissue. This process leads to destruction of normal liver architecture limiting proper organ function. Common associated complications are portal hypertension, ascites, upper gastrointestinal bleeding, jaundice and hepatic encephalopathy²⁷.

The most common causes of liver fibrosis are persistent alcohol abuse, viral hepatitis infections and nonalcoholic fatty liver disease (NAFLD). Regardless of the underlying cause, genetic polymorphisms are strong influencers of susceptibility and severity of the disease. Due to changes in lifestyle leading to increasing numbers of people suffering from metabolic syndrome worldwide, the focus of this study will be on liver fibrosis caused by NAFLD²⁷.

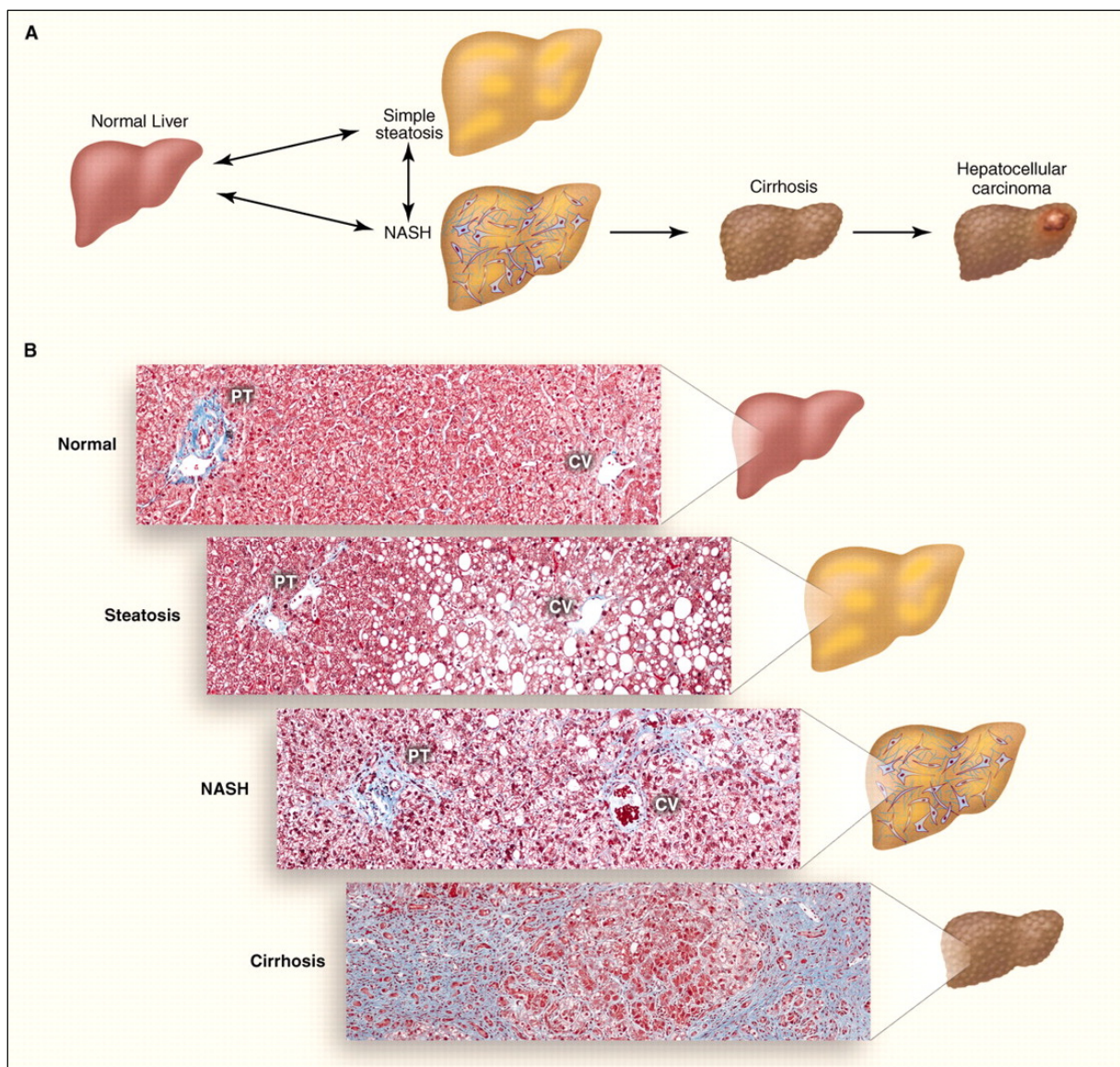


Figure 1: Nonalcoholic fatty liver disease pathogenesis

(A) Schematic of progression of NAFLD. (B) Histological sections illustrating normal liver, steatosis, NASH, and cirrhosis.¹²⁴

NAFLD can be caused by genetic predisposition, but mainly by health problems associated with metabolic syndrome such as obesity, insulin resistance and adipose tissue lipolysis. The diet usually leading to metabolic syndrome is associated with hyperglycaemia and resultant compensatory hyperinsulinaemia. Due to its insulin-sensitivity, the liver is susceptible to hyperglycaemia-induced oxidative stress, leading to derangement of protein, carbohydrate and lipid metabolism and an inflammatory response. Increased lipogenesis and fatty acid uptake with simultaneously reduced very low density lipoprotein (VLDL) export and β -oxidation leads to triglycerides accumulation in the liver, a stage called steatosis. Histological examinations at this disease stage typically show accumulations of fat vesicles in hepatocytes with mild lymphocytic, neutrophilic and other inflammatory infiltrates. This phase may progress to nonalcoholic steatohepatitis (NASH) where lipotoxicity, endoplasmic reticulum (ER) stress, mitochondria dysfunction and inflammation lead over time to varying degrees of fibrosis. Apart from glycogenated nuclei, hepatocytes at this stage often show damaged intermediate filaments (Mallory bodies), necrosis or ballooning, a typical form of hepatocyte cell death. Up to this stage, the fibrotic progress can be halted or in some cases even be reversed. If NASH progresses further to cirrhosis, fibrosis becomes nodular with bridging of fibrous septa. These architectural changes are too severe to be reversible and may eventually progress to hepatocellular carcinoma^{27,28}.

On a cellular and molecular level, liver fibrosis shows ECM accumulation, typical for fibrotic diseases as previously described. In the liver, this leads to loss of hepatocyte microvilli and endothelial fenestration, both being essential for liver function. In the case of liver fibrosis, hepatic stellate cells (HSCs) play a central role in disease onset as they are the main source of myofibroblasts in the liver. In the healthy liver they account for approximately 15 % of liver cells and are located in the perisinosoidal space. Their main function in the healthy quiescent state is storage of vitamin A in form of retinol ester and regulation of the liver immune system. Upon liver damage though, they differentiate into myofibroblasts in a two stage process. First, they are activated by injured neighboring cells – frequently Kupffer cells - through paracrine stimuli, such as reactive oxygen species, transcription factors, growth factors and inflammatory cytokines. In a second step, they undergo a phenotypic change leading to cell proliferation, contractility, fibrogenesis, cytokine release and retinoid loss. In case of elimination of the noxious stimulus, the fibrogenic response is resolved by up-regulation of apoptotic genes and increased secretion of ECM-degrading enzymes. If this process gets out

of control, a vicious circle of autocrine and paracrine signaling sustains the accumulation of ECM^{27,29}. Currently, there are many treatment options under evaluation with special focus on the resolution of noxious stimuli, inhibition of inflammation and deactivation or apoptosis of activated HSCs²⁶.

1.1.2 Lung Fibrosis

Idiopathic pulmonary fibrosis (IPF) is a chronic and fatal form of interstitial lung disease. It typically affects older adults with increased susceptibility in men and has a median survival or time to transplant of 2-5 years. Risk factors associated with IPF are age, exposure to smoke, metal or wood dust and mutation in the MUCB5 allele, which is involved in telomere length regulation. IPF patients suffer from a progressive decline in lung function increasingly limiting their physical activity³⁰⁻³².

From a pathologic point of view, IPF is defined as chronic pulmonary inflammation with areas of fibrosis and clusters of cystic airspaces also referred to as honeycombs (Figure 2). On chest X-rays, these patterns are typically found in the basal and peripheral areas of the lung. In addition, biopsy samples are taken for diagnosis, where fibrosis needs to be confirmed by interstitial scarring and the presence of fibroblast foci, dense collections of myofibroblasts and scar tissue²².

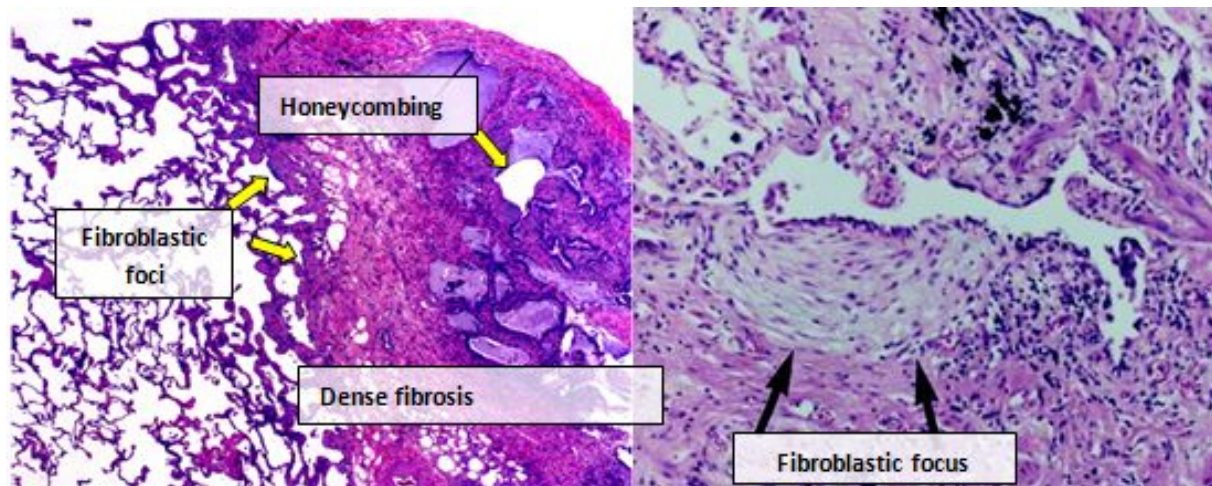


Figure 2: Histopathology of pulmonary fibrosis¹²⁵

The underlying mechanisms leading to IPF are still not fully understood. Previously, inflammation was considered the central driver of fibrosis. However, due to limited treatment success of anti-inflammatory drugs, the paradigm has now shifted towards a model of abnormal wound healing driven by persistent or recurrent alveolar epithelial microinjuries. In

this model, disease onset is considered to be triggered by persistent or recurrent injuries of alveolar epithelial cells (AEC) type II and interruption of the basal lamina (see Figure 3)³³. AECs undergo apoptosis while triggering the coagulation cascade and immune system activation. The resulting gap is filled with a fibrin clot while the activated AECs release profibrotic factors, leading to recruitment, proliferation and differentiation of fibroblasts into myofibroblasts. The resulting gap is filled with a fibrin clot which is then substituted by ECM produced by the surrounding myofibroblasts. Over time, a myofibroblast focus forms, where persistently activated myofibroblasts continue to secrete excessive amounts of ECM components. This process leads to thickening of the air-blood barrier and hence impaired gas exchange and lung compliance. The complexity of this process requires multiple cell-cell and cell-matrix interactions mediated by numerous biochemical factors such as growth factors, chemokines, cytokines, coagulation factors and reactive oxygen species. These factors can easily be influenced by host and environmental factors making disease treatment extremely challenging^{33,34}.

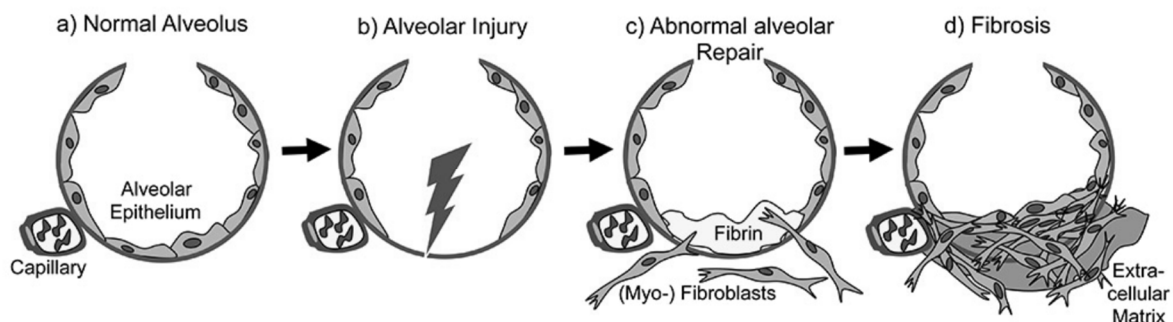


Figure 3: Hypothesis for pathophysiological mechanisms of idiopathic pulmonary fibrosis development³³

The complexity of this process shows quite evidently the necessity of combination therapy targeting multiple pathways. So far treatment options are very limited with pirfenidone and nintedanib being approved for treatment since 2014²⁵. They both exert anti-inflammatory and anti-fibrotic actions^{31,35}, however can only slow and not halt disease progression. New treatment options are urgently required.

1.2 Angiotensin Converting Enzyme 2 (ACE2)

1.2.1 Structure and Function of ACE2

Angiotensin converting enzyme 2 (ACE2) is a close homolog of its counterpart angiotensin converting enzyme (ACE) and has come into research focus during the last two decades. Both enzymes act as metallo-carboxypeptidases within the RAS being well known for its effects on the regulation of blood pressure²⁰. In addition to this main function, several additional physiologic and pathologic functions were discovered, describing nowadays the RAS system as a signaling cascade producing multiple biological active intermediates. These intermediates exert their functions along two main axes (Figure 4). Along the classical axis, ACE produces Angiotensin II (AngII) by cleaving Angiotensin I (AngI). AngII binds to AngII type 1 receptor (AT1R) or to AngII type 2 receptor (AT2R). Along the alternate axis, ACE2 cleaves AngII into Angiotensin (1-7) (Ang-(1-7)) which acts on MAS receptor. The final physiologic effects of the two axes are opposing each other. Stimulation along the classical axis leads to vasoconstriction and stimulation of fibrosis associated processes such as inflammation, epithelial to mesenchymal transition, cell proliferation and hypertrophy. All these effects can be counterbalanced by stimulation of the alternate axis. Under normal conditions, signaling through these two axes is balanced, however is significantly shifted towards increased signaling through the classical axis in case of fibrosis².

Drug development within the RAS system was initially focused around angiotensin converting enzyme inhibitors (ACEi) in the context of blood pressure regulation. However, with increasing knowledge about the physiologic and pathologic properties of the biological intermediates further down the proteolytic cascade, AT1 receptor blockers, AT2 receptor agonists, recombinant ACE2 or ACE2 activators and Ang-(1-7) analogues gained momentum^{7,36}. With the exception of ACE2, the therapeutic purpose of all of these drugs was to either reduce pro-inflammatory and pro-fibrotic signaling through AT1 receptor or to counterbalance AT1 receptor signaling by increased MAS-receptor signaling. The effect of ACE2 regulators however, is unique in the RAS system, as they can achieve both. By cleaving AngII to Ang-(1-7), ACE2 reduces stimulation of AT1 receptor signaling and at the same time increases anti-inflammatory and anti-fibrotic signaling through MAS-receptor. The therapeutic effects of modulating the RAS system as just described were repeatedly shown for both, liver and lung fibrosis^{3-9,37}.

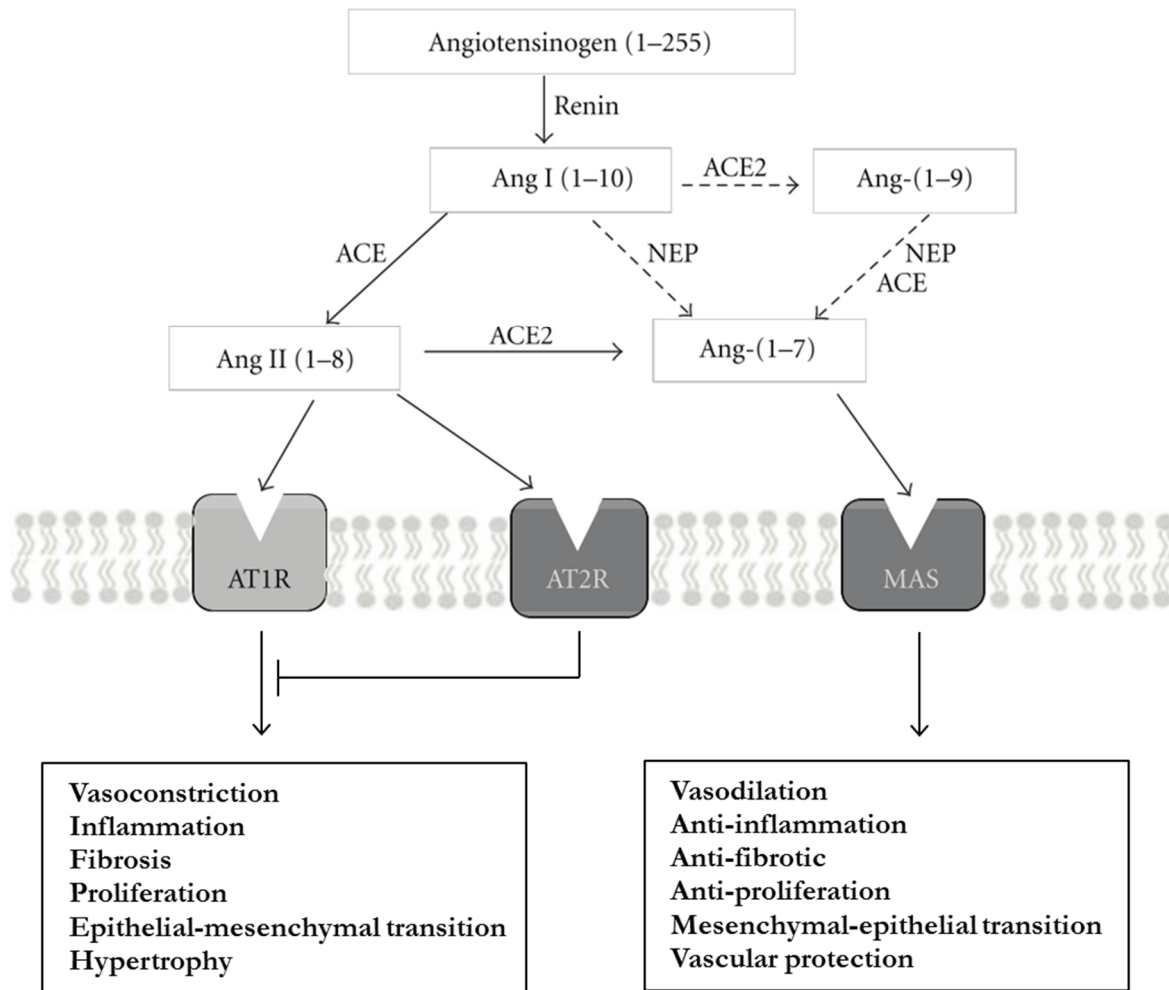


Figure 4: Schematic representation of the RAS system

ACE: angiotensin converting enzyme, ACE2: angiotensin converting enzyme 2, NEP: Neprilysin, AT1R: Ang II type I receptor, AT2R: Ang II type II receptor. Interspaced lines show proteolytic activity of lower effectivity (adapted from Clarke²).

The gene coding for ACE2 is located on chromosome X and is composed of 18 exons encoding for a cDNA with a total length of 3405 nucleotides. The open reading frame (ORF) consists of 2418 nucleotides encoding 805 amino acids, while the 5' untranslated region (UTR) consists of 103 nucleotides and the 3' UTR of 884 nucleotides. ACE2 protein is expressed in endothelial cells mainly in the small intestine, testis, heart and kidney³⁸.

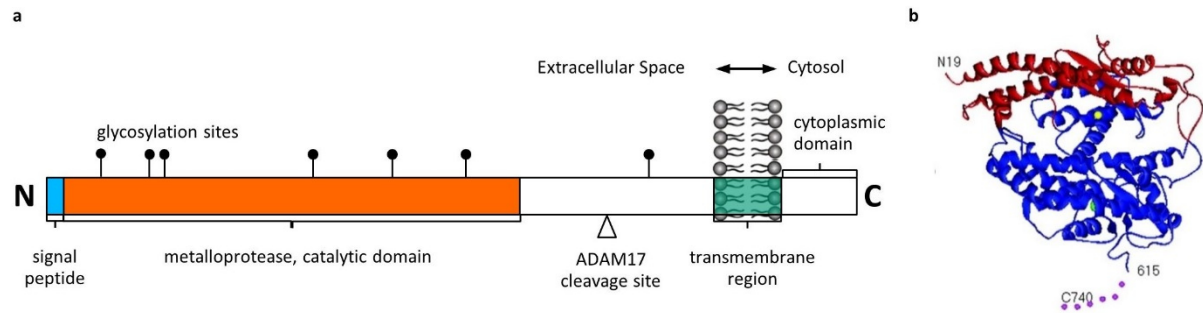


Figure 5: Structure of ACE2 protein

(a) Structure and functional domains of ACE2 protein. (b) Crystal structure of ACE2 protein.

ACE2 is a typical type I integral membrane protein with the carboxyl terminus located in the cytosol. The detailed protein structure is shown in Figure 5 a. The N-terminus is flanked by a 17-amino acid signal peptide followed by a conserved zinc metalloprotease consensus sequence (HEXXH motif). Crystal structure analysis showed seven potential N-linked glycosylation sites reflecting characteristics of a plasma membrane bound protein extracellular domain. Depending on glycosylation status, protein mass varies from approximately 120 kDa for glycosylated to 85 kDa for unglycosylated protein. In addition, the extracellular domain shows various potential phosphorylation sites. Close to the transmembrane domain, the cleavage site for ADAM metallopeptidase domain 17 (ADAM17) can be found generating a secreted form of ACE2³⁹. The transmembrane domain consists of 22 amino acids followed by a cluster of charged residues which may serve as a stop-transfer sequence and leads in combination with calmodulin to retention of protein in the cell membrane^{2,39}. The short cytoplasmic tail shows a regulatory function in ectodomain shedding and severe acute respiratory syndrome infection. ACE2 shows optimal activity in presence of zinc, chloride and fluoride at a pH of 6.5^{40,41}.

The enzymatic core domain can be further divided into catalytic subdomains I and II, shown in red and blue color respectively (Figure 5 b). In the native form, the two domains form a deep open cleft with the zinc ion in its center (yellow sphere). Upon substrate binding to one subdomain, a hinge-bending movement is induced which closes the cleft to allow correct positioning of catalytic residues. A similar movement is induced upon inhibitor binding, closing the enzyme around the inhibitor⁴².

1.2.2 ACE2 in Liver Fibrosis

The complexity of the fibrotic process has brought about numerous treatment attempts to get control of disease progression. Within these attempts, the RAS and its biological active intermediates were subject of intense investigations, as there was increasing evidence of a dysbalanced RAS in liver fibrosis. As reviewed by Moreira de Macedo et al.⁴³, it was frequently observed that in areas of active hepatic fibrogenesis, ACE and AT1 receptor genes were upregulated, triggering inflammation and fibrosis. In addition, stimulation of AT1 receptor with AngII led to contraction and proliferation of HSCs. At the same time, counter-regulatory signaling through the alternate axis was also found to be upregulated in cirrhotic human and rat livers, probably as a protective measure.

Based on this evidence, it has been tried to manipulate RAS signaling by stimulation or inhibition of several of the biological intermediates. Blocking the classical RAS signaling in the liver has been investigated by application of ACE inhibitors (eg. Captopril or Lisinopril) or AngII receptor blockers (ARBs, eg. Telmisartan or Losartan). The anti-fibrotic effects of these treatments have been shown in NASH patients as well as experimental animal models of liver fibrosis⁴⁴⁻⁴⁶. Stimulation of the alternate pathway by treatment with Ang-(1-7) led to improvement in metabolic comorbidities as well as fibrosis in experimental rat models⁴³. However, as already stated, ACE2 would be the most effective enzyme within the RAS to induce a shift in the system's balance due to its dual effect of reducing signaling through the classical axis at the same time of increasing signaling through the alternate axis. Interestingly, unlike observations in IPF patients, the hepatic injury itself is sufficient to trigger this rebalancing process as ACE2 levels in livers from cirrhotic patients with hepatitis C as well as in the livers of bile duct ligated (BDL) rats were markedly increased⁴⁷. These observations were confirmed in an ACE2 knockout (k.o.) model, where the lack of ACE2 was studied in aged k.o. mice as well as in k.o. mice subjected to liver injury by bile duct ligation for 14 days. K.o. mice at 12 months of age showed hepatic inflammation and collagen deposition which was confirmed to be AngII dependent. Upon liver injury, a marked increase in fibrillary collagen deposition was observable in the ACE2 k.o. animals as well as an increased number of activated myofibroblasts and inflammatory cell infiltrates in the liver tissue. In order to evaluate the therapeutic effect of ACE2, a group of BDL ACE2 k.o. animals was treated daily with 2 mg/kg recombinant ACE2 by intraperitoneal injection. This group showed significantly reduction in liver fibrosis⁴. Mak et al. extended the time frame of therapeutic ACE2 delivery in

BDL in two additional models of liver fibrosis by using adeno-associated ACE2 gene therapy and showed ACE2 associated anti-inflammatory and anti-fibrotic effects for a sustained period of up to 8 weeks³.

1.2.3 ACE2 in Lung Fibrosis

There is multiple experimental and clinical evidence that a dysbalanced RAS is actively contributing to lung fibrosis. The gene encoding for Angiotensinogen, was found to be strongly induced in patients with pulmonary fibrosis⁴⁸. Proteolytic cleavage of Angiotensinogen is resulting in increased AngII levels, leading to inflammation, AEC apoptosis and initiation of fibrosis through fibroblast proliferation⁴⁹ and differentiation into myofibroblasts excessively secreting ECM⁵⁰. Apoptotic AEC contribute themselves to increased AngII levels by sustained secretion of angiotensin as well as AngII⁵¹. At the same time, it was found that ACE2 mRNA levels, ACE2 protein expression and activity were severely decreased in lung tissue from IPF patients, may be caused by cell-cycle dependent down-regulation of ACE2⁶. Under normal conditions, ACE2 is mainly secreted by AEC type II cells showing a quiescent phenotype. However, in the case of lung fibrosis, AECII proliferate and at the same time downregulate ACE2 expression⁵². This downregulation of ACE2 additionally contributes to the accumulation of AngII in fibrotic lungs. So far, there have been attempts to decrease AngII levels by treatment with ARBs and ACEi, however they could stabilize lung function only for the first 12 months⁵³, without any positive effects on patient's long-term survival⁵⁴.

The physiologic function as well as therapeutic potential of ACE2 were first studied in ACE2 k.o. models. Although there were no histological changes detectable between the lungs of saline treated wild type animals and ACE2 k.o. animals after 21 days, lung collagen content almost doubled in the k.o. animals. Upon bleomycin induced lung injury however, the effects of loss of ACE2 expression were striking. ACE2 k.o. animals showed increased levels of lung fibrosis compared to all control groups resulting in reduced exercise capacity and lung function. Daily intraperitoneal injection of recombinant human ACE2 of 2 mg/kg could significantly attenuate bleomycin induced lung injury⁵. Wang et al. performed a similar experiment with bleomycin induced lung injury in mice. They studied the therapeutic effect of a single intraperitoneal injection of recombinant human ACE2 at 0.2 mg/kg (given immediately after bleomycin treatment) for a period of 28 days. Their findings showed that ACE2 did not have significant effects on the pathological changes in early disease states, mainly characterized by alveolitis, but showed marked attenuation of fibrosis at later time

points. Closer investigations about the mode of action of ACE2 revealed that ACE2 could inhibit or mitigate early excessive AEC proliferation and subsequent excessive cell loss, as well as fibroblast proliferation and differentiation into myofibroblasts⁵⁵. Based on these encouraging results, lenti-viral application of ACE2 was investigated. For this purpose, rats were pre-treated with lenti-ACE2 viral particles via intratracheal injection. Two weeks later, animals were subjected to bleomycin for establishment of lung fibrosis. Pretreatment with lenti-ACE2 led to a significant reduction in morphologic changes in lungs of bleomycin treated animals as well as in a significant reduction in hydroxyproline content in these lungs. Interestingly, similar effects were achieved by pre-treatment with lenti-Ang-(1-7)⁵⁶. The therapeutic effect of ACE2 was also shown in an experimental mouse model of lung fibrosis by treatment with human umbilical cord mesenchymal stem cells after lentiviral ACE2 gene transfection. Disease progression was analyzed weekly for up to 28 days post treatment. Administration of ACE2 transfected stem cells resulted in significant alleviation of bleomycin induced lung injury already detectable at early time points (7 days) and being sustained until the end of the study (28 days)⁸.

1.3 mRNA Transcript Therapy

1.3.1 mRNA

Messenger RNA (mRNA) is a family of RNA molecules essential for protein translation. The process of protein translation starts inside the nucleus, with transcription of DNA into pre-mRNA. Pre-mRNA is then processed into mature mRNA by splicing, addition of a 5' cap and polyadenylation at the 3' end. In the next step, mature mRNA is exported from the nucleus into the cytoplasm where ribosomes translate the nucleotides of mRNA with the help of transfer RNA into a polymer of amino acids. After post-translational modifications the mature protein is shuttled to its place of destination⁵⁷.

mRNA itself is a single strand sequence whose building blocks are the four ribonucleotides adenosine 5'-monophosphate (AMP), guanosine 5'-monophosphate (GMP), cytidine 5'-monophosphate (CMP) and uridine 5'-monophosphate (UMP). This sequence is encoding the amino acid sequence of the protein. Figure 6 shows the simplified structure of a fully matured mRNA molecule. In the cytoplasm mRNAs are subjected to exo- and endo-nucleases which can cleave RNA. Therefore, mRNA is protected on the 5' end by a 7-methylguanosine cap structure and on the 3' end by a poly-A-tail from enzymatic degradation⁵⁸. The core of the

mRNA consists of a coding region, a sequence of codons which are translated by the ribosomes into proteins, which is flanked by a start codon on the 5' end and a stop codon on the 3' end. UTRs are located upstream and downstream of the coding sequence. They are key elements for translation initiation, elongation and termination as well as intracellular localization and mRNA stability^{57,59,60}.

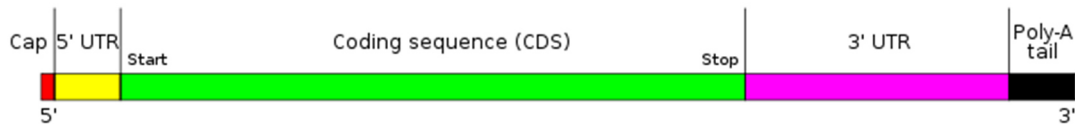


Figure 6: Structure of human mRNA⁵⁷

1.3.2 mRNA Transcript Therapy

During the last decades, therapeutic application of recombinant protein was intensively investigated and moved forward into the clinical setting. In recombinant protein therapy a fully functional protein is administered aiming at raising protein levels to physiological or even higher levels depending on the therapeutic requirements. Upon application, the recombinant protein needs to enter the systemic circulation in order to be delivered to the desired tissue. This implies, that the protein is distributed throughout the body, hence organ or even cell targeting is very challenging. In addition, proteins which exert their function inside the cell or in a membrane bound form, will not reach their targeted location, but are systemically distributed. Depending on the type of protein, short protein half-life may be as well limiting therapeutic application¹⁰. In addition to that, recombinant proteins can be recognized as foreign antigens by the host provoking an immune response, as they were not produced by the host itself¹¹. In gene therapy, DNA is entered with or without the help of a viral delivery system into the cytoplasm. In the case of non-viral gene transfer by pDNA, the transfected plasmid DNA (pDNA) needs to cross the nuclear membrane to reach its final point of destination. However, this entails an increased risk of insertional mutagenesis¹², a problem also faced by retroviral, lentiviral and adeno-associated gene transfer⁶¹.

The limitations faced by recombinant protein and gene therapy fueled research in the field of mRNA transcript therapy (RTT). mRNA exerts its function in the cytoplasm, providing the opportunity to establish protein expression in proliferating as well as quiescent cells, which is especially important in applications in quiescent or harmed tissues. In the cytoplasm, mRNA is translated by the cell's distinct protein translation machinery without need to enter the nucleus, hence there is no risk of insertional mutagenesis. In comparison to recombinant

protein therapy, RTT is not limited to secreted proteins, making it a promising alternative for expression of intracellular or membrane bound proteins. Due to enzymatic mRNA degradation mechanisms in the cytoplasm, protein expression is naturally self-limited. This offers the advantage of well controllable protein expression being key to fine-tunable dosing regimen in clinics^{12,16,62}.

1.3.3 Current Technologies in Transcript Therapy and mRNA Delivery Systems

Despite these favorable properties, progress of RTT into the clinical setting was for a long time hampered by unfavorable immunogenicity, RNA instability and lack of suitable delivery agents. A major improvement was achieved by introduction of chemical modifications in *in vitro* transcribed mRNA (cmRNA). By artificially incorporating naturally occurring modified nucleosides such as pseudouridine, 2-thiouridine, 5-methylcytidine or N6-Methyladenosine, the immune reaction of the cell was markedly reduced as reviewed by Vallazza et al.¹⁷. Most modifications avoid activation of toll like receptor 7 and 8, while some modifications, such as pseudouridine and 2-thiouridine avoid activation of retinoic acid inducible gene I and protein kinase R. Reduced cmRNA recognitions by the immune system consequently leads to reduced clearing of cmRNA by the immune system. This in turn increases cmRNA stability leading to potent protein translation. The optimal choice of chemical modifications and their proportion in relation to unmodified nucleosides heavily depends on the type of protein, the targeted cell type and state and therefore needs to be evaluated for each individual application. Further improvements in cmRNA stability and immunogenicity were achieved by implementing special cap structures as well as optimizing the length of the poly(A) tail¹⁷. Stability as well as amount of protein translated was further increased by substitution of natural UTRs with UTRs from proteins known for strong, stable and sustained expression such as human globins or cytochrome b-245 alpha (CYBA) chain^{16,63-65}. Another technique, frequently used to induce strong protein translation is codon optimization. In this technique, translation rates are markedly increased by replacing rare codons with abundant codons without modifying the amino acid sequence of the encoded protein.^{66,67} Immunogenicity of cmRNA can be mainly attributed to activation of pattern recognition receptors, which are highly effective in identifying and eliminating viral RNA. It has been shown, that modification of specific nucleotides led to markedly reduced activation of the innate immune system and enhanced RNA translation efficiency^{18,19}. Considering the aforementioned properties of RNA transcript therapy, RTT can be considered a strong, adjustable and safe alternative to recombinant ACE2

protein or viral gene delivery for the treatment of liver and lung fibrosis. The main possibilities of mRNA modifications are summarized in Figure 7.

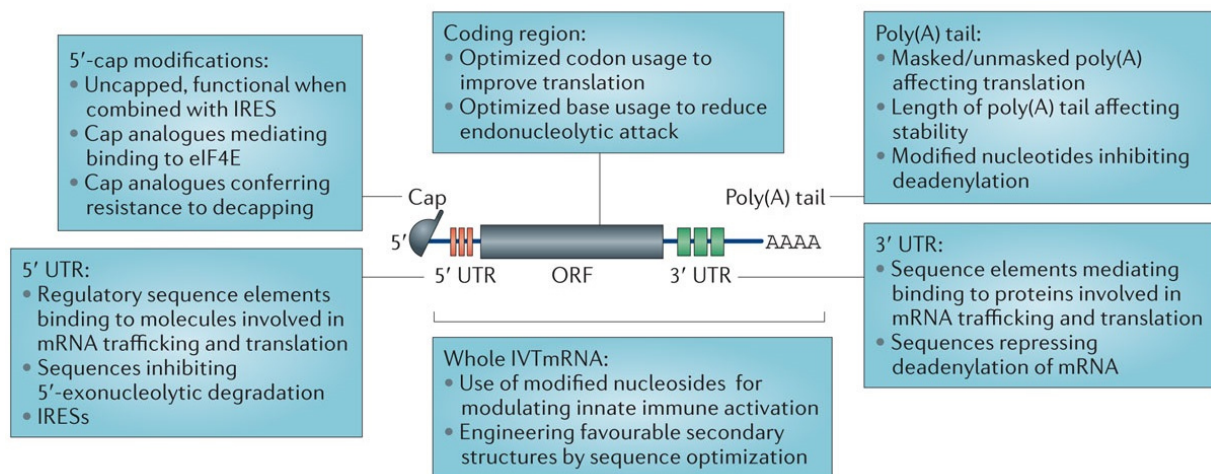


Figure 7: Structural modifications for tuning mRNA pharmacokinetics¹⁶

Despite the fact that many cells can spontaneously uptake naked mRNA, this mechanism is in most cases too inefficient as it is saturated at mRNA doses too low to be used in therapeutic applications⁶⁸. Therefore, suitable formulations are required to facilitate entry into cells and to protect cmRNA against extracellular RNase-mediated degradation. The main challenge in the design of formulations is the achievement of sufficient net level of encoded protein and to reach a high number of cells in a specific organ or a specific cell type.

The liver is an organ with limited cell turnover, hence delivery systems relying on cell division such as viral vectors are very inefficient for hepatocyte transfection. This could be solved by application of adenoviral and adeno-associated viral delivery methods, however both have an increased risk of inducing an immune response. Lipidoid nanoparticles have been proven an interesting alternative for the delivery of small inhibitory RNA (siRNA) in the liver and special adjustment of the nanoparticle composition for the specific purpose could also render them valuable for mRNA delivery^{68,69}. For the *in vivo* experiments presented in this thesis, specifically designed lipoplexes developed by Jarzebinska et al. for targeting hepatocytes will be used. These lipoplexes consist of a cationic lipid, two helper lipids and a polyethylene glycol (PEG) lipid for shielding¹⁴.

Various systems for delivery of nanoparticles in the lung have been studied due to the lungs large alveolar surface area suitable for drug absorption, low thickness of the epithelial barrier and extensive vascularization. mRNA formulations are usually prepared in form of nanoparticle suspension which can be delivered by use of a nebulizer or intratracheal

microspray. In addition to that, recent advances in formulations of polymer-lipid nanoparticles could solve the obstacle of liver uptake of nanoparticles⁷⁰ while specifically targeting lung tissue, which adds systemic administration as an interesting delivery alternative¹³. The choice of the most appropriate delivery system however, heavily depends on the targeted disease and requires intensive fine tuning of carrier, application method and frequency.

1.3.4 Aim of the Study

As previously stated, promising results of ACE2 therapy in experimental liver and lung fibrosis have been reported^{3-5,55,56,71,72}. In human clinical trials, safety and tolerability of systemically applied recombinant ACE2 was shown^{10,73}. However, reestablishing the local RAS balance seems to be most important in the diseased state⁴³, which can best be achieved by a localized translation of membrane anchored ACE2. This may be achieved with the recent advances in RTT¹³⁻¹⁵.

Therefore, the aim of this thesis was to design therapeutic ACE2 cmRNA and combine it with liver and lung targeted formulations. First, *in vitro* validation of ACE2 cmRNA transfection efficiency, protein expression and activity was performed. Second, due to the importance of translation of a membrane anchored protein, necessary post-translational modifications as well as final protein localization were verified.

After this initial *in vitro* proof of concept, liver and lung targeted delivery systems were evaluated for organ specific protein translation by use of reporter cmRNA. In parallel, an *in vitro* screen of eight modified ACE2 sequences was performed as described in the master thesis of Huber M.⁷⁴ to identify the optimal ACE2 cmRNA composition for liver and lung delivery. Upon identification of the respective potent carrier formulations, the best performing ACE2 sequence was administered *in vivo*, leading to substantial ACE2 protein expression in both, liver and lung.

Finally, therapeutic application of organ targeted ACE2 cmRNA was tested in a model of liver and a model of lung fibrosis. These first therapeutic ACE2 cmRNA applications gave a deeper understanding of the strengths and current challenges of therapeutic cmRNA in the treatment of complex fibrotic diseases as well as the pharmacodynamic properties of ACE2 cmRNA in experimental disease models. Based on these results, an outlook for future anti-fibrotic application will be given.

2 MATERIALS and METHODS

The experiments of this thesis are documented in the following laboratory books of the Ethris GmbH: 0063, 0088, 0123 and 0148

2.1 Materials

2.1.1 ACE2 cmRNA Sequences

For the study, one natural and one codon optimized version of the open reading frame (ORF) were designed. The full sequence for both is described in the appendix. In addition 4 different versions of the untranslated regions (UTRs) were designed.

Table 1: UTR sequences used in this study

Abbreviation	Full Name	Sequence
Natural	Human ACE2 with natural 5' and 3' UTRs	GGGAGAC(Nat)GCCACCATG____TGA(Nat)-PolyA
Minimal	Human ACE2 with minimal 5' UTR	GGGAGACGCCACCATG____TGA-PolyA
hαG	Human ACE2 with minimal Human alpha Globin 5' UTR	GGGAGAC(hαG)GCCACCATG____TGA-PolyA
CYBA	Human ACE2 with human cytochrome b-245 alpha polypeptide 5' and 3' UTRs	GGGAGAC(CYBA)GCCACCATG____TGA(CYBA)-PolyA
Luc	Firefly Luciferase	GGGAGAC____ - PolyA

2.1.2 Cell Lines

Table 2: Cell lines used

Product	Supplier	Number	Date of authentication
A549 cells	DSMZ	ACC-107	22.04.2016
HepG2 cells	DSMZ	ACC-180	22.04.2016
HEK293 cells	DSMZ	ACC-305	22.04.2016

The documents for the authentication can be found in the appendix. Cross-contamination was checked by short tandem repeat profiling.

2.1.3 Cell Culture Media and Supplements

Table 3: Cell culture media and supplements used

Product	Supplier
Dulbecco`s Modified Essential Medium (DMEM)/F-12, L-Glutamine, 15 mM HEPES	Gibco Life Technologies
Fetal calf serum (FCS), heat-inactivated	Gibco Life Technologies
Gentamycine	Sigma Aldrich
Hank`s balanced salt solution	Gibco Life Technologies

Hydrocortisone	Rotexmedica
Insulin	Novo Nordisk
Minimum Essential Medium (MEM) GlutaMAX	Gibco Life Technologies
Non Essential Amino Acids	Sigma Aldrich
Normal Horse Serum	Vector Laboratories
Normal Goat Serum	Thermo Fisher Scientific
Phosphate-buffered saline (PBS)	Gibco Life Technologies
Penicillin/Streptomycin solution	Gibco Life Technologies
Roswell Park Memorial Institute (RPMI) 1640 Medium (1X)+ GlutaMAX™	Gibco Life Technologies
Trypsin/EDTA solution	Sigma
TrypLE™	Gibco Life Technologies
Williams' E medium	PAN-Biotech

2.1.4 Transfection Reagents

Table 4: Transfection reagents used

Product	Supplier
In-house transfection reagent (C12-(2-3-2)/DPPC/cholesterol/DMG-PEG2k lipoplexes in aqueous solution)	Ethris GmbH
Lipofectamine® MessengerMAX™	Thermo Fisher Scientific
Liver lipidoid formulation (LLF) – LF92/LF44	Ethris GmbH
Pulmonary Lipid Formulation (PLF) - PEG co-polymer	Ethris GmbH

2.1.5 Kits

Table 5: Assay kits used

Product	Supplier
NucleoSpin® RNA Plus	Machery-Nagel
Pierce™ bicinchoninic assay (BCA) Protein Assay Kit	Thermo Fisher Scientific
Protein Deglycosylation Mix II	New England Biolabs
ProcartaPlex™ Multiplex Immunoassay custom kits	Affymetrix eBioscience
Standard Sensitivity RNA Analysis Kit	Advanced Analytical Technologies
Transcriptor First Strand cDNA Synthesis Kit	Roche Diagnostics

2.1.6 Primers

Table 6: Primers used for qPCR

Name	Species	Sequence (forward)	Sequence (reverse)
<i>Primers supplied by Eurofins</i>			
Angiotensin converting enzyme 2 cmRNA (<i>in vitro</i>)	Artificial	ggccaatcactacgaggact	tccactccgttcacctcata
Angiotensin converting enzyme 2cmRNA (<i>in vivo</i>)	Artificial	aatacgtggtgctgaagaacg	agtcgccgtagtctcctgtag
Angiotensin converting enzyme 2	Homo sapiens	ccagtggatgaaaagtgggtg	gtttcatcatggggcacag

Beta-2-microglobulin	Homo sapiens	ttctggcctggaggctatc	tcaggaatgtgactttccattc
Mitochondrial ribosomal protein L19	Homo sapiens	ggaatgttatcgaaggacaagg	caggaagggcatctcgtaag
Succinate dehydrogenase, subunit A	Homo sapiens	tccactacatgacggagcag	ccatcttcagttctgctaaacg
Mitochondrial ribosomal protein L19	Mus musculus	cgagtacagcacctttgacg	ggcttcattttaactttcagcttg
Succinate dehydrogenase, subunit A	Mus musculus	ttgagatccgtgaaggaagag	tagacgtgtggccagttgc

Primers supplied by Biorad

Beta actin	Homo sapiens	Type: PrimePCR™ SYBR® Green Assay	
Glucuronidase beta	Mus musculus	Type: PrimePCR™ SYBR® Green Assay	
TATA box binding protein	Homo sapiens	Type: PrimePCR™ SYBR® Green Assay	

2.1.7 Antibodies and Dyes

Table 7: Antibodies and dyes used for Western Blot and FACS

Antigen	Catalog#	Supplier
<i>Primary antibodies</i>		
Goat anti Angiotensin converting enzyme 2 pAb	AF933	R&D Systems
Rabbit anti Glycerinaldehyd-3-phosphate-Dehydrogenase mAb	5174	Cell Signaling
Goat anti Luciferase pAb	G7451	Promega
Rabbit anti Vinculin pAb	ab91459	Abcam
<i>Secondary antibodies</i>		
Donkey anti goat Immunoglobulin G (IgG) pAb	sc2020	Santa Cruz Biotechnology
Goat anti rabbit IgG pAb	sc2004	Santa Cruz Biotechnology
Rabbit goat IgG pAb	A-11087	Thermo Fisher Scientific
<i>Dyes and Staining Reagents</i>		
Propidium iodide		Sigma-Aldrich
Hematoxylin		Roth
Tetramethylrhodamine conjugated wheat germ agglutinin	W849	Thermo Fisher Scientific
ImmPRESS HRP anti-goat IgG (peroxidase) polymer detection kit	MP-7405	Vector Laboratories
Vectastain Elite ABC HRP kit (peroxidase)	PK-6100	Vector Laboratories
RNAscope 2.5 HD Reagent Kit-BROWN	322300	Advanced Cell Diagnostics
RNAscope Negative Control Probe – DapB	310043	Advanced Cell Diagnostics
RNAscope Positive Control Probe – Rn-Ppib	313921	Advanced Cell Diagnostics

2.1.8 Chemicals

Table 8: Chemicals used for cell culture

Chemical	Supplier
Angiotensin II human	Sigma Aldrich
Calcium chloride	Sigma Aldrich
CollagenR	Serva
Collagenase (Type NB 4G)	Serva
Collagenase type I	Biochrome
Dimethyl sulfoxide (DMSO)	Sigma Aldrich
Egtazic acid (EGTA)	Sigma Aldrich

Ethanol	Roth
Glucose	Applchem
GTP	New England Biolabs
HEPES	Gibco Life Technologies
Ketamin	Sigma Aldrich
L-Glutamine	Biochrome
MgSO ₄ x 7H ₂ O	Roth
Percoll	GE Healthcare
Potassium dihydrogen phosphate	Sigma Aldrich
Sodium chloride	Roth
Tunicamycin	Sigma Aldrich
Water for injection (WFI)	B. Braun
Xylazin	Sigma Aldrich

Table 9: Chemicals used for *in vitro* transcription

Chemical	Supplier
2-Propanol	Sigma Aldrich
Adenosine triphosphate (ATP)	Sigma Aldrich
Ammonium acetate	Applchem
Bsp199I/BstBI	Thermo Fisher Scientific
Buffer Tango	Thermo Fisher Scientific
Chloroform	Sigma Aldrich
DNASE I	Thermo Fisher Scientific
Ethanol	Roth
Guanosine triphosphate (GTP)	New England Biolabs
Inorganic Pyrophosphatase	Thermo Fisher Scientific
mRNA Cap 2'-o-Methyltransferase	New England Biolabs
Poly(A) Polymerase (E.coli)	NEB
Poly(A) Polymerase Buffer	NEB
RiboLock Rnase Inhibitor	Thermo Fisher Scientific
rATP	Jena Biosciences
rGTP	Jena Biosciences
rCTP	Jena Biosciences
rUTP	Jena Biosciences
5-Iodo-rUTP	Jena Biosciences
5-Iodo-rCTP	Jena Biosciences
S-Methyladenosine	New England Biolabs
Sodium acetate	Roth
T7 polymerase	Thermo Fisher Scientific
Vaccina virus capping enzyme	New England Biolabs
Water for injection (WFI)	B. Braun

Table 10: Other chemicals

Chemical	Supplier
1,4-Dithiothreitol (DTT)	Roth
2-Propanol	Sigma Aldrich
2-Mercaptoethanol	Sigma Aldrich
3,3'Diaminobenzidine	Roth
4-(Dimethylamino)benzaldehyde	Sigma Aldrich
Bolt® Lithium Dodecyl Sulfate (LDS) sample buffer (4 x)	Thermo Fisher Scientific
Bolt® sample reducing agent (10 x)	Thermo Fisher Scientific
Bolt® 2-(N-morpholino)ethanesulfonic acid (MES) buffer	Thermo Fisher Scientific
Bolt® 3-(N-morpholino)propanesulfonic acid (MOPS) buffer	Thermo Fisher Scientific
Bovine serum albumin	Sigma Aldrich
Branched poly(ethylenimine)	Sigma Aldrich
Captopril	Santa Cruz Biotech
Chloramine-T hydrate	Sigma Aldrich
Citric Acid	Sigma Aldrich
Coenzyme A	Sigma Aldrich
Complete, EDTA-free	Roche
Dimethyl sulfoxide	Sigma Aldrich
D-Luciferin	Synchem
DX600	Bachem
Edetic acid (EDTA)	Roth
Ethanol	Roth
FluorSave	Merck Chemicals
Gelatine alba	Caesar&Loretz GmbH
Hydrochloric acid (10 mol/l)	Applichem
Hydrochloric acid (1 N)	Roth
Hydrogene peroxide	Roth
Laemmli Sample Buffer (4X)	Biorad
L-Hydroxyproline	Millipore
Magnesium sulfate	Roth
Mca-YVADAPK(Dnp)-OH	R&D Systems
Mca-APK(Dnp)	Caslo
MES	Roth
Methanol ≥ 99 %	Roth
MgCO ₃	Roth
(MgCO ₃)4Mg(OH) ₂ x 5H ₂ O	Roth
MLN4760	Exclusive Chemistry Ltd
NuPage® Antioxidant	Thermo Fisher Scientific
NuPage® Sample Reducing Agent	Thermo Fisher Scientific
NuPAGE® LDS Sample Buffer (4X)	Thermo Fisher Scientific
NuPAGE® MOPS SDS Running Buffer (20X)	Thermo Fisher Scientific
Paraformaldehyde 20 % Solution	Electron Microscopy Sciences
p-Dimethylaminobezaldehyde	Sigma Aldrich
Perchloric acid (70 %)	Sigma Aldrich

Potassium chloride	Roth
Powdered milk	Roth
Precision Plus Protein™ Dual Color Standards	Bio-Rad
Pierce™ Protease and Phosphatase Inhibitor Mini Tablets	Thermo Fisher Scientific
Recombinant human ACE2	R&D Systems
RNAlater™	Invitrogen
Sodium chloride	Roth
Sodium deoxycholate	Roth
Sodium dodecyl sulfate (SDS)	Roth
Sodium hydroxide	Roth
Tris buffered saline (TBS)	Bio-Rad
Tricine	Roth
Tri sodium citrate dihydrate	Roth
Tris(hydroxymethyl)aminomethane (Tris)	Roth
Tris-HCl	Roth
Triton X-100	Sigma Aldrich
Tween®	Roth
Water for injection (WFI)	B. Braun
Xylol	Roth
ZnCl ₂	Roth

2.1.9 Consumables

Table 11: Consumables used in this work

Product	Supplier
0.2 µm 4 mm sterile filters	EMD Millipore
Bolt® 8 % Bis-Tris Plus gels (10 pockets)	Thermo Fisher Scientific
Bolt® 4-12 % Bis-Tris Plus gels (10, 12 and 15 pockets)	Thermo Fisher Scientific
Centrifuge Tube 15 and 50 mL	Corning Incorporated
Corning® 96 Well Black Flat Bottom Polystyrene Not Treated Microplate	Corning Incorporated
Costar™ 96-Well White Plates	Thermo Fisher Scientific
Costar™ cell culture plate, flat bottom, 96, 24 and 6 wells	Corning Incorporated
Costar Microcentrifuge Tube: 0.65 mL, 1.50 mL, 2.00 mL, 5.00 mL	Corning Incorporated
Costar™ Stripette 5, 10, 25, 50 mL	Corning Incorporated
Countess™ Counting Slides	Thermo Fisher Scientific
Diamond® Tipack™ D1200ST, D300ST, D200ST and DL10ST	Gilson
Eppendorf Safe-Lock Tubes 0,65; 1,7; 2,0 mL	Eppendorf
LightCycler® 480 Multiwell Plate 96, white	Roche
Luminata Western HRP	Merck Chemicals

NuPAGE™ Novex™ 4-12% Bis-Tris Midi Protein gels (20 and 26 pockets)	Thermo Fisher Scientific
T75 Corning® cell culture flasks, angled neck, cap (vented)	Sigma Aldrich
T175 Corning® cell culture flasks, angled neck, cap (vented)	Sigma Aldrich
Trans-Blot® Turbo Transfer Pack Midi 0.2 µm PVDF	Bio-Rad
Trans-Blot® Turbo Transfer Pack Mini 0.2 µm PVDF	Bio-Rad
Vivaspin 20 - 100 kDA MWCO PES Filter	Sartorius

2.1.10 Technical Equipment

Table 12: List of technical equipment used in this work

Name	Device	Supplier
15-300 µL (12 channels), I39816B	Multichannel pipette	Eppendorf
15-300 µL (8 channels), L29846B	Multichannel pipette	Eppendorf
Aeroneb Solo	Mesh nebulizer	Aerogen
Attune® acoustic focusing cytometer	Flow cytometer	Thermo Fisher Scientific
Axiovert 25	Microscope	Carl Zeiss AG
BoltR® Mini Gel Tank	Gel electrophoresis tank	Thermo Fisher Scientific
BIOSAFE®-System	Nitrogen tank	Cryotherm
Centrifuge 5810R	RNA-Centrifuge	Eppendorf
ChemiDoc™ XRS System	Molecular imager	BIO-RAD
Duomax 1030	Plate shaker	Heidolph Instruments
Fragment Analyzer	Fragment Analyzer	Advanced Analytical Technologies
Hettich Mikro 220	Centrifuge	Hettich Zentrifugen
Invitrogen™ countess automated cell counter	Cell counter	Invitrogen™
IR Sensor MCO-17AIC CO ₂ Incubator	Cell incubator	Sanyo
IVIS® Lumina XR	Imaging System	Caliper Life Sciences
KDS-210-CE	Dual Syringe Infusion/Withdrawal Pump	KD Scientific
Laminar Flow	Flow BDK	Luft- und Reinraumtechnik GmbH
Leica DMI8	Inverted Light Microscope	Leica Mikrosysteme
Leica DM2000 LED	Light Microscope	Leica Mikrosysteme
LightCycler® 96 Real-Time PCR System	qPCR machine	Roche

Lumat LB 9507	Single Tube Luminometer	Berthold Technologies
MagPix® Luminex	CCD Imager	Xmap Technologies
Mastercycler® gradient	Thermocycler	Eppendorf
Microcentrifuge 5415R/5415D	Microcentrifuge	Eppendorf
NanoDrop2000 UV-Vis	Spectrophotometer	Thermo Fisher Scientific
New Brunswick™ Innova® Upright Freezers	Freezer	New Brunswick
Pipetboy acu	Pipette	INTEGRA Biosciences AG
PIPETMAN Classic™: 2, 20, 200 and 1000 µl	Pipettes	Gilson
PowerPac3000	Power supply	BIO-RAD
Reacti-Therm™ III	Heating/Stirring module	Pierce
Refrigerated centrifuge 3K15	Refrigerated centrifuge	Sigma
Tecan Infinite® 200 PRO	Plate reader	Tecan
Thermomixer® compact	Thermomixer C	Eppendorf
Titramax 1000	Plate shaker	Heidolph instruments
Trans-BlotR Turbo™ Transfer System	Western blotting transfer system	BIO-RAD
Varifuge 3.0®	Centrifuge	Heraeus Sepatech GmbH
Vortex Genie 2	Vortexer	Scientific Industries
Wallac Victor2 1420 Multilabel counter	Plate reader	PerkinElmer Inc
Water bath model 1003	Water bath	GFL
Zetasizer™ Nanoseries	Particle and molecular size analyzer	Malvern

2.1.11 Software

Table 13: Software used for measurements and analysis

Product	Supplier
Attune® Cytometric Software V2.1	Thermo Fisher Scientific
ChemiDoc™XRS System	BIO-RAD
FlowJo® V10	FlowJo
GraphPad Prism® Version 6.01	GraphPad Software Inc.
Image Lab™ Software	BIO-RAD
Living Image V 4.3.1	Caliper Life Sciences Inc.
Magellan™ - Data Analysis Software	Tecan
LightCycler® 96 System	Roche

2.2 Methods

2.2.1 cmRNA and Lipoplex Preparation

2.2.1.1 cmRNA Preparation

Chemically modified mRNA (cmRNA) was synthesized by *in vitro* transcription of the respective plasmid DNA templates. For this purpose, plasmid vectors were digested with BstBI/BsP119I and purified chloroform/ethanol precipitation. Prior *in vitro* transcription, a mix of ribonucleotides was prepared containing adenosine-triphosphate (25 mM), guanosine-triphosphate (25 mM), uridine-triphosphate (16.25 mM), cytosine-triphosphate (23.125 mM) as well as the chemically modified ribonucleotides 5-iodo-cytosine-triphosphate (1.875 mM) and 5-iodo-uridine-triphosphate (8.75 mM). For *in vitro* transcription, the ribonucleotides were mixed with the linearized plasmid template and T7 RNA polymerase and incubated for 6 h at 37 °C. Afterwards, residual DNA was digested with DNase I for 45 min at 37 °C and the mix was twice precipitated with ammonium-acetate at 2.5 M at 4 °C for a minimum of 30 min and washed with 70 % ethanol. The final cmRNA pellet was re-suspended in water for injection (WFI) and concentration and purity was determined with NanoDrop 2000C spectrophotometer. Additional quality control was performed by running the cmRNA on a 1 % agarose gel. The RNA was then purified by ultrafiltration through a PES spinfilter (100 kDa). To enhance RNA stability at the 5' end of the transcript, a C1-m7G cap structure was enzymatically added by incubation with 0.5 mM guanosine-triphosphate, 0.2 mM S-Methyladenosine, mRNA Cap 2'-O-Methyltransferase and vaccinia virus capping enzyme for 75 min at 37 °C. Afterwards, mRNA was subjected twice to ammonium-acetate precipitation followed by two washing steps in 70 % ethanol. The RNA was then filtered through a 0.2 µm sterile filter and denatured for 20 min at 68 °C for post polyadenylation. For this purpose, denatured RNA was mixed with adenosine-triphosphate and Poly(A) polymerase and incubated for 60 min at 37 °C. Postpolyadenylation was stopped by addition of ice cold ammonium-acetate and two washing steps with 70 % ethanol. This process was repeated twice. The cmRNA was filtered through a 0.2 µm sterile filter and concentration and quality was measured on a NanoDop 2000C spectrophotometer and with the Standard Sensitivity RNA Analysis Kit on a Fragment Analyzer.

Table 1 gives an overview of the different cmRNA sequences designed. The structure of the natural human ACE2 UTRs (Nat) was retrieved from NCBI GenBank (NM_021804.2). The human alpha globin (hαG) 5' UTR was designed with omission of the first 30 nucleotides of

the hαG reference sequence (NM_000517.4) and introduction of an additional 'G' to give a full Kozak element upstream of ATG. Cytochrome b-245 alpha (CYBA) UTRs were designed as previously described⁷⁵.

2.2.1.2 cmRNA Lipoplex Formation and Application

For initial proof of concept, in-house transfection reagent was used at an N/P ratio (molar ratio of amino groups of lipid to phosphate groups of cmRNA) of 8. In brief, cmRNA in aqueous solution was rapidly injected into the appropriate amount of in-house transfection reagent, followed by 5 min incubation at room temperature (RT) for self-assembly of cmRNA and lipoplexes. Lipofectamine MessengerMax was used for transfection of murine primary cells according to manufacturer's protocol. cmRNA was prepared at a concentration of 1 µg/µl in H₂O and mixed with Lipofectamine MessengerMax with a cmRNA-to-transfection reagent ratio of 1:1.5 (vol/vol). In general, 2 µg of cmRNA per well was used for experiments performed in 6-well plates, 250 ng and 25 ng of cmRNA per well for 24-well plates. For all experiments, cells were seeded in a number to reach 70 % confluence within 24 h. After 24 h, medium was renewed and lipoplexes were added dropwise. Medium was replaced 4 h after transfection for cells transfected with Lipofectamine MessengerMAX.

For liver targeted *in vivo* experiments, cmRNA was formulated in LLF as previously described¹⁴. Polyethylenimine (PEI) formulation for aerosol application was prepared by mixing equal volumes of branched polyethylenimine (brPEI) at a concentration of 0.65 mg/ml with cmRNA at a concentration of 0.5 mg/ml in a total volume of 10 ml at a speed of 40 ml/min using a syringe pump system. The mix was incubated for 20 min at RT for complex formulation and then kept on ice until application. Particles were then analyzed on a Zeta-Sizer and showed a diameter of 80-120 nm. Lung targeted lipoplexes were prepared by mixing cmRNA with PLF in aqueous solution and applying it to a mix of preassembled lipid micelles. After incubation for 15 min at RT for self-assembly of cmRNA in this pulmonary lipid formulation, the mix was transferred into Dulbecco's phosphate-buffered saline (PBS) supplemented with 2 % sucrose. Lipoplexes were injected in the tail vein at a final volume of 150 µl per animal with a cmRNA dose of 1 mg/kg.

2.2.2 Cell Culture

2.2.2.1 Primary Murine Liver Cells

Liver cells were isolated from 8 weeks old male C57BL/6J mice. For hepatocyte isolation, animals were sacrificed and liver was perfused *via* the portal vein with EGTA buffer (25 mM HEPES [pH 8.5], glucose 5.7 g/l, 103 mM NaCl, 2.4 mM KCl, 1.23 mM KH₂PO₄, 0.480 mM L-Glutamine, 15 % (v/v) non essential amino acids and 0.5 mM EGTA) followed by a 10 min perfusion with collagenase buffer (25 mM HEPES [pH 8.5], glucose 5.7 g/l, 103 mM NaCl, 2.4 mM KCl, 1.23 mM KH₂PO₄, 0.480 mM L-Glutamine, 12 % (v/v) Amino acids, 2 mM CaCl₂, 3.5 mM MgCl₂ supplemented with 0.12 U/ml type NB 4G collagenase). In the next step, liver was excised, transferred to a petri dish and cut open to flush out hepatocytes with suspension buffer (25 mM HEPES [pH 7.6], glucose 5.7 g/l, 103 mM NaCl, 2.4 mM KCl, 1.23 mM KH₂PO₄, 0.480 mM L-Glutamine, 15 % (v/v) Amino acids, 1.1 mM CaCl₂, 0.4 mM MgSO₄, 0.17 % bovine serum albumin). Cells were washed twice with suspension buffer and were then subjected to a Percoll gradient. In brief, the cell suspension was fractionated by centrifugation at 600 g for 20 min, without brake. The upper layer containing dead cells was removed and the lowest layer was filled up with suspension buffer. Cells were once washed with suspension buffer, counted with Trypan blue and seeded on CollageneR coated 6-well plates in Williams' E medium supplemented with 0.22 mM L-Glutamine, 0.02 M HEPES [pH 7.4], 0.5 % Penicillin/Streptomycin, 100 mg/l Gentamycine, 110 nM Hydrocortisone, Insulin, 1.6 % dimethyl sulfoxide (DMSO) and 10 % fetal calf serum (FCS). After cell attachment, medium was changed to culture medium including 1 % FCS. Cells were cultured in a humidified 5 % CO₂ incubator at 37 °C with exchange of culture medium every 2-3 days.

2.2.2.2 Primary Murine Lung Cells

For isolation of lung fibroblasts 16 weeks old male C57BL/6J mice were anesthetized with Ketamin/Xylazin and lungs were flushed with PBS *via* the right heart ventricle. Lung tissue was removed, transferred into a petri dish, cut in small pieces and digested in collagenase solution DMEM/F-12, supplemented with 26.5 U/ml collagenase type I for 2 h at 37 °C and gentle shaking. The digested tissue was filtered, washed with PBS and seeded in culture medium (DMEM/F-12, 10 % heat-inactivated FCS and 1 % Penicillin/Streptomycin). Cells were passaged when reaching 90-95 % confluency. Cells were cultured in a humidified 5 % CO₂ incubator at

37 °C with exchange of culture medium every 2-3 days and all experiments were performed within passage 4 and 6.

2.2.2.3 Human Cell Lines

A549 and HEK293 cells were purchased from DSMZ and cultured in MEM GlutaMAX. HepG2 were purchased from DSMZ and cultured in RPMI 1640 + GlutaMAX. Absence of cross-contaminations within the cell lines were regularly checked by short tandem repeat profiling within the 2 years of *in vitro* experiments. Medium of all three cell lines was supplemented with 10 % heat-inactivated FCS and 1 % Penicillin/Streptomycin. Cells were cultured in a humidified 5 % CO₂ incubator at 37 °C. Cell culture medium was renewed twice a week and cells were passaged at 70 % confluency. For long term storage, cells were transferred in cell culture medium containing 20 % heat inactivated FCS and 10 % DMSO and brought to -80 °C at a controlled cooling rate of minus 1 °C per minute. Afterwards, they were transferred to liquid nitrogen. For thawing, cells were heated to 37 °C by dropwise addition of cell culture medium including all supplements. Residual DMSO was removed by centrifugation before transferring cells into cell culture flasks. Freshly thawed cells were kept in culture for at least one week before starting experiments.

2.2.3 Animal Studies

All studies were approved by the Government of Upper Bavaria or by the 'Norddeutsches Landesamt für Verbraucherschutz und Lebensmittelsicherheit' (LAVES) (Germany) and all animal experiments were carried out according to the guidelines of the German law of protection of animal life. Studies in the STAM model of liver fibroses were performed in Japan approved by the Japanese ministry of environment and all animal experiments were carried out according to the Japanese standards relating to the care and management of laboratory animals and relief of pain and the Japanese guidelines for proper conduct of animal experiments.

2.2.3.1 Mice

Animal studies for evaluation of organ targeted delivery were performed in female Balb/c at Ethris GmbH. The study of ACE2 application in a bleomycin induced model of pulmonary fibrosis was performed in male C57Bl/6J mice at Fraunhofer ITEM (Hannover). All animals were purchased from Charles River (Sulzfeld, Germany). The study of ACE2 application in the

STAM model for analysis of liver fibrosis was performed at Stelic MC, Inc. (Tokyo, Japan) in Japan and animals were purchased and treated by Stelic. At the start of the experiment they were 9-11 weeks of age weighing approximately 20 g. At the end of the study, organs were collected and stored at -80 °C or transferred into RNALater. 200 µl of blood serum was collected for analysis of blood parameters and stored at -80 °C for later analysis.

2.2.3.2 Rats

Studies in rats were performed by Fraunhofer ITEM (Hannover) with male Wistar rats, purchased from Charles River. They were 7 weeks old and around 330 g of weight at the start of the experiments. At the end of the experiment lungs were excised, transferred to a petri-dish and stored at -80 °C for examination.

2.2.4 cmRNA Quantification and Relative Gene Expression Analysis

For total RNA isolation, fresh tissue sections were incubated in RNA Later overnight at 4 °C. Tissues were then transferred into Eppendorf tubes and stored at -80 °C for later analysis. Total RNA was isolated with the Nucleospin RNA Plus Kit. For analysis of *in vivo* samples, 30 mg of tissue was homogenized in 350 µl lysis buffer using FastPrep-24 tissue / cell homogenizer. *In vitro* samples were lysed directly by addition of lysis buffer (LBP) into cell culture plates. All samples were processed with the Nucleospin RNA Plus kit following manufacturers' instructions. RNA quality and quantity was analysed on a NanoDrop. 1 µg of total RNA was transcribed into cDNA using Transcriptor First Strand cDNA Synthesis Kit using oligo dT primers. Samples were heated with the Mastercycler to 65 °C for 10 min, then RNase inhibitor, dNTP mix and reverse transcriptase were added and heated to 55 °C for 30 min. Reverse transcriptase was inactivated by heating to 85 °C for 5 min. For determination of absolute cmRNA values, cDNA standard series with cmRNA spike in (from 1.0×10^{-7} to 1 ng) in untransfected tissue samples were prepared. Real-time qPCR was performed with SsoAdvanced Universal SYBR Green Supermix on a Roche Light Cycler 96. The program setting was as follows:

Table 14: Settings for real-time qPCR measurement

Pre-incubation	1 cycle	95 °C for 600 sec
3 step amplification	45 cycles	95 °C for 5 sec
		60 °C for 1 sec
		72 °C for 1 sec
Melting	1 cycle	Ramp up to 95 °C in 10 sec

Experiments were performed in triplicates with the following reference genes:

- Determination of human endogenous ACE2 mRNA (Figure 9): β -2-microglobulin, MRPL19 and SDHA
- Determination of murine endogenous ACE2 mRNA (Figure 9): GusB, MRPL19 and SDHA
- *In vitro* analysis of ACE2 cmRNA uptake in human cells (Figure 10): β -actin and TATA-box binding protein
- *In vitro* analysis of ACE2 cmRNA uptake in murine cells (Figure 10): MRPL19, SDHA and GUSB

Δ ct (ACE2 cmRNA – mean reference genes) was calculated for relative gene expression according to Pfaffl⁷⁶, while absolute cmRNA values were interpolated using Graph-Pad prism. Half-life was calculated applying a one phase exponential decay function with automatic outlier elimination in Graph-Pad prism.

2.2.5 Protein Analysis

2.2.5.1 Hydroxyproline Assay

Hydroxyproline is a major structural component of collagen and can therefore be used for indirect collagen quantification in tissues. For the assay, approximately 50 mg of frozen liver tissue was transferred into 500 μ l WFI and homogenized in a FastPrep-24 tissue homogenizer. For hydrolysis, the homogenate was supplemented with HCl at a final concentration of 5 N and boiled overnight at 120 °C. After passing the homogenate through a 0.2 μ m filter, 10 μ l of the homogenate or L-Hydroxyproline standard (from 3.15 ng/ μ l to 150 ng/ μ l) was transferred into a clear 96-well plate and dried at 70 °C until complete liquid evaporation. Samples were then incubated with 100 μ l chloramine-T solution (0.84 % chloramine-T, 42 mM sodium acetate, 2.6 mM citric acid and 39.5 % (vol/vol) isopropanol at pH 6.0) for 10 min at RT. Next, 100 μ l of DMAB solution (0.248 g p-dimethylaminobezaldehyde dissolved in 0.27 ml 60 % perchloric acid and 0.73 ml isopropanol) was added and heated to 50 °C for 60 min. Absorption measurement was performed at 558 nm on a plate reader.

2.2.5.2 Flow Cytometry Analysis

Correct protein integration into the plasma membrane was assessed by flow cytometry. Cells were washed with PBS, detached with TrypLE and re-suspended in flow cytometry buffer (PBS supplemented with 10 % FCS). Then, cells were incubated with primary antibody against ACE2

in flow cytometry buffer (concentration 5 $\mu\text{g}/\mu\text{l}$) for one hour at 4 °C. After washing with flow cytometry buffer, anti-goat AF488 antibody was added (dilution 1:400) for one hour at 4 °C. Cells were washed again in flow cytometry buffer, stained with propidium iodide (concentration 1 $\mu\text{g}/\text{ml}$) for discrimination between live and dead cells and analyzed on a flow cytometer.

2.2.5.3 Protein Quantification by Western Blot

In vitro samples were washed once with ice cold PBS and lysed either in 200 μl (6-well plates) or 75 μl (48-well plates) ACE2 lysis buffer ((1 M NaCl, 0.5 mM ZnCl_2 and 75 mM TrisHCl [pH 7.5], 0.5 % Triton X-100) for 10 min on ice. Cells were then scratched off the plates and lysate was transferred into Eppendorf tubes. For *in vivo* samples, tissue pieces were transferred in RIPA buffer (50 mM Tris [pH 8.0], 150 mmol/l NaCl, 1.0 % Triton X-100, 0.5 % sodium deoxycholate, and 0.1 % sodium dodecyl sulfate) and homogenized using FastPrep-24 homogenizer. All lysates were centrifuged for 10 min at 14000 rpm at 4 °C to remove cell debris and supernatant was collected for protein analysis.

The amount of total protein in the cell lysates was determined by BCA (bicinchoninic assay) Protein Assay Kit according to manufacturer's instruction. The assay was performed in 96-well plates with 5 μl of *in vitro* cell lysate or 10 μl of *in vivo* cell lysate and 200 μl of BCA reaction reagent. After incubation for 20-30 min at 37 °C, the colorimetric reaction was measured at 590 nm with a plate reader.

For the experiment proofing full glycosylation of ACE2 protein, parts of the lysates enzymatically deglycosylized by treatment with the NEB Protein Deglycosylation Mix II following manufacturer's instructions for denaturing conditions. Cell lysates were then separated by SDS-PAGE. For this purpose, 2-75 μg of total protein was supplemented with Bolt LDS Sample Buffer and Bolt Sample Reducing Agent and heated to 70 °C for 10 min at 350 rpm for protein denaturation. Samples were then loaded on a 4-12 % polyacrylamide gel and run for 30 to 45 min at 160 V. For verification of disulfide bonds, 2 μg of total protein was supplemented with Laemmli Sample Buffer with or without 2-mercaptoethanol and heated to 90 °C for 5 min at 350 rpm. Then, samples were loaded on a 8 % polyacrylamide gel and run for 30 min at 160 V. After protein separation, proteins were transferred from the gel to a polyvinylidene membrane using preassembled transfer packages (Trans-Blot Turbo Transfer Packages) placed in a Trans-Blot Turbo Transfer system for 30 min at 25 V. Membranes were

then transferred in NET-gelatin buffer (50 mM Tris [pH 7.5], 150 mM NaCl, 0.05 % Triton X-100, 5 mM EDTA and 0.25 % gelatin) for 1 h at RT to block free protein bindings sites on the membrane. Incubation with primary antibody (ACE2 0.1 µg/ml, GAPDH 1:10000, Luciferase 1:300, Vinculin 1:10000) was performed in NET-gelatin overnight at 4 °C and gentle shaking. After washing membranes three times for 10 min in NET-gelatin buffer, they were incubated for one hour at RT with secondary antibody at a dilution of 1:10000 coupled to horse radish peroxidase. Membranes were washed again three times for 10 min in NET-gelatin buffer and then incubated for 5 min with peroxidase substrate (Luminata Western HRP). For chemiluminescence signal detection, membranes developed in a ChemiDoc XRS System.

2.2.5.4 ACE2 Activity Assay

ACE2 activity was determined by cleavage of a fluorogenic peptide substrate (Mca-Y-V-A-D-A-P-K(Dnp)-OH). Once the substrate is cleaved, the fluorophore (Mca) is separated from its quencher (Dnp), resulting in increased fluorescence intensity of the sample. In order to distinguish fluorescence created by ACE2 from fluorescence created by other peptidases, a specific ACE2 inhibitor (DX600) was used. The difference in fluorescence intensity of inhibitor treated versus untreated samples corresponds to ACE2 activity.

For ACE2 activity determination in cell culture, samples were lysed as described for western blotting. 30 µg of total protein extract was incubated ± DX600 for 20 min at RT in ACE2 reaction buffer ((1 M NaCl, 0.5 mM ZnCl₂ and 75 mM TrisHCl [pH 7.5]). 10 µM of synthetic substrate Mca-Y-V-A-D-A-P-K(Dnp)-OH was added to a total volume of 100 µl and incubated for at least 60 min at 37 °C.

Ex vivo samples were prepared as described by Joyner et al. (Joyner). In brief, frozen liver and lung samples were homogenized in ACE2 reaction buffer (1X Complete, 25 mM HEPES buffer, 125 mM NaCl, 10 µM ZnCl₂ [pH 7.4]) followed by a centrifugation at 2500 g for 5 min. Supernatant was collected and spun for 10 min at 28000 g. The resulting pellet was re-suspended in reaction buffer before over-night incubation with 0.5 % Triton X-100 at 4 °C and gentle shaking. Samples were centrifuged for 5 min at 28000 g, supernatant was collected and total protein content measured by BCA. For the assay, 20 µg of protein was incubated for 20 min at RT in ACE2 reaction buffer containing 10 µM ACE inhibitor Captopril. 1 mM of ACE2 inhibitor MLN4760 was added followed by another incubation for 20 min at RT. Finally, 1 mM of substrate Mca-A-P-K(DnP) was added and samples were incubated for 1 h at 37 °C.

Fluorescence of all samples was measured on a Tecan Infinite 200 PRO plate reader with excitation at 320 nm and emission at 405 nm.

2.2.5.5 Firefly Luciferase Activity Measurements

For determination of *in vivo* luciferase activity, animals having received Luc2 cmRNA were anesthetized followed by 3 mg intraperitoneal and 1.5 mg intra-nasal application of D-luciferin substrate dissolved in PBS at 30 mg/ml [pH 7.0]. Bioluminescence for the whole animal was measured 10 min later using an IVIS Lumina XR Imaging System with an exposure time of 1 min. Then, organs were excised, placed on a petri-dish and reimaged on the IVIS system.

For quantification of *ex vivo* firefly luciferase activity, 60-90 mg of frozen lung tissue were lysed in luciferase lysis buffer (25mM Tris-HCL, 1 % Triton X-100, 1X Complete). 100 µl of luciferin substrate (0.47 mM D-Luciferin, 0.27 mM Coenzyme A, 33.3 mM 1,4-Dithiothreitol, 0.53 mM ATP, 1.1 mM MgCO₃, 2.7 mM Magnesium sulphate heptahydrate, 20 mM Tricine, 0.1 mM EDTA disodiumsalt dihydrate) was added to the tissue homogenate and photon emission was measured for 1 sec in a tube luminometer.

2.2.5.6 Cytokine Measurements

Cytokine levels in plasma were determined with ProcartaPlex™ Multiplex Immunoassay custom kits provided by Affymetrix eBioscience on a Magpix instrument. The assay uses 6.5 µm magnetic beads labelled with a pattern of red and infrared fluorophores, giving each bead a unique spectral signature. On each magnetic bead, a monoclonal capture antibody is attached which binds to the targeted cytokine and in a second step to a biotinylated secondary antibody coupled to streptavidin-phycoerythrin. For signal detection, the magnetic beads are first captured by a magnet in front of a CCD camera. Then, the red light emitting diodes (LEDs) excite the dye mixture inside the bead, which identifies the cytokine measured. Finally, the green LEDs excite the phycoerythrin reporter tag which generates the analytical signal used to quantify the cytokine level.

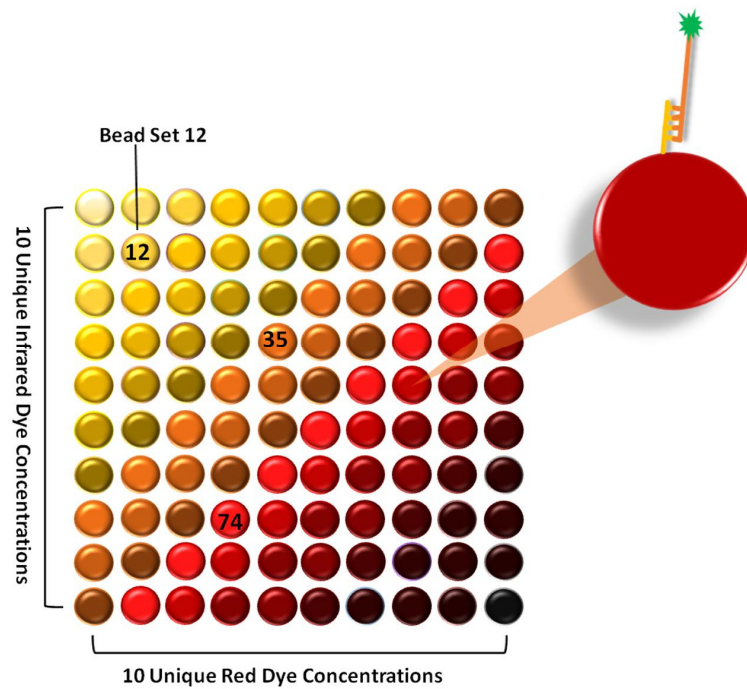


Figure 8: Principle of the cytokine measurement

Each bead set identifies a specific cytokine measured.¹²⁶

75 μ L of plasma was treated according to manufacturer's instruction. In brief, upon standard preparation, antibody magnetic beads were prepared and 50 μ L were transferred to each well of the 96-well plate provided in the kit. After one washing step with washing buffer at RT, 25 μ L of standards and samples were added to the dedicated wells. While shaking, the plate was incubated for 15 min at RT. Subsequently, the plate was transferred to 4 $^{\circ}$ C and incubated overnight. The next day, the plate was shaken at RT for 15 min. Following two washing steps at RT, 25 μ L of the detection antibody was added and incubated for 20 min at RT. After two more washing steps, 50 μ L streptavidin-phycoerythrin was added and incubated for 30 min at RT. After two additional washing steps and bead suspension data acquisition was done with the Magpix instrument. The following cytokines were measured: IL-10, IL-1 β , IL-2, IP-10, IL-6, IFN α , IFN γ , IL-12p70 and TNF α . Cytokine data were analyzed by nonlinear regression.

2.2.6 Immunocyto- and Immunohistochemistry

2.2.6.1 Immunocytochemistry

For visualisation of ACE2, cells were cultured on coverslips in 6-well plates and afterwards co-stained for immunofluorogenic detection of ACE2 protein at the cell membrane. After washing with PBS, cell membranes were stained by addition of tetramethylrhodamine conjugated wheat germ agglutinin in Hank's balanced salt solution (concentration 20 µg/ml) and incubation for 10 min in the incubator. Samples were washed with PBS and fixed in 4 % paraformaldehyde for 10 min at RT. Cells were washed again and permeabilized for 10 min in PBS supplemented with 0.2 % Triton X-100 at RT. After another washing step, cells were blocked in blocking solution (PBS supplemented with 10 % FCS and 0.05 % Triton X-100) for 30 min at RT. Slides were then incubated for one hour with primary antibody against ACE2 in blocking solution at RT followed by another washing step in PBS. Secondary anti-goat AF488 antibody and DAPI for visualisation of the nuclei, were diluted in blocking solution and samples incubated for 1 h at RT. After a final wash, slides were mounted in FluorSave and viewed under a Leica DMI8 microscope.

2.2.6.2 Immunohistochemistry

Liver and lung tissues were excised, fixed for 24 h in 4 % buffered formaldehyde solution and embedded in paraffin for histological examination. Tissues were then sectioned into 3-4 µm slices, deparaffinized in Xylol and rehydrated in a decreasing ethanol series. For antigen retrieval, tissue sections were incubated in 10 mM sodium citrate buffer [pH 6.0] for 30 min using a waterbath at 96 °C. The tissues were washed in PBS, quenched for 5 min in 3 % H₂O₂ and washed again.

For luciferase staining, sections were blocked for 1 h at room temperature in 2.5 % horse serum in PBS. The sections were then incubated with primary anti-luciferase antibody in PBS supplemented with 0.3 % Triton X-100 at 4 °C overnight. Tissue sections were washed in PBS and incubated with ImmPRESS Reagent for 30 min at RT. The ImmPRESS reagent is a peroxidase micropolymer coupled to a secondary anti-goat antibody, allowing highly sensitive signal detection with reduced background signals. After washing again with PBS, 3,3'-diaminobenzidine substrate at 0.5 mg/ml in PBS was added for 1-8 min at RT.

For ACE2 staining, the tissue sections were additionally subjected to an avidin/biotin block for 15 min at RT, followed by a brief wash. Then tissues were blocked in Vectastain serum blocking

reagent D for 30 min at RT, followed by an overnight incubation at 4 °C with primary anti-ACE2 antibody in 10 % normal goat serum in PBS supplemented with 0.2 % Triton X-100. After washing with PBS, the sections were incubated with Vectastain biotinylated secondary anti-goat IgG antibody diluted according to manufacturer's protocol for 30 min at RT. Slides were washed again and incubated in Vectastain ABC complex, a preformed Avidin/Biotinylated enzyme complex, which serves as a signal multiplier due to very high affinity of avidin for biotin and four biotin binding sites. After incubation for 30 min at RT, 3,3'-Diaminobenzidine substrate was added at 0.5 mg/ml in PBS for 1 min at RT and the reaction was stopped by washing tissue sections in distilled water. For counterstaining, sections were briefly dipped in hematoxylin and then washed under running water. Evaluation was performed with a Leica DM2000 LED.

2.2.6.3 Sirius red Staining

Sirius red staining is a dye used for staining collagen and amyloid. As excessive collagen deposition is a major hallmark of fibrotic diseases, quantitative analysis of the percentage of sirius red staining area in tissue sections is frequently used for fibrosis scoring. Sample preparation, sirius red staining, hematoxylin staining and tissue analysis for the liver disease model was done by Stelic MC, Inc. Tokyo, Japan.

2.2.6.4 In situ Hybridisation

In situ hybridization of liver tissues was performed by ACD (Advanced Cell Diagnostics, Hayward, CA, USA), and lung tissues were analyzed by ITEM (Hannover, Germany) using RNAscope 2.5 HD Reagent Kit-Brown following manufacturer's instructions. For detection of ACE2 cmRNA, a targeted probe was designed by ACD based on the cmRNA sequence provided, while a probe detecting murine ACE2 was derived from GenBank (NM_027286.4). RNAscope dapB (bacterial dapB) was used as a negative and RNAscope PPIB (Cyclophilin B) as a positive control. Samples were counterstained with hematoxylin and viewed under a brightfield microscope.

2.2.7 Statistical Analysis

Each experiment was performed with at least three technical replicates per sample. In addition, quantitative analysis of flow cytometry samples was performed with a minimum of three biological replicates. Results are shown as mean \pm standard error. Statistical analysis was performed using GraphPad Prism 6. Pair-wise comparison of *in vitro* experiments was conducted by two-tailed Student's t-test and group comparisons of *in vivo* experiments were done by one-way ANOVA, followed by Dunnett's multiple comparison test. A P value ≤ 0.05 was considered statistically significant (* ≤ 0.05 , ** ≤ 0.01).

3 RESULTS

3.1 Proof of Concept for ACE2 Delivery *in vitro*

3.1.1 ACE2 cmRNA Transfection and Translation *in vitro*

In the first set of experiments, RNA delivery of in-vitro-transcribed (IVT) chemically modified ACE2 RNA (ACE2 cmRNA) and its successful translation into ACE2 protein was investigated. As a generic test system, human embryonic kidney cells HEK293 were chosen as they are frequently used for transient transfection experiments. Additionally, with the aim of liver and lung targeted protein translation in subsequent *in vivo* studies, the following cells were selected: alveolar epithelial derived cells A549 and hepatoma derived cells HepG2 as human cell lines and hepatocytes and lung fibroblasts as primary murine cells.

First, all cells were screened for their endogenous levels of ACE2 mRNA (Figure 9). Endogenous levels in pulmonary cells were either not detectable as in the case of lung fibroblasts or at detection limit in the case of A549. All other cells showed moderate levels of ACE2 mRNA relative to the reference gene panel.

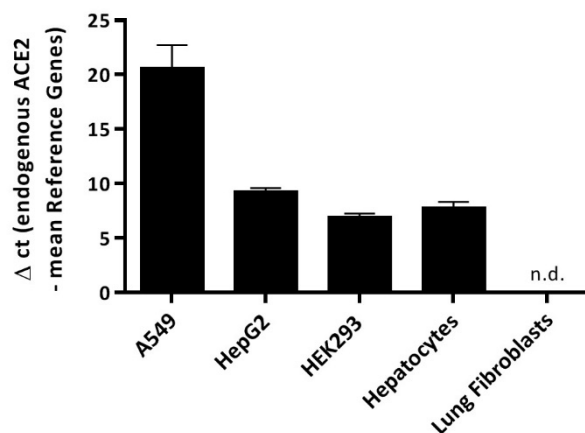


Figure 9: Levels of endogenous ACE2 mRNA

Endogenous ACE2 mRNA for all cells, normalized to a panel of reference genes for each cell type. n.d. not detectable.

Next, cells were transfected with ACE2 cmRNA or Luciferase cmRNA as control and analyzed 24 h after transfection (Figure 10). In order to analyze cellular uptake of cmRNA, total RNA was collected and 1 μ g was transcribed into first-strand cDNA. Relative expression of ACE2 cmRNA was analyzed by real-time PCR against a set of reference genes (Figure 10 a).

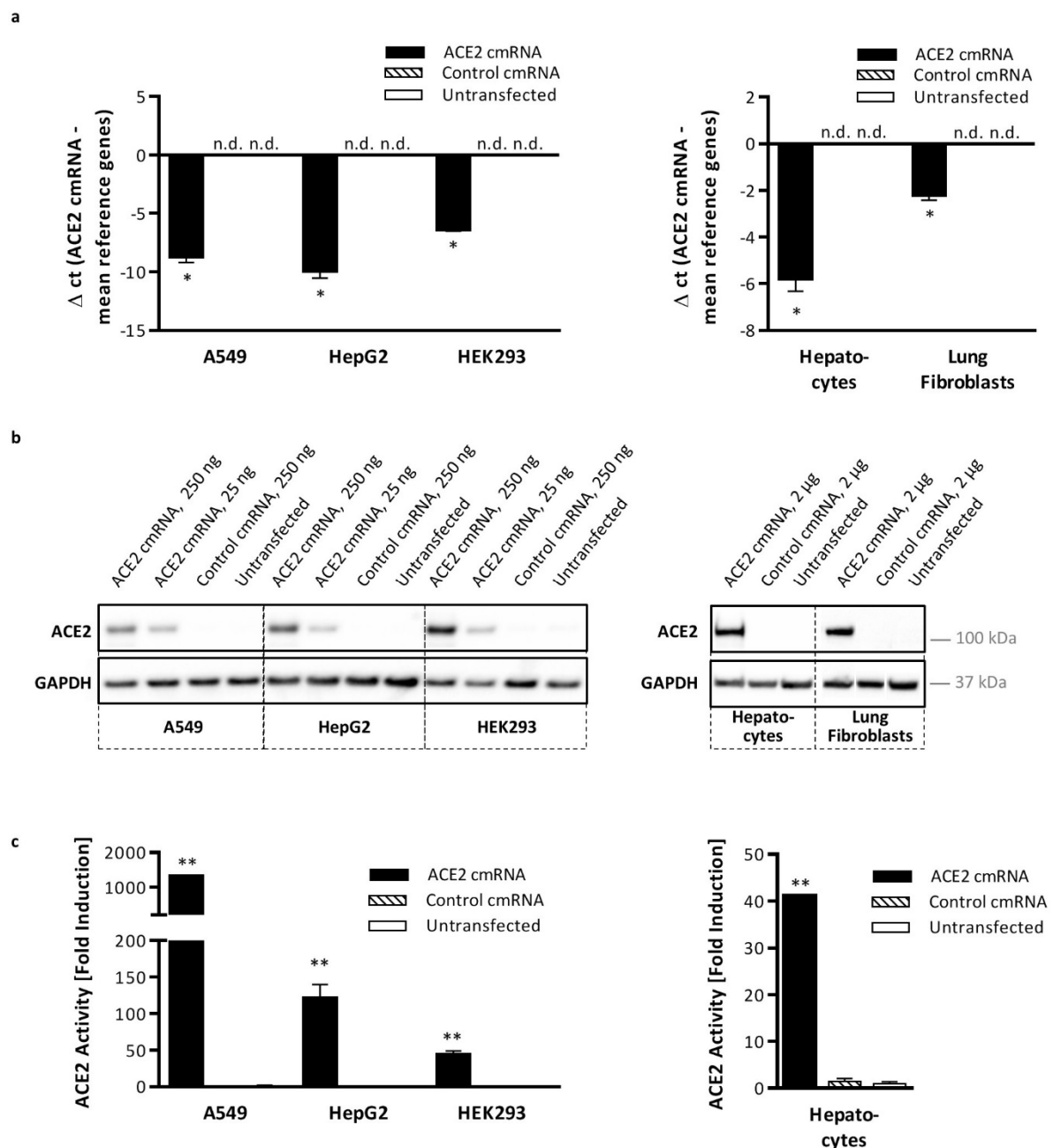


Figure 10: Detection of cmRNA and encoded protein 24 h after transfection in different cell types

(a) Relative expression of ACE2 cmRNA. (b) ACE2 protein expression with GAPDH as loading control. (c) ACE2 activity. * $p < 0.05$, ** $p < 0.01$

The difference in abundance (ct values) of ACE2 cmRNA to the mean abundance of reference genes is shown (Δ ct). Strongly negative Δ ct values indicate prominent ACE2 cmRNA abundance in samples compared to reference gene abundance. In all ACE2 cmRNA treated cells, cmRNA was successfully taken up, while no ACE2 cmRNA could be detected in control cmRNA or untransfected samples.

In a next step, it was verified whether ACE2 cmRNA was successfully translated into ACE2 protein (Figure 10 b). For this purpose, A549, HepG2 and HEK293 were seeded in 24-well plates and transfected with 250 or 25 ng of ACE2 cmRNA, while primary cells were seeded in 6-well plates and transfected with 2 µg of ACE2 cmRNA. Cells were lysed after 24 h and total protein concentration was determined by bicinchoninic assay (BCA). 5-10 µg of total protein was loaded on by SDS-PAGE and probed for ACE2 and glyceraldehyde 3-phosphate dehydrogenase (GAPDH) as a loading control. The three human cell lines showed clear dose dependent expression levels for ACE2 protein. Likewise, transfection of primary liver and lung cells with ACE2 cmRNA led to clearly detectable ACE2 protein levels. Weak ACE2 signals in control or untransfected samples especially in HEK293 may be explained by detection of endogenous ACE2 by the antibody used as the antibody does not discriminate between cmRNA derived and endogenous ACE2 protein.

Finally, it was determined if the ACE2 protein detected by Western Blot shows enzymatic activity. ACE2 activity assay was performed with 30 µg of total protein (Figure 10 c). ACE2 activity is shown as fold induction to ACE2 activity measured in untransfected samples. All ACE2 cmRNA transfected samples showed a significant signal induction in ACE2 activity with p-values < 0.01. As for Western Blotting, the ACE2 activity assay cannot differentiate between ACE2 activity derived from endogenous or cmRNA derived protein, hence ACE2 activity in the different cell lines shall not be compared side by side.

These findings demonstrate, that ACE2 cmRNA transfection leads to translation of an enzymatically active protein in human and murine liver and lung cells.

3.1.2 ACE2 Posttranslational Modifications

ACE2 is a type I integral membrane protein with the core domain located at the extracellular surface. For correct integration into the membrane, these proteins have to undergo posttranslational modifications. This process and its results were analyzed in a next set of experiments.

Glycans are pivotal for proper folding, assembly and trafficking of membrane proteins. In order to verify N-linked glycosylation of ACE2 protein, a transfection experiment was set up with A549 cells, in which half of the samples were treated with Tunicamycin prior transfection (Figure 11 a). Tunicamycin prevents glycosylation of asparagine residues by inhibition of N-Acetylglucosamine transferase, hence protein size will be reduced due to reduced number of

glycans bound to the protein⁷⁷. Cells were seeded in 6-well plates and transfected with 2 µg ACE2 cmRNA of luciferase cmRNA as control and lysed 24 h after transfection. Part of the cell lysate of the ACE2 cmRNA transfected sample which was not treated with Tunicamycin was subjected to enzymatic deglycosylation. 10 µg of total protein was used for Western Blotting. ACE2 cmRNA transfected samples without Tunicamycin pretreatment, showed an ACE2 protein with a size of 120 kDa, which corresponds to the mature, fully glycosylated form of the protein⁷⁸. Upon treatment with Tunicamycin or retrospective deglycosylation, the size of ACE2 protein was markedly decreased. These findings indicate glycosylation of ACE2 cmRNA derived protein. In addition, ACE2 forms 3 disulfide bridges during posttranslational maturation⁷⁹, which was shown by processing of ACE2 transfected cell lysate under reducing and non reducing conditions on SDS PAGE. Reducing conditions led to unfolding of protein, resulting in reduced migration capacity of the protein, hence the ACE2 protein band was detected at a higher level than under non reducing conditions (Figure 11 a).

Correct protein integration and expression on the cell surface was verified by fluorescence activated cell sorting. All three human cell lines were transfected with ACE2 cmRNA and 24 h later a surface staining for ACE2 protein was performed (Figure 11 b and c). If ACE2 is correctly integrated into the plasma membrane, the core domain faces towards the extracellular space and will be recognized by the antibody. The experiment was repeated three times for each cell line (Figure 11 b) and showed that ACE2 cmRNA transfection leads to a significant induction in fluorescent intensity in these samples compared to control transfected and untransfected samples. Figure 11 c shows respective representative histograms for each cell line, where increased ACE2 expression in ACE2 transfected cells leads to a shift to the right of the curve for these samples. As the primary antibody used in this experiment is not able to discriminate between endogenous and cmRNA derived protein, a direct side by side comparison of the expression levels in the different cell lines is not appropriate.

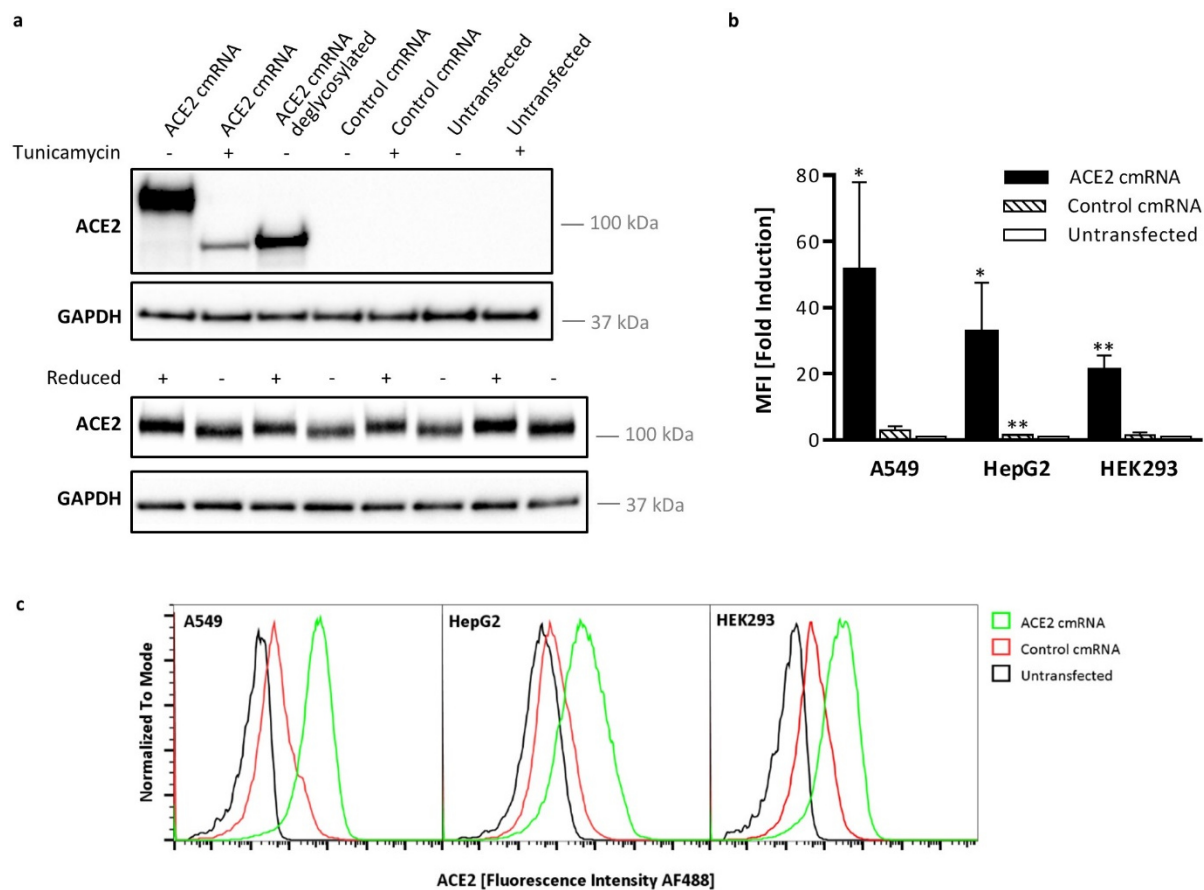


Figure 11: Posttranslational processing of ACE2 protein

(a) Upper panel: glycosylation of ACE2 protein in presence/absence of Tunicamycin. Lower panel: breaking of disulfide bonds under reducing conditions. The same sample was applied repeatedly. (b) Flow cytometry analysis of ACE2 expression on the cell surface. * $p < 0.05$, ** $p < 0.01$. (c) Representative histograms of flow cytometry experiment for each cell line.

To localize cmRNA derived protein, A549 and HepG2 were transfected with ACE2 cmRNA and stained 24 h after transfection. By additional staining of the plasma membrane with a membrane marker (wheat germ agglutinin) it can be visually verified that the protein is located at the plasma membrane indicating integration into the membrane (Figure 12). In both cell lines, samples transfected with ACE2 cmRNA stained positive for ACE2 protein, while transfection with control cmRNA (luciferase) showed weak background signal in HepG2, which may be due to staining of endogenous levels of ACE2 protein in these cells. The immunocytochemical images revealed ACE2 protein localization throughout the cytoplasm and on the plasma membrane. The accumulations found throughout the cytoplasm showed a dotted pattern, indicating for protein enrichment in vesicular structures probably involved in protein maturation or trafficking to the plasma membrane. Presence of ACE2 protein at the plasma

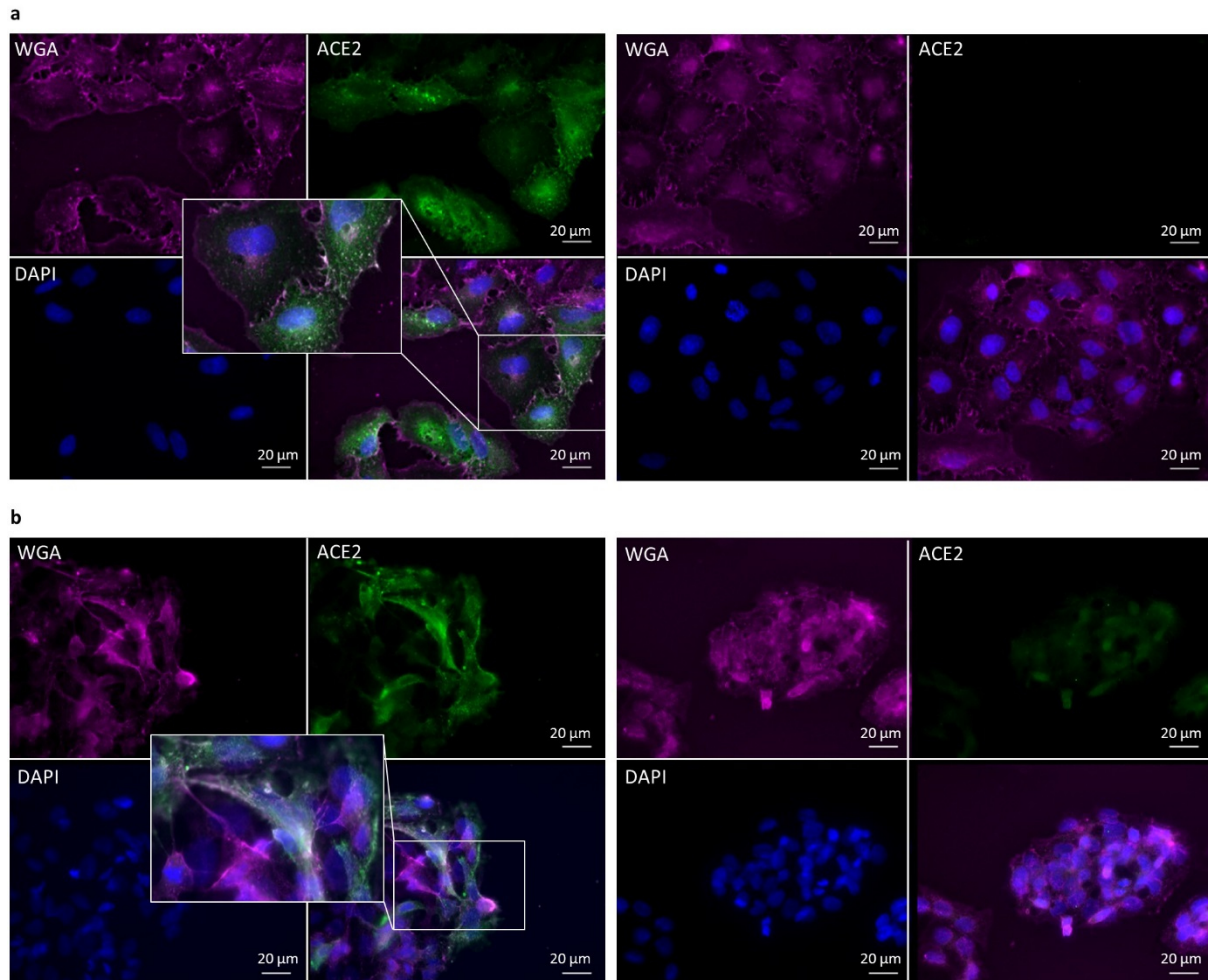


Figure 12: Immunofluorescent staining for ACE2

Left panels – ACE2 cmRNA transfected, Right panels – control cmRNA transfected green: A549, blue: nucleus, violet: cell membrane, white: green and violet overlay (a) A549. (b) HepG2.

membrane was apparent by co-localization of ACE2 protein with wheat germ agglutinin which is shown in white color in the overlay images.

Taken together, it was shown that ACE2 cmRNA derived ACE2 protein undergoes biological post-translational modifications leading to correct protein integration into the plasma membrane.

3.1.3 Optimization of ACE2 cmRNA for *in vivo* Application

After having successfully verified that the sequence of ACE2 cmRNA leads to the translation of an active membrane bound form of ACE2 protein, a separate comprehensive evaluation was set up to further optimize the cmRNA sequence for strong protein translation. This evaluation was done in form of a master thesis project by Huber M⁷⁴. The major findings are summarized in the following.

For sequence optimization, eight different ACE2 cmRNA sequences were designed. They shared the same open reading frame (ORF) encoding ACE2, a C1-m7G cap and a poly(A) tail of approximately 120 nucleotides which was found to be the optimal length⁶⁵. In addition to the natural ACE2 untranslated region (UTR) mRNA sequence, three different modifications of the UTR being known for high level of protein translation^{75,80,81} were introduced, namely minimal 5' UTR, human alpha globin (hαG) 5' UTR and cytochrome b-245 alpha (CYBA) 5' with 3' UTR. For all four sequences, one natural and one codon optimized version of the ORF were designed.

For the cmRNA sequence evaluation, A549 and HepG2 cells were transfected and lysed after 5 different time points for cmRNA and protein kinetics evaluation. ACE2 protein expression analyzed by Western Blot showed ACE2 translation in both cell lines upon transfection with

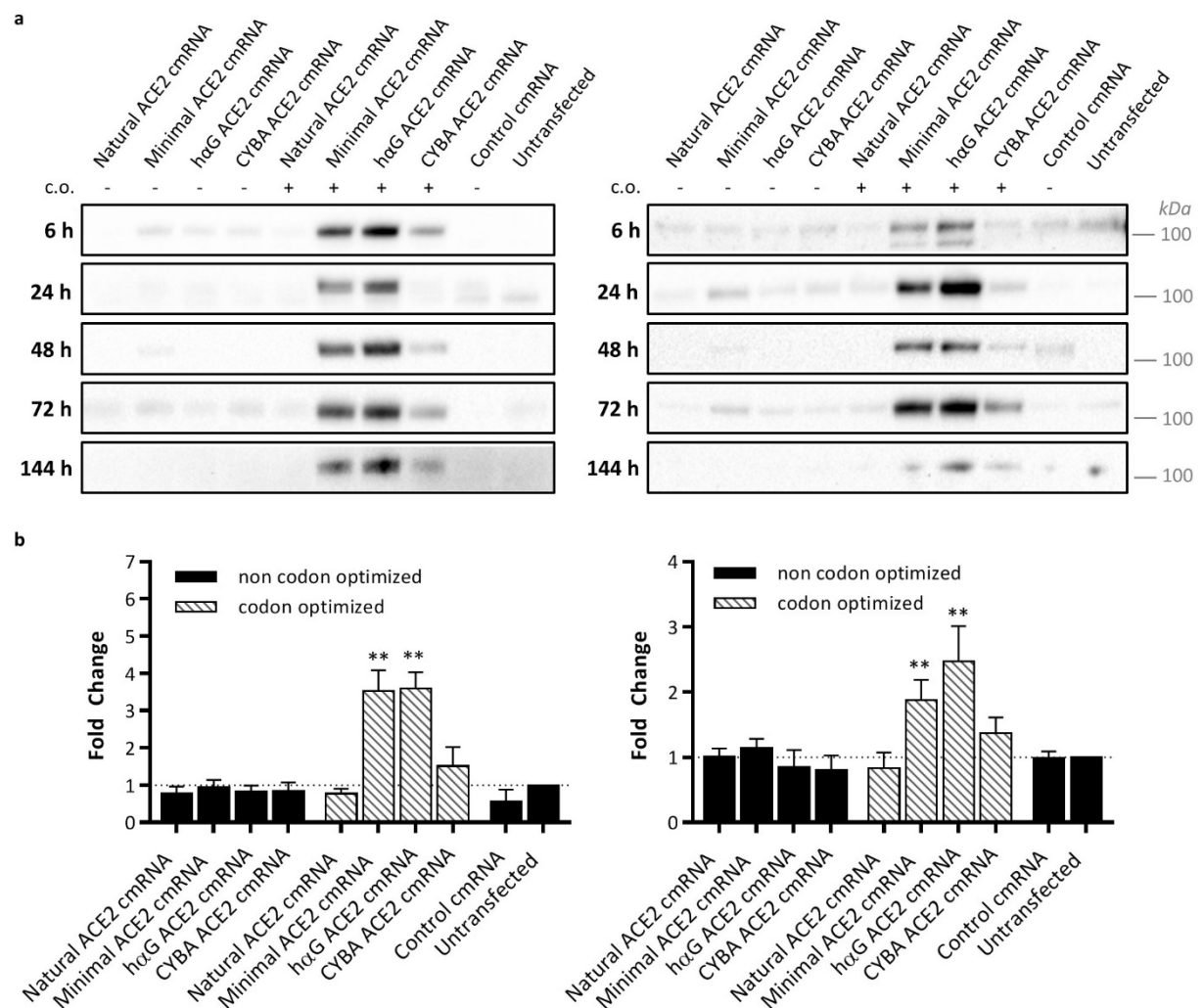


Figure 13: Screening of ACE2 cmRNA sequences

(a) Western Blot for samples taken after 6 h, 24 h, 48 h, 72 h and 144 h. (b) ACE2 Activity assay 24 h after transfection. c.o. codon optimized

codon optimized ACE2 cmRNA sequences for up to 144 h (Figure 13 a, A549 left panel, HepG2 right panel). Strongest protein translation was observed for codon optimized hαG cmRNA followed by codon optimized minimal cmRNA. Data obtained by Western Blot were confirmed by an ACE2 activity assay (Figure 13 b; A549 left panel, HepG2 right panel). In both cell lines, ACE2 enzymatic activity was significantly increased for samples transfected with codon optimized hαG cmRNA and codon optimized minimal cmRNA relative to untransfected samples.

Based on these results, codon optimized minimal and codon optimized hαG cmRNA were identified as the best performing sequences with regards to cmRNA stability, protein translation and kinetics. As the codon optimized hαG cmRNA sequence showed a slightly longer half-life (approximately 13 h in A549 and 9 h in HepG2) than the minimal sequence, it was used in all subsequent *in vivo* studies.

3.2 Proof of Concept for ACE2 Transcript Therapy in the Liver

Dysregulation of the local RAS system is significantly contributing to inflammation and fibrosis in liver fibrosis^{82,83}, and counterbalancing this process has been shown to have promising therapeutic effects^{4,6,8,55,56}. In order to establish ACE2 cmRNA delivery in the liver, a set of experiments was planned. First, a carrier formulation was selected which was selectively targeting liver tissue, leading to substantial local protein translation without causing intolerable toxicity. These requirements were best verified by *in vivo* application of a formulation holding luciferase cmRNA. Upon successful transfection, organ targeting can easily be verified by whole animal imaging and by *ex vivo* luciferase activity. In a next step, the experiment was repeated with ACE2 cmRNA instead of luciferase cmRNA and ACE2 protein translation was validated. Finally, the ACE2 cmRNA formulation was tested in a disease model of liver fibrosis and tolerability, protein expression and therapeutic effects were evaluated.

3.2.1 Liver Targeted cmRNA Delivery

For the purpose of liver targeted cmRNA delivery, lipoplexes (LLF (liver lipidoid formulation) in the following) as described by Jarzebinska et al. were used¹⁴. These lipoplexes consist of a cationic lipid, two helper lipids and a polyethylene glycol (PEG) lipid for shielding. In a first study, firefly luciferase cmRNA was formulated in LLF. This formulation was intravenously (i.v.) applied in female Balb/c mice at 1 mg/kg while the sham group was treated with phosphate-buffered saline (PBS). All animals were sacrificed 6 h after application. Immediately after death, D-luciferin was injected intraperitoneally and IVIS images were taken. All animals showed strong and selective cmRNA uptake in the liver (Figure 14 a). Afterwards, liver, lung and spleen of each animal were dissected and reimaged in the IVIS. A clear signal was detected in the liver, but not in the other organs (Figure 14 a). Organs were then homogenized and luciferase activity was measured (Figure 14 b). The results confirmed the IVIS data as there was significant luciferase activity in liver homogenates compared to spleen and lung.

Parts of the dissected livers were embedded in paraffin and stained for luciferase protein with anti-luciferase antibody. Figure 14 c shows the typical structure of a liver lobule. In the case of intravenous injection, lipoplexes enter the liver via the interlobular artery and then diffuse to the central vein. Looking at the venous blood flow through the liver, an oxygenation and nutrient gradient with strong enrichment close to the afferent vessels and low enrichment close to the efferent vessels is typical (Figure 14 d). The stainings for luciferase protein showed

a very similar protein distribution, mirroring the blood flow through the organ. Strong protein enrichment was observed close to the portal region, where afferent vessels enter the liver, with a gradual decrease towards the efferent central vein (Figure 14 e). In the sham treated animals, no luciferase protein could be detected.

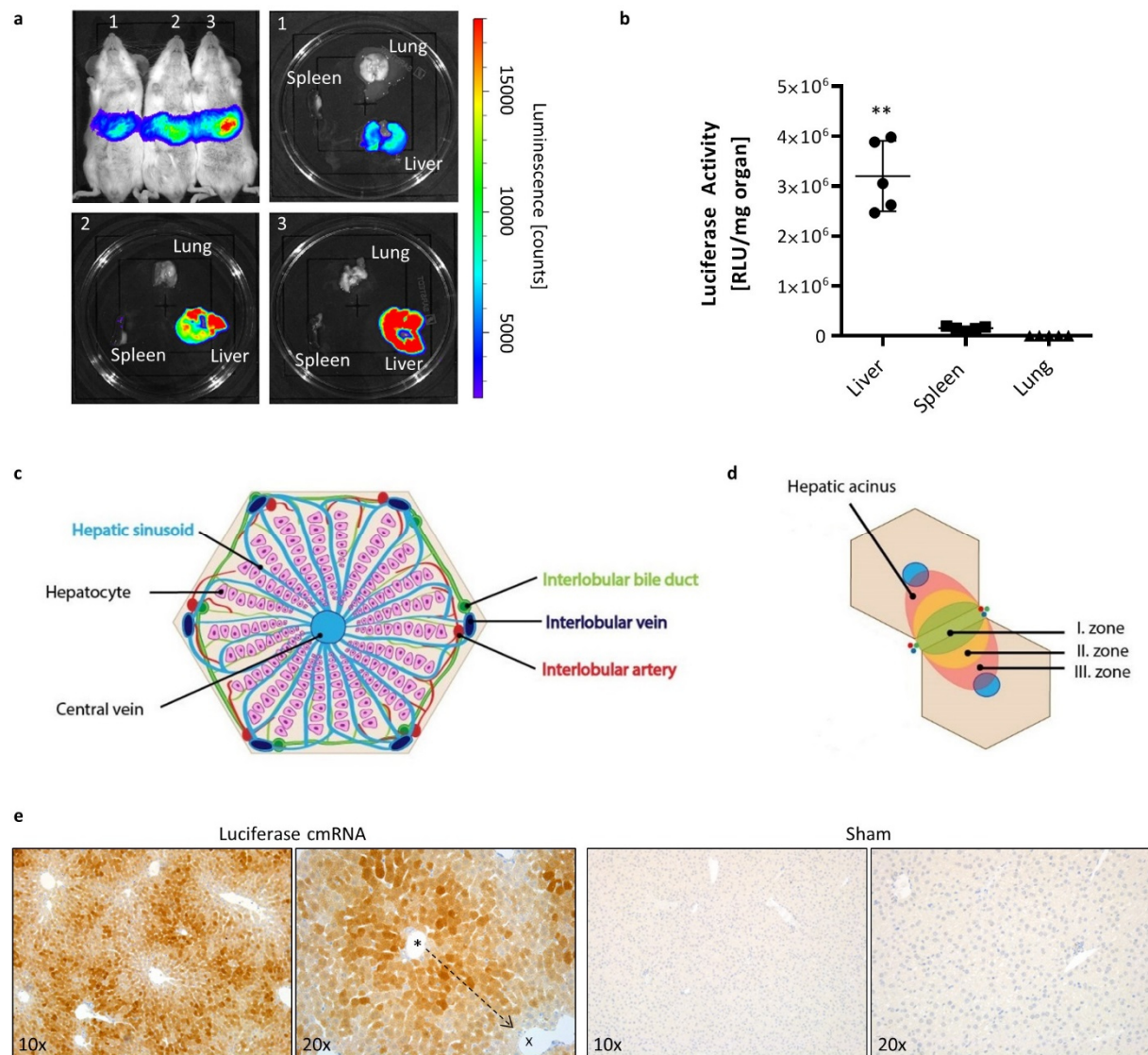


Figure 14: Liver targeted delivery of firefly luciferase cmRNA

i.v. administration of 1 mg/kg luciferase cmRNA in LLF, 6 h post treatment

(a) Firefly luciferase activity detected by IVIS imaging. (b) Luciferase activity in organ homogenates. RLU relative light units**p<0.01 (c) Architecture of liver lobule¹²⁷. (d) Oxygenation and nutrient zones in the liver lobule¹²⁷. (e) Luciferase stainings for cmRNA and Sham treated animals.

3.2.2 Liver Targeted ACE2 cmRNA Delivery

After having successfully verified targeted and selective enrichment of LLF complexed cmRNA and protein translation in the liver using reporter cmRNA, delivery of ACE2 cmRNA in LLF was evaluated. Two doses of ACE2 cmRNA (4 and 2 mg/kg) and a single dose (2 mg/kg) of control cmRNA in LLF was formulated and intravenously injected in female Balb/c mice, while sham treated animals received PBS. Animals were sacrificed 6 h after treatment and organs were taken.

First, the amount of ACE2 cmRNA taken up by the liver was analyzed by real-time PCR (Figure 15 a). For this purpose, total RNA of liver tissue was extracted and transcribed into first-strand cDNA. Absolute values of ACE2 cmRNA in the liver were measured by real time PCR using an ACE2 cmRNA dilution series. PCR analysis showed a clear dose-dependent uptake of 0.032 ± 0.007 ng ACE2 cmRNA/ μ g total RNA for a dose of 4 mg/kg and 0.016 ± 0.002 ACE2 cmRNA/ μ g total RNA for a dose of 2 mg/kg. There was no ACE2 cmRNA detected in the control group. Second, part of the liver was embedded in paraffin and *in situ* hybridization was performed to see where the cmRNA is deposited. ACE2 cmRNA was visualized in black and endogenous ACE2 mRNA in pink color. ACE2 treated animals showed clear cmRNA uptake by hepatocytes next to diffuse detection of cmRNA in liver sinusoids throughout the organ (Figure 15 b). Sham treated animals showed only endogenous levels of ACE2 mRNA. Part of the liver was homogenized and analyzed by Western Blot (Figure 15 c). GAPDH was used as a loading control while cell lysate of ACE2 cmRNA transfected hepatocytes was used as a positive control. ACE2 cmRNA was successfully translated as shown by a clear increase of ACE2 protein abundance in the ACE2 treatment groups. Control cmRNA treated animals showed background levels of ACE2 protein. Successful glycosylation of ACE2 protein was verified by retrospective enzymatic deglycosylation. In order to confirm full protein functionality, part of the liver was used to perform an ACE2 activity assay (Figure 15 d). Control cmRNA treated animals showed endogenous levels of ACE2 activity while significant increase in ACE2 activity of ACE2 cmRNA treated groups was detected.

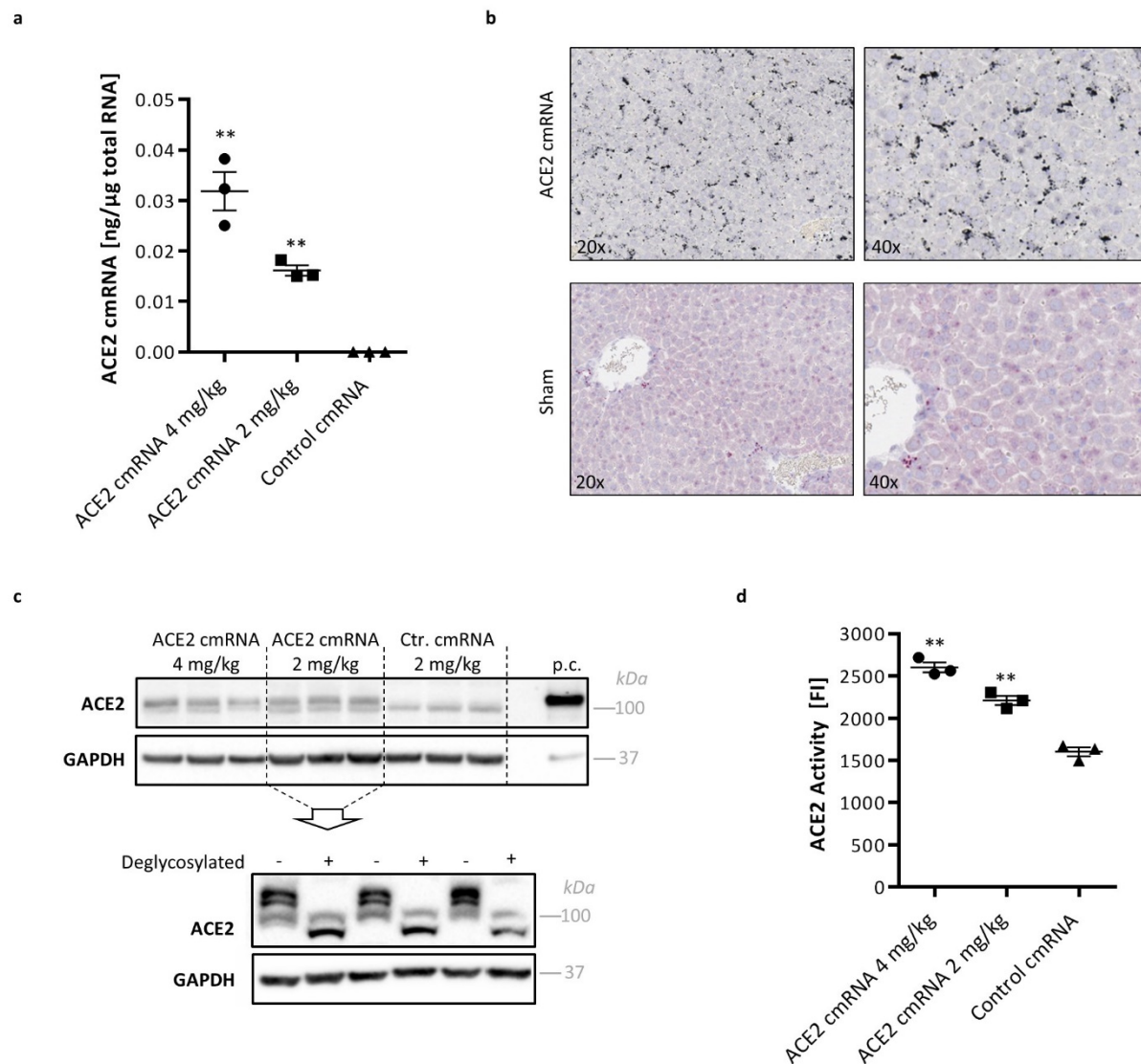


Figure 15: Liver targeted delivery of ACE2 cmRNA

i.v. administration of 4 and 2 mg/kg ACE2 cmRNA in LLF, 6 h post treatment

(a) Absolute quantification of ACE2 cmRNA. (b) *In situ* hybridization of liver tissue; black: ACE2 cmRNA, red: endogenous ACE2. (c) Upper panel: ACE2 protein abundance. Lower panel: glycosylation of ACE2 cmRNA derived protein. (d) ACE2 activity. FI Fluorescence intensity ** $p < 0.01$

Overall, *in vivo* studies using reporter cmRNA have confirmed that LLF is a suitable delivery agent for selectively targeting cmRNA to the liver. Subsequent formulation of ACE2 cmRNA in LLF led to a homogenous ACE2 cmRNA in the liver leading to a significant increase of ACE2 protein translation and activity in the liver.

3.2.3 ACE2 cmRNA Application in a Model of Non Alcoholic Steatohepatitis

Based on the results of cmRNA application in healthy mice, a study for therapeutic application of cmRNA in a NASH model was designed. For the investigations, a two-hit model was selected, established and provided by Stelic Inc. (STAM™). The selected model uses one chemical and one diet based challenge for disease establishment in male C57/Bl6 mice (Figure 16). The first challenge is given after birth by a subcutaneous injection of 200 µg Streptozotocin leading to harm of β -cells in the pancreas with subsequent induction of mild diabetes⁸⁴. The second challenge starts in week 4 by continuous feeding of high fat diet leading to obesity, impaired glucose tolerance, dyslipidemia, increased expression of regulators of lipogenesis and expression of proinflammatory cytokines⁸⁵.

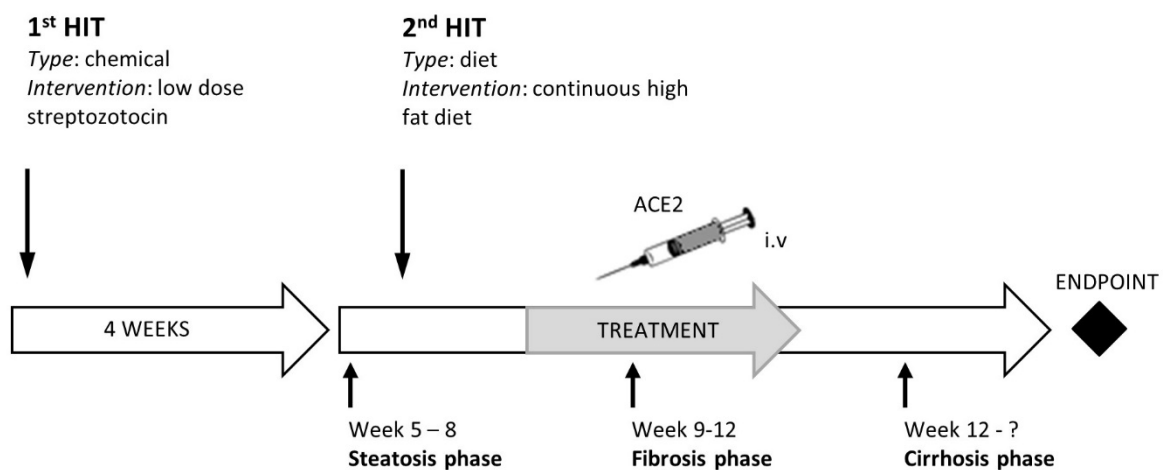


Figure 16: Establishment of STAM model and study outline

In the liver, export of triglycerides to the periphery is hampered, leading to significant lipid accumulation in the organ which results in increased liver weights in the animals while total body weight is decreased⁸⁶. This leads to an increased liver to body weight ratio in diseased animals. The associated liver damage is usually associated with increase liver parameters. The effects of the high fat diet is also apparent in serum parameters such as glucose and cholesterol, resembling the situation in humans, where these parameters are increased in patients suffering from metabolic syndrome⁸⁷.

Between week 5 and 6, steatosis onset can be observed which progresses to fibrosis between week 9 and 12 and at later stages to cirrhosis and finally hepatocellular carcinoma. Patients usually present in the late steatosis or early fibrosis phase. In the animal model on hand, this correlates to a time window between week 6 and 9 after the initial first hit. Therefore, the

treatment was started at the beginning of week 6 and was followed for a time frame of 3 weeks. Mice were randomly allocated to the following groups:

Table 15: Group allocation for NASH model

Group Number	STAM established?	Treatment	Group size (start)	Group size (end)
1	Yes	ACE2 cmRNA - 2x/week	8	5
2	Yes	ACE2 cmRNA - 1x/week	8	8
3	Yes	Sham (2 % sucrose) - 2x/week	8	7
4	No	None	8	8

In an additional pre-experiment for dose determination in Balb/c mice (data not shown), substantial ACE2 protein expression was seen down to a cmRNA dose of 0.25 mg/kg. Therefore, and for the purpose of keeping toxicity at a minimum, the dose for this study was set at 0.25 mg/kg/treatment formulated in LLF. The sham group received 2 % sucrose per treatment. The treatment was repeated iteratively every 3 or 4 days for group 1 and group 3, while group 2 was treated every 7 days. Group 4 was used as healthy control group, hence neither disease was established nor any treatment was applied. The treatment regimen was followed for 3 consecutive weeks, with final treatment at the beginning of week 4. In total, seven administrations were given to group 1 and 3 and four administrations to group 2. Animals were sacrificed 24 h after final treatment and body and liver weights were recorded. In addition, part of the liver was embedded in paraffin for histological examination, while the remaining part and blood serum were frozen and stored at -80 °C for later analysis.

Figure 17 a summarizes body and liver weight data at the end of the study. Body weight was not changed due to ACE2 treatment, while liver weight was significantly increased in both ACE2 treatment groups. The resulting liver to body weight ratio did not show any changes due to ACE2 treatment. Metabolic parameters such as glucose and cholesterol were not improved after ACE2 treatment. In group 2, glucose levels were increased compared to group 1 and group 3. The status of liver injury was evaluated by a panel of liver parameters (Figure 17 b). Lactate dehydrogenase (LDH) is an enzyme which is released into blood stream only upon tissue damage. As LDH is widely distributed in the body, it is a rather generic parameter used for identification of acute or chronic tissue damage.⁸⁸ Treatment with ACE2 cmRNA led to significant increase of this enzyme. In order to identify the organ being the cause of increased LDH levels, additional parameters need to be considered. In the case of liver injury, alanine

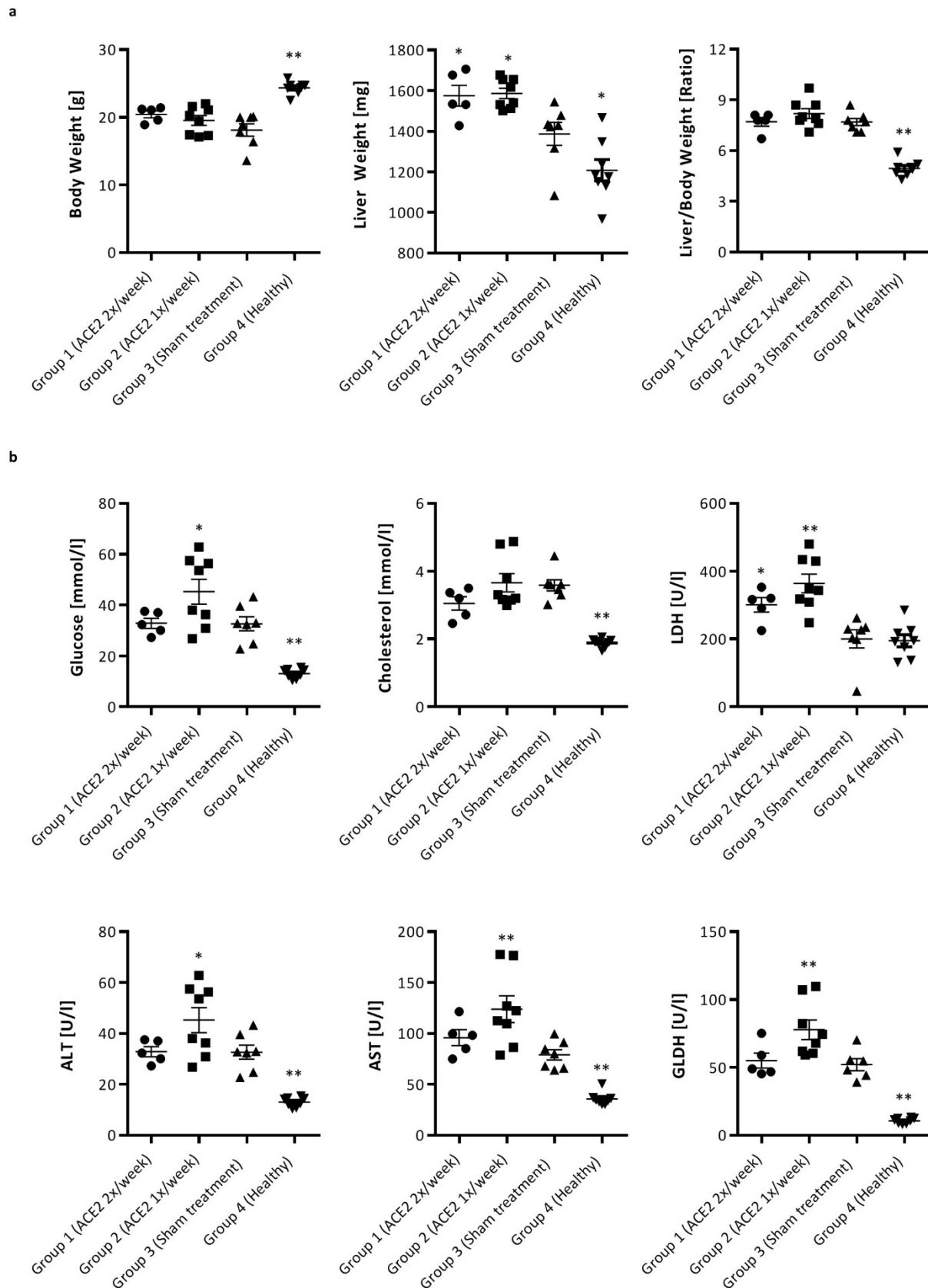


Figure 17: Weight and serum parameters after ACE2 cmRNA treatment

i.v. administration of 0.25 mg/kg ACE2 cmRNA in LLF, 24 h post treatment

(a) Body, liver weight and liver to body weight ratio at the end of treatment period. (b) Serum parameters at the end of treatment. For all statistical calculations, group 3 was used as reference group; *p<0.05, **p<0.01

For qualitative evaluation of fibrosis, sirius red and hematoxylin stainings of liver tissue slides were prepared. Sirius red is frequently used for staining of hepatic collagen as it binds to most hepatic collagens with collagen type I and III being the major components. These binding properties correlate well with the readout of the hydroxyproline assay⁹², hence the combination of these two techniques allows a comprehensive evaluation of fibrosis stage. Figure 19 shows one representative sirius red image of each group. Animals of group 1, 2 and 3 showed mild to moderate hepatic fibrosis with collagen deposition around large vessels and between hepatocytic plates. Quantitative evaluation of the sirius red stainings showed a slight decrease in collagen due to treatment with ACE2 once per week and a significant decrease in the group treated twice per week.

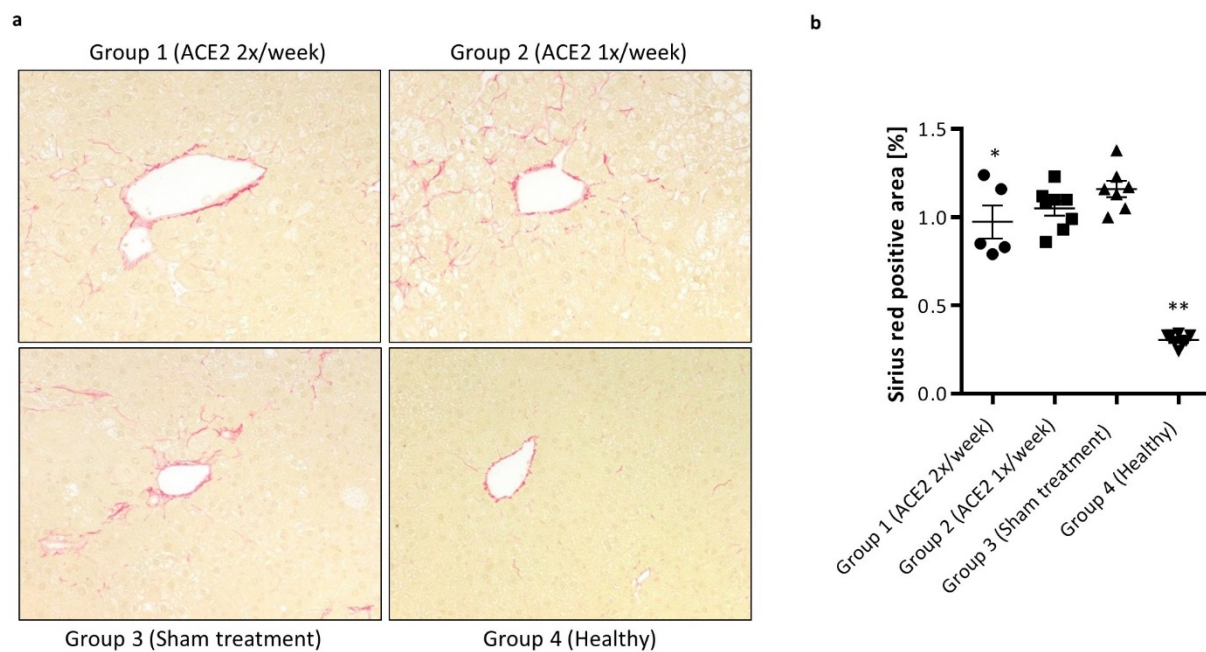


Figure 19: Effects of ACE2 cmRNA treatment on fibrosis

i.v. administration of 0.25 mg/kg ACE2 cmRNA in LLF, 24 h post treatment

(a) Representative sirius red images of each group. (b) Quantification of sirius red staining area

In order to evaluate disease progression, hematoxylin stainings were evaluated using a three step scoring system. The scoring system is summarized in Table 16 and consists of three individual scores (steatosis, inflammation and ballooning) which are added up to an overall score reflecting NAFLD status. Steatosis is an abnormal accumulation of lipid droplets in the cytoplasm of hepatocytes resulting from metabolic or toxic insults, among others. Ballooning reflects hepatocyte injury caused by alterations of the intermediate filament cytoskeleton. These cells appear to be swollen with a rarefied cytoplasm and a centrally located small, dark

nucleus. Finally inflammation is characterized by a mixed inflammatory cell infiltrate mostly found between lobuli⁹³.

Table 16: NAFLD scoring system⁹³

Item	Definition	Score
Steatosis	% of hepatocytes showing abnormal accumulation of fat droplets:	
	< 5 %	0
	5 % - 33 %	1
	> 33 % - 66 %	2
Lobular inflammation	> 66 %	3
	No foci	0
	< 2 foci per 200 x field	1
	2-4 foci per 200 x field	2
Ballooning	> 4 foci per 200 x field	3
	None	0
	Few balloon cells	1
	Many cells / prominent ballooning	2

All groups presented with an overall mild steatosis without any ACE2 treatment effect observable. For ballooning, no clear statement of the effect of ACE2 cmRNA treatment can be postulated as both ACE2 treatment groups showed mild to moderate ballooning in the majority of the animals compared to an overall mild ballooning in the vehicle group (Figure 20 a and Figure 20 c). Inflammation was present in predominantly moderate intensity in the sham treated group (Figure 20 a and d). For ACE2 treatment groups, there was a trend towards lower grade of inflammation observable with increasing ACE2 cmRNA dosing. Healthy untreated animals did not show steatosis, ballooning or inflammation. The unweighted sum of these individual scores are summarized in Figure 20 e. There was a trends towards decreased NAFLD level visible, however the effect did not reach significance value.

Overall, evaluation of liver collagen content and histologic examination of liver tissues lead to the conclusion that ACE2 cmRNA treatment could not halt or reverse disease progression. However, there is a trend observable that frequent ACE2 cmRNA administration of two applications per week leads to amelioration of inflammation and fibrosis as well as improvement of acute liver injury parameters.

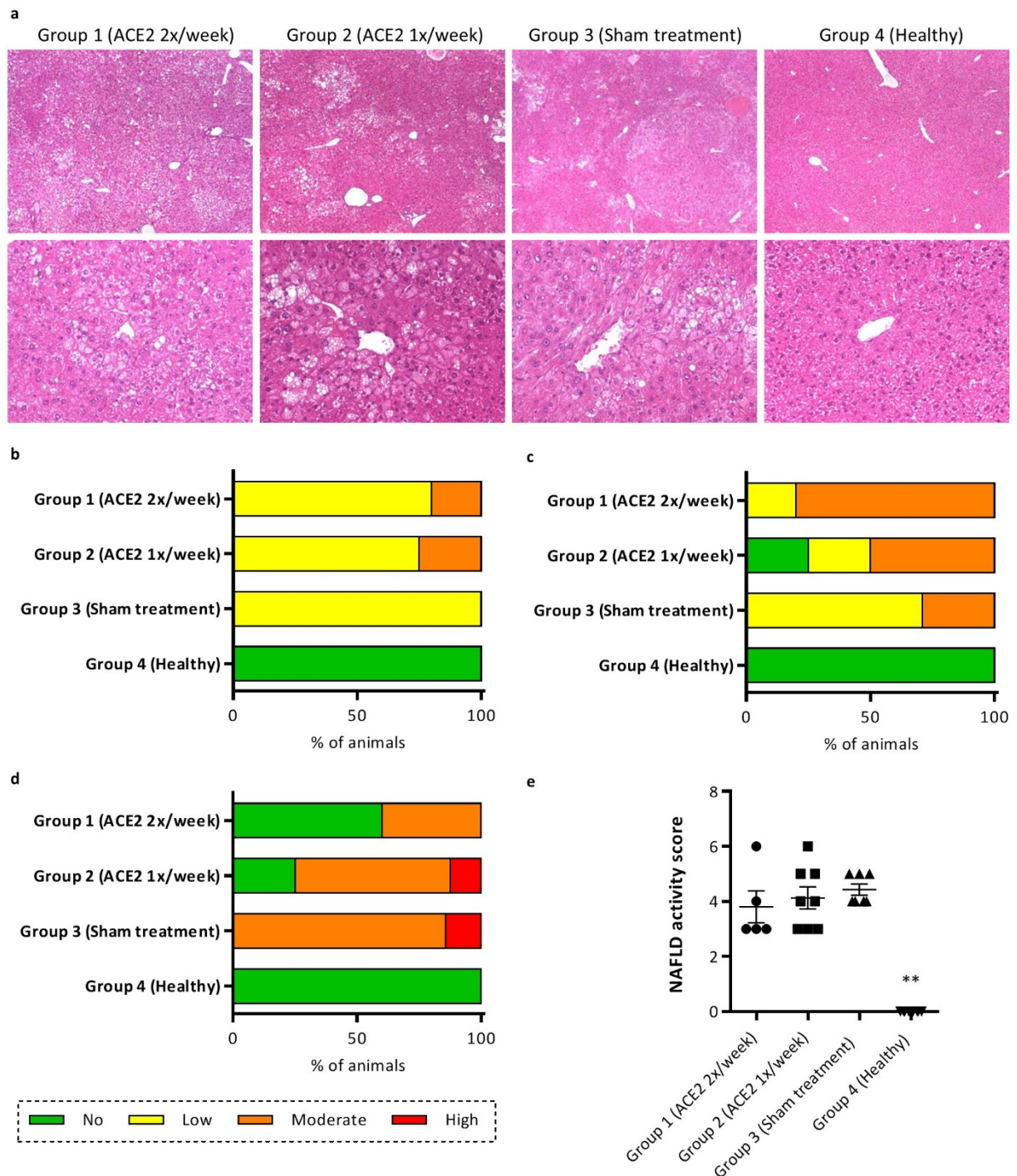


Figure 20: NAFLD scoring

i.v. administration of 0.25 mg/kg ACE2 cmRNA in LLF, 24 h post treatment

(a) Representative hematoxylin stainings for each group used for NAFLD scoring. Distribution of scores within each group: (b) Steatosis, (c) Ballooning and (d) Inflammation. (e) Overall NAFLD score per group.

3.3 Proof of Concept of ACE2 Transcript Therapy in the Lung

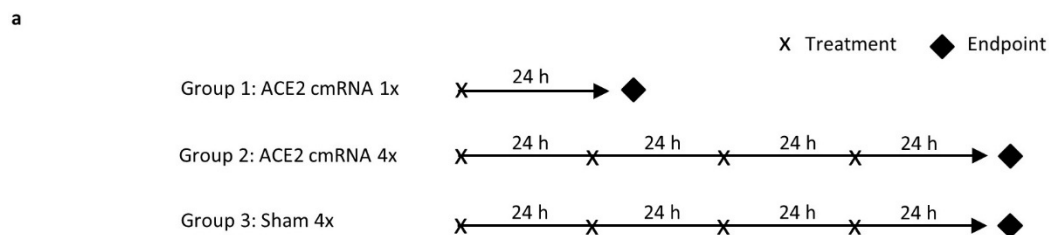
Similar to liver fibrosis, the local RAS system is dysbalanced in lung fibrosis. Contrary to liver fibrosis, local ACE2 expression is downregulated and reestablishment of pulmonary ACE2 expression showed therapeutic effects^{5,8,55,56}. In order to establish lung targeted ACE2 cmRNA delivery, a similar study outline as for liver targeted treatment was chosen. First, a carrier formulation for selective delivery into the lungs was identified by use of reporter cmRNA or a mix of reporter and target cmRNA. In a second step, reporter cmRNA was replaced by ACE2 cmRNA, in order to verify substantial translation of ACE2 upon cmRNA delivery with the delivery method established in step one. In a third step, the same formulation was applied in a disease model in order to evaluate therapeutic effects.

There are two main administration routes for drug delivery into the lung, namely pulmonary and systemic delivery. Due to the differences in the drug clearance mechanisms of each route and due to morphologic changes in diseased tissue, considerable differences between the two application routes with regards to drug bio-availability have to be considered. The most common techniques for pulmonary delivery of cmRNA are aerosol inhalation (nebulization) and intratracheal (i.t.) instillation. Systemic delivery is usually performed by intravenous (i.v.) or intraperitoneal (i.p.) injection.

3.3.1 Nebulization of cmRNA

Aerosol application offers a convenient and minimal invasive way of delivering small particles into the lung. It has been shown that protein expression can be induced upon delivery of pDNA or mRNA^{94,95}, however it had to be tested, if sufficient quantities of ACE2 protein can be expressed by this delivery route to rebalance the local RAS system. As aerosol application of branched polyethylenimine (brPEI) formulations is usually well tolerated by the mice, repeated dosing potentially leading to cmRNA accumulation and hence stronger protein translation was included in the experimental set up. For the experiment, 3 groups of six animals of female Balb/c mice were formed (Figure 21 a). Group 1 received a single aerosol application, group 2 received aerosol on 4 consecutive days and group 3 received sham treatment (nebulization of water) on 4 consecutive days. The aerosol consisting of 1.8 mg (90 %) ACE2 cmRNA and 0.2 mg (10 %) luciferase cmRNA formulated in brPEI was freshly prepared every day directly before application. 10 % luciferase cmRNA was included for the

purpose of additional proof of cmRNA delivery and for exclusion of cmRNA enrichment in other organs. For the treatment, all animals of one group were placed in a whole body nebulization chamber connected to a mesh nebulizer (Figure 21 b). The nebulizer was further connected to a pariboy compressor, which generated the pressure necessary for nebulization. For continuous airflow generation, the nebulization chamber was equipped with a fume extractor. Nebulization treatment lasted for approximately 15-20 min. The animals were sacrificed 24 h after the last treatment and lung, liver and spleen were excised and homogenized for luciferase assay and Western Blot.



b

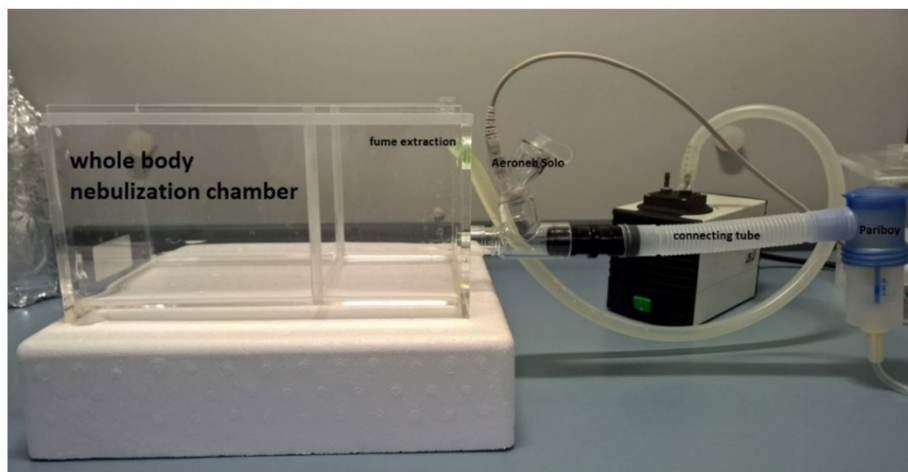


Figure 21: Study outline and nebulization apparatus

(a) Study outline. (b) Nebulization apparatus.

Luciferase activity was selectively measurable in the lung, while liver and spleen did not show any activity (Figure 22). Luciferase was detectable in animals treated once, though it was not of significant magnitude compared to sham treated animals. Repeated aerosol application however led to significant increased luciferase activity compared to single aerosol as well as sham treatment with $p < 0.01$ in both cases.

3.3.2 Intratracheal Application of cmRNA

Based on the weak protein expression achieved in the nebulization experiment, a new set of experiments was planned.

3.3.2.1 *Polymer versus Lipidoid Formulation of cmRNA*

The previous experiments showed that LLF based formulation led to strong protein translation in the liver upon i.v. delivery. However, its administration via the airways was not yet investigated. Pre-experiments have shown that nebulization is not suitable for delivery of lipid nanoparticles but that they need to be applied directly into the lung by use of an i.t. spray. The spray is introduced into the trachea and down the primary bronchi to the first bifurcation, a procedure which requires full anesthesia of the animal. The formulation is then delivered by manual force application producing an aerosol of the liquid formulation. The first i.t. experiment was designed as a side by side comparison between polymer and lipidoid based formulation to identify the best delivery agent. The evaluation was done with luciferase cmRNA in male Wistar rats, which were divided in two groups of 3 animals each. Based on the dosing regimen of the previous mouse experiments, the dose was set 10 times higher for rats. The animals were of 330 g at the start of the experiment, resulting in a dose of 0.45 mg/kg. The first group was treated with luciferase cmRNA formulated in brPEI and the second group received the same cmRNA formulated in LLF. The animals were sacrificed 6 h after application and lungs were collected.

Given the nature of the i.t. spray device, aerosol delivery in the lung is not as homogeneously distributed as in the case of nebulization. Final deposition of the aerosol heavily depends on the exact positioning of the device inside the trachea as well as the exact positioning of the animal. Therefore, considerable variations in the final distribution of the aerosol have to be expected. In order to avoid false results with regards to transfection efficiency and protein expression, lung samples of all lung lobes as well as the central respiratory system were taken for homogenization. Western Blot analysis of these homogenates revealed a clear band for luciferase protein delivered in lipidoid formulation with no band detectable for the polymer formulation (Figure 23 a). Vinculin served as a loading control and homogenized heart tissue was used as negative control, as the heart tissue will not be transfected by i.t. delivery. The luciferase activity assay performed with the lung homogenates confirmed these results. Figure 23 b shows the results per animal in the same order as on the Western Blot. There was no

signal detectable for the polymer based formulation and strong signal for the lipidoid based formulation.

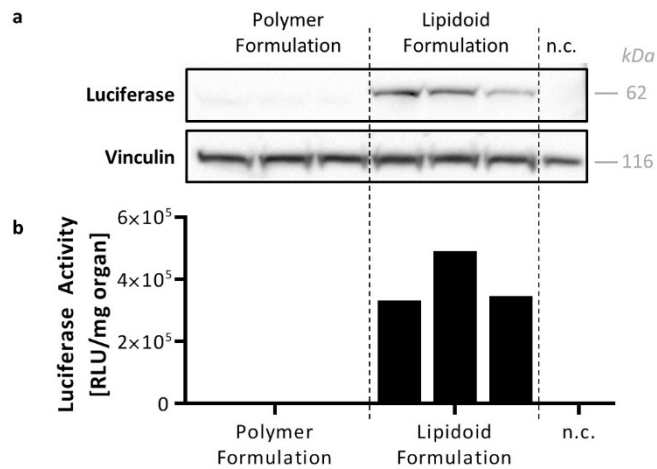


Figure 23: Luciferase translation post intratracheal cmRNA application

i.t. administration of 0.45 mg/kg ACE2 cmRNA in brPEI or LLF, 6 h post treatment

(a) Luciferase protein expression with Vinculin as loading control. (b) Luciferase activity of lung homogenates

The side by side comparison of these two formulations demonstrated that the lipidoid based formulation was superior in inducing protein translation upon i.t. spray application.

3.3.2.2 Intratracheal Delivery of ACE2 cmRNA in Lipidoid Formulation

Based on the results of the previous experiment, lipidoid based formulation was selected for i.t. ACE2 cmRNA delivery. Due to the strong protein signals achieved with 0.45 mg/kg cmRNA and due to increased toxicity of lipidoid based formulation compared to polymer based formulation observed in the previous experiment, dosing was reduced to 0.3 mg/kg in rats. Three groups of 5 animals each were formed with group 1 receiving ACE2 cmRNA, group 2 receiving control cmRNA and group 3 receiving sham treatment. The control cmRNA, all start codons of the ACE2 cmRNA sequence were scrambled to stop codons, leading to abortion of the protein translation process. Again, 10 % of luciferase cmRNA was included in each formulation. Sham treated animals received a single instillation of PBS. Animals were again sacrificed 6 h after treatment and lungs were excised. The left lung was fixed in formalin and embedded in paraffin while the right lung was frozen at -80 °C.

As described in the previous experiment, a mixture of lung tissue was homogenized and a luciferase activity assay performed (Figure 24 a). The results showed significant luciferase activity in cmRNA treated animals compared to sham treated animals, indicating successful

protein translation due to cmRNA transfection of pulmonary cells. In order to quantify ACE2 cmRNA delivered into the lung, total RNA was extracted from a mix of lung tissue and 1 μg of total RNA was used for cDNA production (Figure 24 b). Total ACE2 cmRNA was determined against an ACE2 cmRNA dilution series. ACE2 cmRNA treated animals showed significant uptake of ACE2 cmRNA in lung tissue. It has to be noted that the absolute values have to be interpreted with care as the i.t. application method and sampling lead to high variance in data. *In situ* hybridization and hematoxylin stainings were done in paraffin embedded lung tissues. *In situ* hybridization is a sensitive method to detect RNA, but does not allow conclusions about ACE2 protein expression. In the *in situ* hybridization, ACE2 treated animals showed high ACE2 cmRNA deposition close to central airways, while lung periphery showed only scattered ACE2 cmRNA staining (Figure 24 c, upper left panel). Strong signal enrichment was seen in cytoplasm rich cells located in alveolar walls, often being situated in alveolar angles, indicative for alveolar epithelial cells (AEC) type II (Figure 24 c, lower left panel) or macrophages.

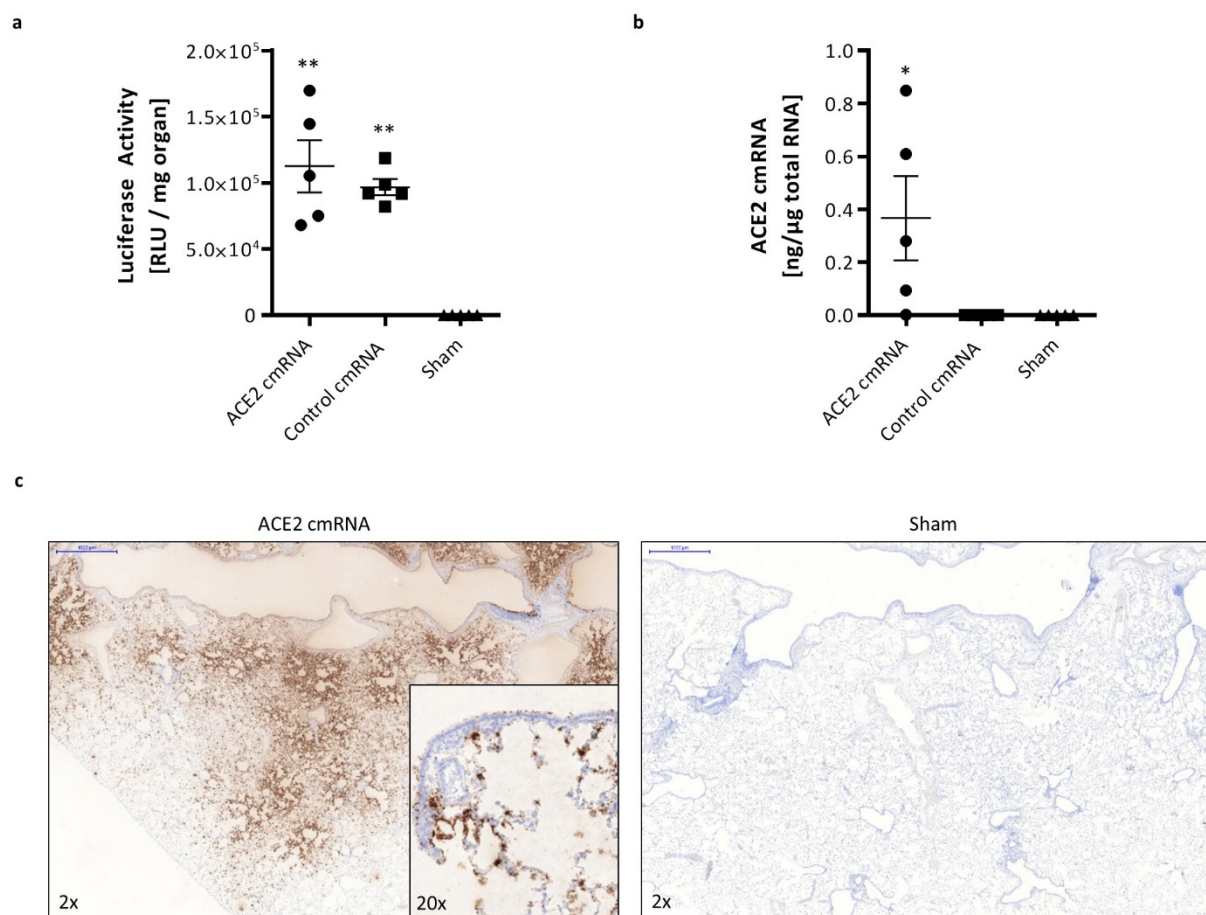


Figure 24: Reporter protein translation and ACE2 cmRNA abundance post i.t. application of ACE2 cmRNA

i.t. administration of 0.3 mg/kg ACE2 cmRNA in or LLF, 6 h post treatment

(a) Luciferase Activity. (b) Absolute quantification of ACE2 cmRNA. (c) *In situ* hybridization for a representative ACE2 cmRNA treated (left panel) and sham treated (right panel) animal.

Furthermore, there were numerous free small positively staining particles in bronchial airways, deposited on top of ciliated cells as well as in alveolar lumina. No positive signal was seen in the *in situ* hybridization of the PBS control group (Figure 24 c, right panel).

Lung homogenates of four animals per group were analyzed by Western Blot (Figure 25 a). GAPDH was used as loading control and recombinant human ACE2 protein as positive control. Control treated animals showed endogenous levels of ACE2 protein⁹⁶, while ACE2 treated animals showed increased levels of protein. Part of the lysate was then used for an ACE2 activity assay (Figure 25 b). As already observed in the Western Blot, ACE2 treated animals showed induced ACE2 activity while animals of the control group showed endogenous levels of ACE2. In the hematoxylin-eosin stained lung tissue of ACE2 treated animals, up to moderate, alveolar infiltration with neutrophils and mild fibrin extravasation was found. Both was accentuated to central regions of the lung (Figure 25 c).

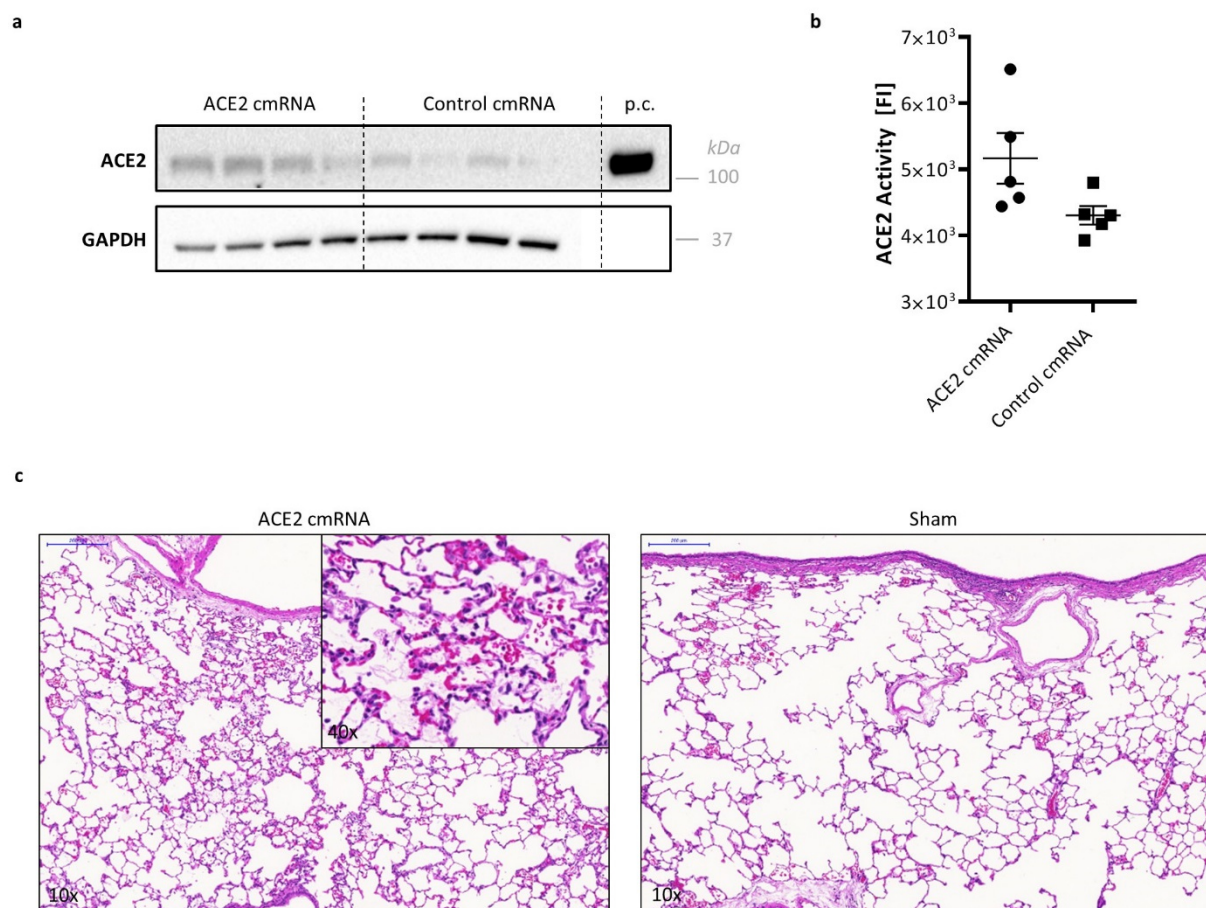


Figure 25: ACE2 protein translation post i.t. application and inflammatory reaction

i.t. administration of 0.3 mg/kg ACE2 cmRNA in or LLF, 6 h post treatment

(a) ACE2 Protein expression with GAPDH as a loading control. (b) ACE2 activity. * $p < 0.05$, ** $p < 0.01$. (c) Representative hematoxylin-eosin stainings.

These data lead to the conclusion that ACE2 cmRNA administered by i.t. spray application leads to moderately induced ACE2 protein expression. This protein induction is accompanied by an acute inflammatory reaction.

3.3.3 Intravenous Application of cmRNA

The previous experiments based on i.t. application showed an inflammatory reaction which raised doubts about its tolerability in diseased animals. In addition to that, protein expression was not more than moderately induced in i.t. treated healthy lungs and due to low ventilation in fibrotic lungs of IPF patients, even lower protein expression had to be expected. Therefore, i.v. application as the second delivery route to the lung was investigated.

3.3.3.1 Pulmonary Lipid Formulation of cmRNA

For the investigations, a lipoplex containing an Ethris in-house PEG co-polymer (called PLF (pulmonary lipid formulation) in the following) was identified in pre-experiments which showed strong and selective enrichment in the lungs. As for liver specific cmRNA delivery, targeted cmRNA delivery was first evaluated by use of reporter cmRNA. For this purpose, firefly luciferase cmRNA was formulated in a PLF and intravenously injected in mice at a dose of 1 mg/kg. 6 h after injection, animals were sacrificed and in vivo luciferase activity was determined. Two representative animals and their organs (lung, liver, heart, kidney, brain and spleen) are shown in Figure 26 a. Strong luciferase signal was detected selectively in lungs, whereas other organs did not show any signal.

Having identified PLF as a selective delivery agent for lung application, a mixture of 90 % ACE2 cmRNA or 90 % control cmRNA and 10 % luciferase cmRNA in PLF was prepared. This formulation was intravenously applied to Balb/c mice at a dose of 1 mg/kg while sham treated animals received a single injection of phosphate buffered saline. After 6 h, animals were sacrificed and lung, liver, spleen, heart and kidney were collected. Half of the lung was embedded in paraffin for histologic analysis. The organs were then homogenized and luciferase activity was determined for each organ (Figure 26 b). Pairwise comparison of the organs gave significantly stronger luciferase activity in lungs compared to other organs. Next, paraffin embedded lung tissue was stained for ACE2 protein (Figure 26 c, left panels). Due to the fact, that the antibody did not differentiate between murine (endogenous) and human ACE2 protein, cells containing endogenous and/or exogenous ACE2 stained with a brown

color. The lung tissue of sham treated animals showed patterns related to endogenous ACE2 expression⁹⁶. Additionally, ACE2 cmRNA treated animals showed positive staining of cells in the alveolar walls with strong membrane and moderate cytoplasmic staining. The morphology of these cells is indicative for both, AEC type I and for AEC type II. Furthermore, staining of macrophages is suspected. Overall, the application of cmRNA resulted in mild to moderate focally disseminated free alveolar erythrocytes (Figure 26 c, right panels). Sham treated animals did not show morphologic reactions to the treatment. Protein abundance in organ homogenates was determined by Western Blot with GAPDH as a loading control and recombinant human ACE2 protein as positive control. Sham and control treated animals showed endogenous ACE2 activity analogue to the immunohistochemical stainings, while ACE2 treated animals showed clearly induced bands for ACE2 (Figure 26 d).

Taken together, this experiment proved that intravenous administration of ACE2 cmRNA in the respective lipid formulation selectively targeted to the lung and is able to induce ACE2 protein translation.

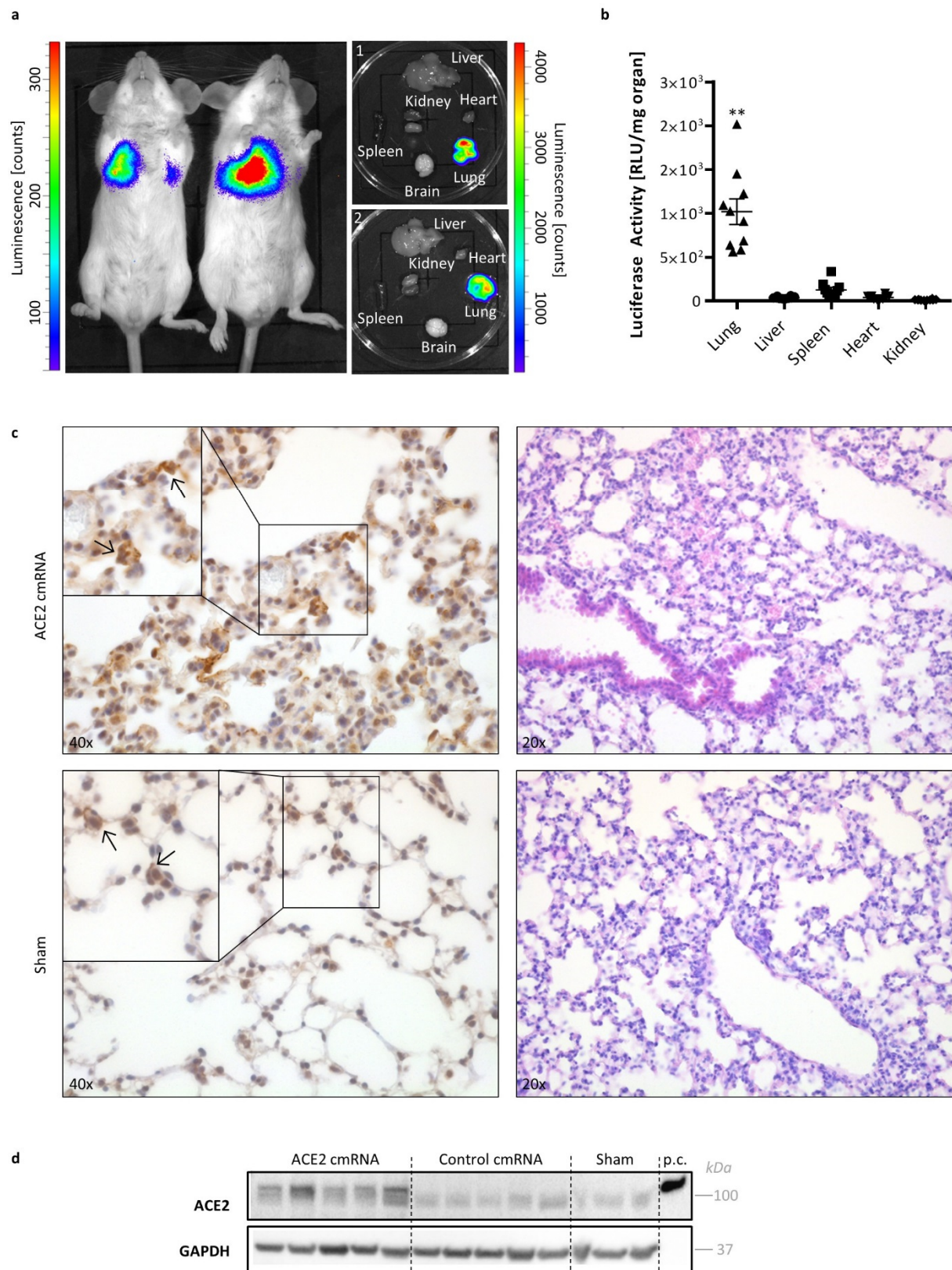


Figure 26: Intravenous application of ACE2 cmRNA

i.v. administration of 1 mg/kg ACE2 cmRNA in or PLF, 24 h post treatment

(a) Firefly luciferase activity detected by IVIS imaging. (b) Luciferase activity in organ homogenates. ** $p < 0.01$. (c) Immunohistochemical stainings for ACE2 – left panel. Hematoxylin-eosin stainings – right panel. (d) ACE2 protein abundance with GAPDH as loading control and recombinant human ACE2 as positive control.

3.3.3.2 ACE2 cmRNA Application in a Model of Idiopathic Pulmonary Fibrosis

Having identified a carrier formulation for selective ACE2 cmRNA delivery into the lung resulting in significant ACE2 protein abundance, a disease model for lung fibrosis was selected. Bleomycin induced lung fibrosis is frequently used to study drug effectiveness in the treatment for IPF. In this model a single or repeated bleomycin administration is used to trigger lung fibrosis. This leads to an acute inflammatory reaction followed by a fibrotic response. The underlying mechanism is not fully understood but clearly involves tissue damage by reactive oxygen species. Although the model does not fully mimic disease progression in humans especially in the acute inflammatory phase, it offers the advantage of high reproducibility and a clear defined disease staging^{97,98}. In the current study, the model was induced by a single i.t. bleomycin administration of 0.05 units in C57Bl/6 mice. All animals were given bleomycin on day 0 and treated by intravenous injection of ACE2 cmRNA or 2 % sucrose on day 7 according to the following outline:

Table 17: Group allocation for IPF model

Group Number	Treatment	Group size (start)	Group size (end)	Endpoint
1	Sham (2 % sucrose)	4	3	6 h
2	Sham (2 % sucrose)	4	3	5 days
3	cmRNA (ACE2 90 %, Luc 10 %)	4	4	6 h
4	cmRNA (ACE2 90 %, Luc 10 %)	4	4	48 h
5	cmRNA (ACE2 90 %, Luc 10 %)	4	3	5 days

As already described in previous experiments, a mixture of ACE2 cmRNA and reporter cmRNA was applied for additional verification of cmRNA delivery. cmRNA treated animals received a dose of 1 mg/kg cmRNA formulated in PLF, while sham treated animals received 2 % sucrose in PBS. The total volume applied was 150 µl. In order to get a first understanding of the *in vivo* kinetics, different endpoints were chosen for the groups. The first endpoint was set 6 h in post application order to evaluate effectiveness of transfection and for comparison with previous experiments. For this endpoint, a separate control group was allocated. The next endpoint was set after 48 h to verify cmRNA half life and protein expression at that time point. The last endpoint was set after 5 days again for evaluation of cmRNA and protein expression as well as for verification of anti-fibrotic effects of the treatment. An additional control group was included for day 5 in order to evaluate disease progression. At each endpoint, blood plasma

was taken for analysis of cytokines and lungs were excised. The left lungs were prepared for immunohistochemical evaluation and the right lungs were frozen for cmRNA and protein analysis.

Luciferase assay of lung homogenates proofed lung targeted delivery of cmRNA. Luciferase activity was detectable 6 h post application (Figure 27 a). Luciferase activity was not measurable at later time points, which may be due to the short half-life of luciferase protein. However, one animal did not show luciferase activity at any timepoint, indicative for a failed treatment. This animal is shown in the figures but was excluded from statistical analysis.

For ACE2 cmRNA quantification, total RNA was extracted and 500 ng was transcribed to cDNA. Real time PCR analysis showed uptake of 0.4 ng ACE2 cmRNA per μg total RNA after 6 h (Figure 27 b). As shown in the luciferase activity assay, one animal was excluded for analysis, being the major reason for limited statistical relevance of the data. Following the 6 h timepoint, there was a gradual decrease of ACE2 cmRNA detectable with little, but still measurable amounts of cmRNA even 5 days after treatment. Based on these data, a half-life of approximately 15 h was calculated (Figure 27 c). ACE2 cmRNA was then visualized in the *in situ* hybridization of embedded lung tissues (Figure 27 d). The cmRNA shows up as brown colored dots and with a homogenous distribution of positive stained cells in the alveolar walls of ACE2 treated animals, which were interpreted to be AEC type I and type II cells. Furthermore, single alveolar macrophages as well as single endothelial cells of large vessels with ACE2 cmRNA were found. As expected, no staining for ACE2 cmRNA was found in the sham treated group.

Lung homogenates were then probed for ACE2 protein by Western Blot. There was no induction in ACE2 protein expression detectable between ACE2 treated and sham treated animals.

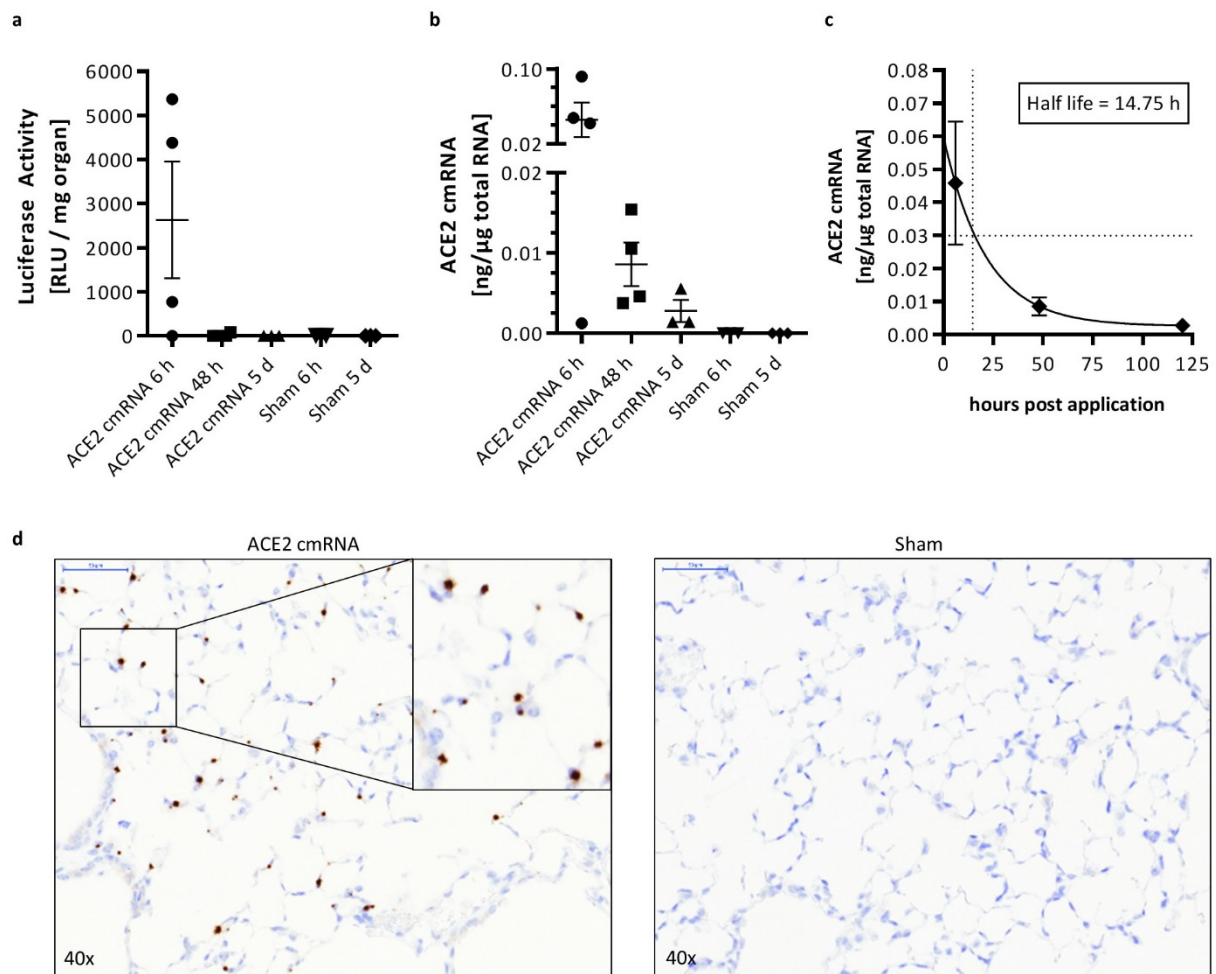


Figure 27: Reporter protein translation and ACE2 cmRNA abundance post i.v. application of ACE2 cmRNA

i.v. administration of 1 mg/kg ACE2 cmRNA in or PLF, 24 h post treatment

(a) Luciferase Activity. (b, c) Absolute quantification of ACE2 cmRNA. (d) *In situ* hybridization for a representative ACE2 cmRNA treated (left panel) and sham treated (right panel) animal.

The immune response following cmRNA treatment was analyzed using a standard cytokine panel reflecting both Th1 as well as Th2 response including IL-10, IL-1 β , IL-2, IP-10, IL-6, IFN α , IFN γ , IL-12p70 and TNF α (Figure 28). Values obtained for IL-1 β , IL-2 and IL-12p70 were below detection limit, hence neither disease nor cmRNA treatment stimulated secretion of these cytokines. IL-6 and TNF α being two acute phase cytokines were moderately and slightly increased 6 h post application. The single high value of IL-6 in the 6 h sham group is considered to be an outlier as all other animals showed low levels of IL-6. The acute inflammation in the first 6 h post cmRNA treatment triggered a slight increase in IL-10, a negative regulator of the immune response. Administration of cmRNA typically induces upregulation of interferons, due to presence of single stranded RNA. This was reflected by a minor induction of the IFN γ levels.

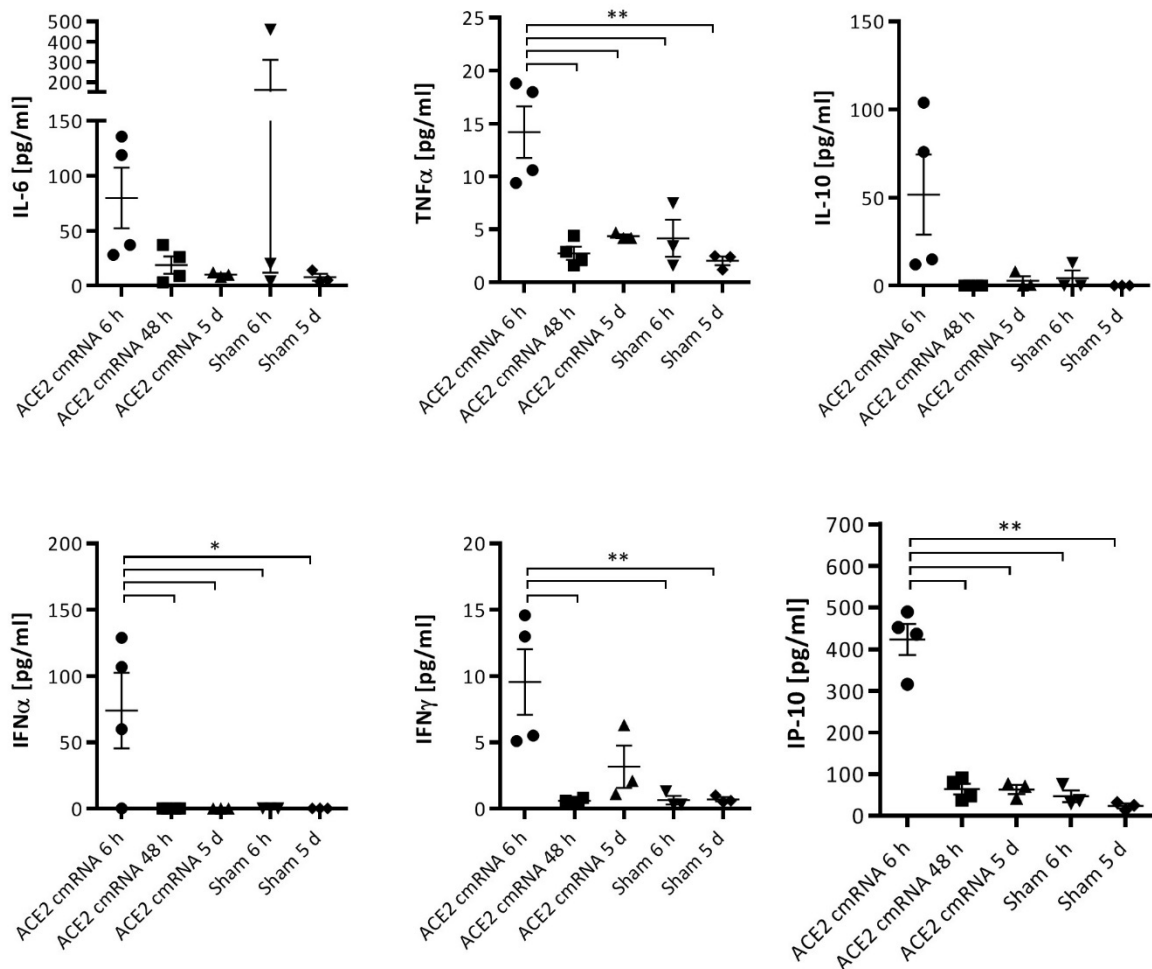


Figure 28: Cytokine analysis

Subsequently, interferons trigger upregulation of IP-10, important for immune cell recruitment. Taken together, all cytokines show a similar pattern over time. cmRNA treatment seems to stimulate an acute immune response briefly after application which is resolved within 48 h. The disease itself does not seem to provoke strong induction of any of the analyzed cytokines.

For disease evaluation all slides were stained with hematoxylin-eosin (Figure 29). Fibrosis was detectable by fibrous thickening of alveolar walls as well as in peribronchial and perivascular regions leading to disruption of normal lung architecture. Furthermore, chronic inflammation was detectable by alveolar and interstitial cellular infiltration.

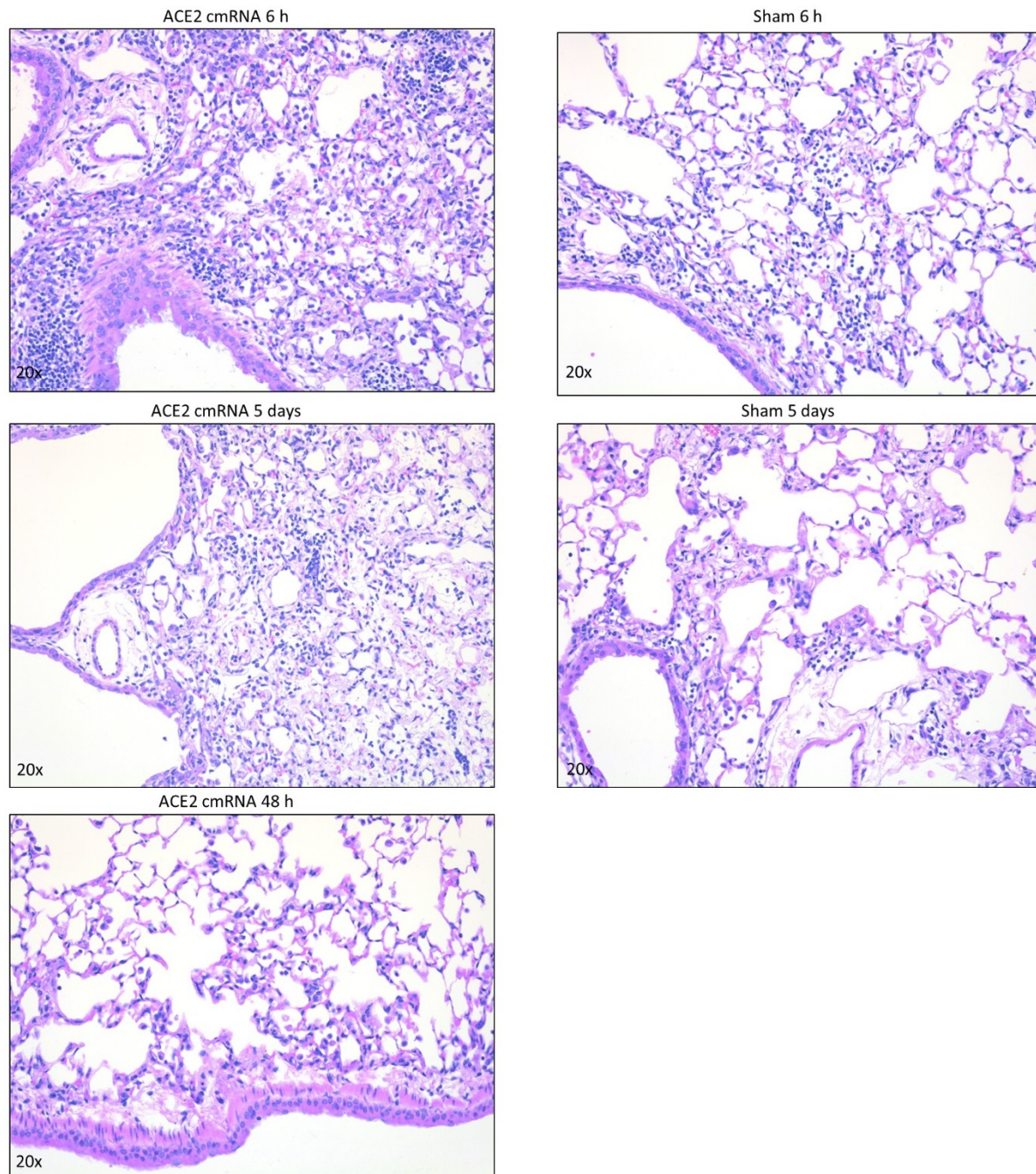


Figure 29: Representative hematoxylin-eosin stainings of ACE2 treatment lungs

i.v. administration of 1 mg/kg ACE2 cmRNA in or PLF, 24 h post treatment

A grading for fibrosis and inflammation with a scoring system from 0 (none) to 5 (very severe) was applied. As shown in Table 18, scoring data of inflammatory reaction and fibrosis differed in between animals in each group. Thus, no obvious reduction of inflammatory reaction or fibrotic progression could be seen. Nevertheless, no enhancing effect on disease progression could be seen either.

Table 18: Fibrosis and Inflammation scores

ACE2 cmRNA Treatment Groups				Sham Treatment Groups			
Animal	Group	Fibrosis	Inflammation	Animal	Group	Fibrosis	Inflammation
301	3	2	3	101	1	2	3
302	3	2	2	102	1	1	1
303	3	2	3	103	1	2	3
304	3	1	2	Mean		1.67	2.33
Mean		1.75	2.50	±SEM		±0.33	±0.67
±SEM		±0.25	±0.29				
Animal	Group	Fibrosis	Inflammation	Animal	Group	Fibrosis	Inflammation
401	4	1	1	201	2	2	2
402	4	1	1	202	2	1	1
403	4	1	0	203	2	2	2
404	4	2	2	Mean		1.67	1.67
Mean		1.25	1.00	±SEM		±0.33	±0.33
±SEM		±0.25	±0.41				
Animal	Group	Fibrosis	Inflammation	Grading			
501	5	2	2	0 none	3 moderate		
502	5	2	2	1 very slight	4 severe		
503	5	3	2	2 slight	5 very severe		
Mean		2.33	2.00				
±SEM		±0.33	±0.00				

Overall, ACE2 cmRNA could be detected in lungs of bleomycin induced pulmonary fibrosis. However, ACE2 protein was below detection limit and ACE2 treatment did not have any effect disease progression.

4 DISCUSSION

In the treatment of liver and lung fibrosis, reestablishment of a well-balanced renin-angiotensin-system (RAS) was repeatedly shown to have promising therapeutic effects.^{4,5,8,20,37,44,45,55,56,71} The most effective intermediate of the RAS system to achieve this goal is ACE2 due to its dual function of downregulating the RAS classical axis and upregulating the RAS alternate axis. The topic of this thesis was a comprehensive *in vitro* and *in vivo* evaluation of the therapeutic application of ACE2 transcript therapy in the treatment of liver and lung fibrosis.

4.1 *In vitro* Analysis

Having identified ACE2 as target protein, an in-vitro-transcribed chemically modified ACE2 sequence was designed. This sequence was subjected to an intense *in vitro* screen in HEK293 cells as a generic test system as well as human and murine cells of liver (HepG2 and primary hepatocytes) and pulmonary (A549 and primary lung fibroblasts) origin in order to reflect future application in liver and lung. ACE2 cmRNA was successfully taken up by all tested cells and translated into an enzymatically active protein (Figure 10).

As described in Figure 5, the extracellular domain of ACE2 protein holds a cleavage site which generates a secreted form of ACE2 upon cleavage by ADAM17³⁹. The mode of action of a secreted molecule resembles the situation after administration of a recombinant protein, which enters systemic circulation and is distributed throughout the body. Administration of recombinant human ACE2 in experimental liver⁴ and lung fibrosis⁵⁵ showed first promising but also negative results. On the one hand, the treatments showed overall anti-inflammatory and anti-fibrotic progresses, but could on the other hand not halt collagen deposition, a major problem in fibrosis in a model of lung fibrosis⁶. This raises the question if it would be more effective to increase the dosing of recombinant protein or to aim for a local delivery system with greater efficacy. The current state of knowledge points more towards higher effectiveness of local delivery. For instance, high tissue AngII levels are frequently found in fibrosis, while systemic AngII levels are barely affected⁴³. In addition to these findings, there is limited understanding of the physiological relevance of soluble ACE2 and the terminal half-life of recombinant ACE2 protein in humans⁷ is limited to 10 h, both being strong indicators for the need of an effective organ targeted local delivery system for ACE2 cmRNA. With the latest advances in mRNA transcript therapy (RTT), organ targeted local delivery as well as local

protein translation should be feasible. Therefore, it was essential to first clarify *in vitro* if cmRNA derived ACE2 protein is processed to a stably expressed transmembrane protein. First of all, it was verified that ACE2 is glycosylated and forms disulfide bonds, crucial steps for integration into the plasma membrane (Figure 11). In a next step it was confirmed that the direction of ACE2 integration into the plasma membrane is in the correct orientation with the N-terminus in the extracellular space and the C-terminus in the cytoplasm. This was shown by a flow cytometry experiment of unpermeabilized cells detecting the ACE2 core domain located on the cellular surface (Figure 11). In addition, fluorescent stainings of ACE2 cmRNA transfected A549 and HepG2 showed co-localisation of ACE2 protein with a plasma membrane marker. It was further observed that ACE2 seems to be enriched in vesicular structures which may be part of the posttranslational maturation machinery (Figure 12).

After verification that ACE2 cmRNA meets all requirements to be expressed in form of a local membrane anchored protein, the ACE2 cmRNA sequence was further optimized with regard to its pharmacokinetic and pharmacodynamics properties in liver and lung cell lines. These evaluations are summarized in the master thesis of Huber M.⁷⁴ and consisted of a screen of eight different ACE2 cmRNA sequences which were manipulated in their UTRs and codon usage. The sequences were analyzed for their intracellular half-life, protein abundance, enzymatic activity and translation kinetics in A549 and HepG2 and resulted in the identification of two codon-optimized ACE2 cmRNA sequences being the most promising candidates. Due to its prolonged half-life, the ACE2 cmRNA sequence flanked by 5' human alpha globin 5' UTR element was chosen for subsequent *in vivo* evaluations.

4.2 *In vivo* Analysis

After having verified full functionality and integrity of ACE2 cmRNA derived protein, liver and lung *in vivo* application was tested.

4.2.1 Liver

Liver targeted cmRNA delivery was first evaluated by a formulation of luciferase cmRNA in lipidoid nanoparticles as described by Jarzebinska et al.¹⁴ These particles were intravenously applied in mice and led to strong and liver specific protein translation (Figure 14 a and b). Immunohistochemical stainings indicate that systemic application of a lipidoid based cmRNA formulation seems to be a potent delivery mechanism for reaching a high number of hepatocytes, which was already shown for delivery of siRNA as well as mRNA^{16,99–101}. The

current understanding of the underlying mechanism is, that lipoplexes enter the liver lobuli *via* fenestrated capillaries, which - unlike other type of capillaries - lack a diaphragm. This makes them highly permeable for small molecules, and lipoplexes are easily taken up into the interstitium, where they are transported by ligand-based targeting or diffusion from the afferent to the efferent vessels¹⁰⁰⁻¹⁰². This is clearly visible in the histochemical stainings for luciferase protein showing a gradual decrease of protein abundance from the afferent to the efferent vessels as observed for nutrients and oxygen saturation in the liver (Figure 14 e). This observation highlights a major advantage of RTT over recombinant protein therapy and viral pDNA delivery, namely the ability to reach a large pool of cells even beyond physical barriers such as endothelium in both mitotic and non-mitotic cells. With the aim of shifting the local balance of the RAS system towards resolution of fibrosis, reaching hepatocytes, being the most abundant cell type in the liver, can be considered a major achievement for strong translation of the target protein. In a second step, the same delivery method was applied to ACE2 cmRNA and led to a markedly increased ACE2 protein translation and activity 6 h after treatment (Figure 15). Based on previous *in vitro* findings about ACE2 cmRNA kinetics, ACE2 protein translation for up to 5 days can be expected. This time frame lies above levels reached by recombinant ACE2 therapy in human and experimental models¹⁰, and below levels reached by adeno-associated viral ACE2 therapy³, emphasizing once more the advantages of RTT for a flexible dosing regimen for potential future clinical application.

Next, a first evaluation of ACE2 cmRNA application in a NASH disease model was set up in order to get an understanding of cmRNA deposition, protein expression kinetics and anti-fibrotic effects of ACE2 for future large scale preclinical experiments. So far multiple NAFLD/NASH models have been established resembling human disease progression in its macroscopic and microscopic morphology, the degree of inflammation and fibrosis. However, a gene expression analysis between disease models and human tissue samples disclosed that the gene expression patterns between models and humans are more distinct than previously thought. Within this analysis, high fat diet enriched models showed a closer link to human NAFLD than other models¹⁰³. Due to high prevalence of NAFLD within patients suffering from metabolic syndrome and the increasing problems associated with western diet, a model based on high fat diet was considered most appropriate. Compared to other high fat diet based models, the STAM model does not only reproduce NAFLD associated indications but as well NASH associated indications. The model is based on induced insulin resistance in combination

with high-fat diet and induces physiological alterations associated with metabolic syndrome simultaneously to pathologic patterns associated with NAFLD and NASH in humans with high reproducibility¹⁰⁴. It has previously been used in multiple studies for evaluation of anti-fibrotic treatment¹⁰⁵ and was therefore considered appropriate for the investigation of ACE2 RTT in the progression of NASH.

Treatment with ACE2 was started in the late phase of NAFLD, which correlates to the timepoint where NAFLD patients present with elevated liver parameters for the first time¹⁰⁶. The treatment regimen was followed for 3 consecutive weeks with a dose of 0.25 mg/kg ACE2 cmRNA in LLF once (group 2) or twice (group 1) per week. First, establishment of the disease model was verified by increased liver/body weight ratio (Figure 17), elevated blood parameters (Figure 17) and elevated levels of hydroxyproline in the liver (Figure 18). With regards to ACE2 treatment, body weight, plasma glucose and cholesterol were not affected while liver weights were increased in ACE2 treated animals (Figure 17 a and b). Evaluation of fibrosis progression was based on observed accumulation of liver collagen as well as on histologic examinations of liver tissue for steatosis, ballooning and inflammation. Collagen content was determined quantitatively in a hydroxyproline assay and qualitatively on histologic slides stained for sirius red. While there was no treatment effect seen in the quantitative evaluation, a significant reduction in collagen was detected in the histologic examination. Despite the proposed correlation of the readouts of these two assays⁹², the hydroxyproline assay may be less sensitive in detecting therapeutic effects as the differences between control groups and all other groups were less pronounced than in the sirius red analysis. Evaluation of histologic sections showed no effect of ACE2 cmRNA treatment on steatosis and ballooning. Inflammation however, seemed to improve with increased ACE2 dosing. These observations are in line with findings by Mak et al.³, who found ACE2 gene therapy instilled by an adeno associated viral vector to be anti-inflammatory in acute as well as chronic liver injury. However, these findings are contradictory to the results of Österreicher et al.⁴, who concluded post recombinant protein therapy that ACE2 does not play a role in acute but in chronic liver injury⁴. These differences may be explained by the fact that Österreicher et al. started the treatment at the timepoint of disease initiation, while in the study at hand and the study by Mak et al. ACE2 therapy was started 2 weeks after disease establishment. Steatosis, ballooning and inflammation were combined to an overall NAFLD

score which showed a minor trend towards NAFLD improvement with increasing frequency of ACE2 treatment.

Taken together, ACE2 cmRNA treatment did not have any effect on metabolic syndrome which is contradictory to previous studies having shown a protective role of the alternate RAS axis on obesity-associated complications⁴³. Despite the high transfection efficiency of lipidoid based formulation in the liver, it may be worth considering a different carrier solution in a model already challenged by high amounts of lipids in a high fat diet. Similar considerations about the suitability of a lipidoid carrier may be drawn from the animal dropout rates which were highest in group 1 undergoing two treatments per week. While the group sizes were too small to allow a judgement about treatment toxicity, the dropout rates observed emphasize the need of low toxicity of the formulation due to disease severity. With regards to fibrosis progression, ACE2 cmRNA treatment did not halt or reverse liver fibrosis, but there was a trend towards disease improvement observable for the group treated twice per week. One of the underlying reasons for the limited therapeutic efficacy in this experiment could be found in deposited ACE2 cmRNA levels 20 fold lower than expected. As shown in the earlier experiments for evaluation of organ targeted ACE2 delivery (Figure 15 b), a dose dependent deposition of ACE2 in the liver was observed. Extrapolating these values to the ACE2 cmRNA dose applied in the NASH study (0.25 mg/kg), one would expect an ACE2 cmRNA deposition of at least 0.002 ng/ μ g total RNA compared to the achieved 0.1 pg/ μ g total RNA. The most evident causes for the low transfection efficiency are either differences in the mouse strains used (Balb/c in organ targeted experiments versus C57BL/6 in NASH study) or limited nanoparticle uptake due to loss of endothelium fenestration in liver fibrosis, as already observed in liver tumors⁶⁹.

In conclusion, intravenous administration of codon-optimized ACE2 cmRNA with h α G 5' UTR formulated in lipidoid nanoparticles leads to strong protein translation in the liver. Application of ACE2 in a NASH disease model showed a first trend towards reduction of inflammation and fibrosis.

4.2.2 Lung

With the objective of clinical application of ACE2 treatment, the *in vivo* investigations were started with the least invasive form of pulmonary delivery in form of nebulization. It was previously shown that delivery of pDNA or mRNA is able to enhance protein translation in the

lung^{94,95} and that brPEI is an effective delivery agent for aerosol application of pDNA^{107,108}. However, it had to be determined if mRNA formulations with brPEI would be effective enough to establish ACE2 expression levels high enough to shift the local RAS balance towards anti-inflammatory and anti-fibrotic signaling. It was speculated, that even higher ACE2 protein expression could be achieved by repeated dosing every 24 hours due to protein accumulation. The results of the experiment showed, that protein accumulation *per se* was achievable for luciferase (Figure 22), however protein accumulation for ACE2 protein was not high enough to lead to detectable protein levels. There are multiple reasons for the low protein expression, one of them being the route of application in form of nebulization which does not guarantee deposition of a predefined amount of nanoparticles. On the way through the nebulization chamber, the particles interact with different types of surfaces and it has to be assumed that a large amount of particles are lost without reaching the animal's pulmonary system. Once reaching the pulmonary system, particle deposition may also show high intra-individual variances due to differences in breathing rates and depths as well as differences in direct contact time with the aerosol due to animal movements and body position during the nebulization procedure. Many of these obstacles can be avoided by i.t. microspray application, though the application is much more invasive and would be less convenient in use for future patients. By installation of a tube down the trachea, it is guaranteed that no particles will be lost outside the pulmonary system or in the upper respiratory tract. I.t. microspray application is suitable for both, polyplex as well as lipidoid based carriers. Therefore, a side-by-side comparison between a polyplex based carrier (brPEI) and a lipidoid based carrier (LF44) was set up in order to identify the most effective carrier. In this side by side comparison done in rats, protein activity achieved by 0.45 mg/kg reporter cmRNA in the lipidoid based formulation was markedly stronger than protein activity achieved by the polyplex based formulation (Figure 23). These findings are in line with previous investigations, showing that interaction of poly- and lipoplexes with bronchoalveolar lavage fluid components can alter the particles' surface charge and consequently have a strong impact on transfection efficiency¹⁰⁹. It was shown that lipoplexes kept an overall positive charge, while polyplexes changed from a positive to a negative surface charge. A negative surface charge hinders interaction of the polyplex with the negative charged cell surface resulting in lower transfection efficiency. Based on these findings, a lipidoid based formulation of ACE2 cmRNA was applied i.t. which resulted in a weak but detectable induction of ACE2 protein expression. Histologic evaluations

showed deposition of larger amounts of ACE2 cmRNA in the central airways compared to distant alveoli. This observation confirms on the one hand, that the droplets created by the microspray device are small enough to reach alveoli, but highlights on the other hand the devices' limitations in homogenous aerosol distribution. The predominantly central deposition of the ACE2 cmRNA may also explain the overall weak induction in ACE2 protein expression as most of the particles do not seem to reach the alveoli as their final destination but are caught in the bronchial system. The bronchial system is equipped with the mucociliary escalator, an effective clearing system pushing trapped material in a layer of mucus towards the mouth¹¹⁰. Transfection efficiency of the remaining ACE2 cmRNA having reached the alveoli is determined by the rate of deposition and the rate of clearance by macrophages as well as the immune response evoked by macrophage activation.

The treatment itself led to slightly increased breathing rates and temporary unresponsive behavior of the animals. 6 h after treatment, neutrophil infiltration and fibrin extravasation reaching up to moderate levels were found in the lung tissues of ACE2 cmRNA transfected animals (Figure 25 b). These findings indicate an acute pulmonary inflammatory reaction to the i.t. application of lipoplexed cmRNA since none of the PBS-treated animals presented with histopathological findings. Unfortunately, time and resource constraints did not allow detailed investigations if toxicity is caused by the lipoplex, by the ACE2 cmRNA or by both molecules. The combination of weak ACE2 protein expression and the observed inflammatory reaction – although maybe being solely an interim acute reaction to the aerosol – led to the conclusion, that i.t. microspray application of ACE2 cmRNA may not be the appropriate treatment for severely diseased animals, needing strong ACE2 protein expression in order to shift the RAS balance. Therefore, it was decided to continue *in vivo* investigations for lung application *via* systemic cmRNA delivery.

Despite the inconvenience of intravenous drug administration, which may need to be repetitive in the case of cmRNA, systemic drug delivery may be more effective than pulmonary delivery for several reasons. First, IPF is characterized by an interstitial pneumonia with basal predominance and epithelial cell stress and apoptosis especially adjacent to fibroblast foci¹¹¹. Previous *in vitro* studies have shown that AEC produce more AngII in response to injury, while at the same time ACE2 mRNA is reduced. This makes AEC even more prone to injury and AngII induced apoptosis^{6,112–114}. Therefore delivering ACE2 cmRNA especially to these areas of epithelial cell death may be essential for therapeutic success. Unfortunately, due to

destruction of the lung parenchyma, these areas are poorly ventilated, making them hard to reach for drug delivery *via* the airways. Looking at the vascularization of fibrotic lungs, it was shown that fibroblast foci themselves are poorly vascularized while adjacent non-fibrotic areas, where AEC apoptosis is taking place, are highly vascularized^{115,116}. Second, in a study comparing the distribution and uptake patterns of oligonucleotides and pDNA packed in lung targeted cationic lipoplexes showed that i.v. administration resulted in a very homogenous distribution of oligonucleotides and pDNA in the lung, while i.t. distribution led to highly localized distribution as observed in the previous experiment¹¹⁷. It has to be noted, that in the study just mentioned, i.t. application was done by instillation as compared to microspray in this thesis. Based on these findings and the limited success of markedly inducing ACE2 protein expression upon i.t. cmRNA delivery, a lipid based cmRNA formulation for intravenous application in mice was prepared. Identical to the previous *in vivo* studies, organ selectivity of the formulation had to be evaluated first. This was verified by application of 1 mg/kg luciferase cmRNA in mice, which induced strong and selective protein translation in the lung (Figure 26 a and b). All other organs did not show significant protein levels which is especially important for application of ACE2 due to its potential effects on blood pressure regulation. Administration of the same proprietary lipid formulation containing 1 mg/kg ACE2 cmRNA led to equally strong ACE2 protein translation in the lung (Figure 26 d). Histologic evaluation showed a very homogenous expression of ACE2 cmRNA derived protein in AECs throughout the whole organ, confirming externalization of i.v. applied lipid nanoparticles from systemic circulation into the lung parenchyma and successful transfection of lung epithelial cells (Figure 26 c). The externalization mechanism was not studied further and it is assumed that a combination of particle size as shown for antibody conjugated nanoparticles by Azarmi et al.⁷⁰ and electrostatic interaction between charged molecules and the cell surface¹¹⁷ lead to retention of the nanoparticle in the lung and subsequently to externalization of the particle. Closer evaluations of the immunostainings showed that sham treated animals expressed ACE2 in AEC type II cells, which is in line with endogenous ACE2 expression patterns previously observed in mice¹¹⁸. ACE2 cmRNA treated lungs also expressed ACE2 in macrophages and more importantly AEC type I. These findings are especially valuable for therapeutic application in IPF, as unlike rodent lungs, human lungs also express ACE2 in AEC type I^{96,119}, rendering them an enormous pool for locally active ACE2 protein to break the vicious circle of AngII stimulated ACE2 downregulation and apoptosis. Establishing ACE2 translation in AEC type I

could so far neither be achieved by recombinant protein therapy⁵⁵ nor by lentiviral-mediated ACE2 overexpression⁵⁶.

Based on these promising results, a first evaluation of ACE2 cmRNA application in a bleomycin induced mouse model of lung fibrosis was designed for evaluation of cmRNA deposition and protein expression kinetics. 1 mg/kg ACE2 cmRNA including 10 % luciferase cmRNA spike was prepared in PLF and intravenously applied. The treatment provoked an acute inflammatory reaction as shown by a panel of representative cytokines (Figure 28) which was resolved within 48 h. It was not investigated, whether the acute inflammatory reaction was triggered by the cmRNA or the lipid formulation. With cmRNA being optimized for minimal immune reaction, part of the cytokine induction can also be attributed to the liposomes, which has already been observed before¹²⁰. ACE2 cmRNA was successfully taken up in the lung tissue and was detectable up to 5 days. The calculated half-life of approximately 15 h is similar to the half-life achieved *in vitro*⁷⁴ (approximately 13 h) and gives important information for the calculation of treatment regimens for future studies. However, ACE2 protein could not be detected in this study as compared to i.v. application in healthy Balb/c mice (Figure 26). Taking into considerations the low luciferase activity levels, the reasons for ACE2 protein expression below detection limit may be found in low transfection efficiency due to differences in lung architecture between healthy and diseased lungs, differences in genetic backgrounds of the two mouse strains or both. The changes in lung architecture are clearly visible comparing histological images of Figure 26 b of a healthy lung to Figure 29 b of bleomycin treated lungs. Bleomycin treatment led to an obvious fibrotic reaction, though still graded on average as 'slight', resulting in thickening of the air-blood-barrier, possibly severe enough to block transfection or nanoparticle extravasation. Apart from this apparent optical difference in lung architecture, differences in mouse strains (Balb/c versus C57BL/6) may as well contribute to differences in transfection efficiency. Considerable differences in gene expression between mouse strains were already observed following i.v.¹²¹ as well as aerosol based pDNA mediated gene delivery¹²². It is speculated that differences in the genetic background lead to differences in immune system mediated nanoparticle clearance, nanoparticle uptake, intracellular trafficking, endosomal release and translation rates¹²². Due to undetectable ACE2 protein expression, there was no significant positive effect on inflammation and fibrosis detectable at the end of the study. However, there was a minor trend towards improvement in inflammation and fibrosis observable 48 h after treatment. Due to the limited group size,

these data would need additional experimental confirmation. At this point it has to be noted, that in all other previous studies ACE2 overexpression was established either before⁵⁶ or at the time point of disease initiation^{5,123}, which calls into question the clinical applicability of these findings. Apart from the study performed by Min et al.⁸, this study is the first to provide data with ACE2 treatment started after clear establishment of lung fibrosis which resembles much closer the setting in future therapeutic applications.

4.2.3 Conclusion and Outlook

In summary, it was shown that establishment of sustained local ACE2 translation selectively in liver or lung is achievable with latest RNA technology. This was accomplished by a combination of lipidoid and lipid nanoparticles serving as carrier systems and especially designed ACE2 cmRNA sequences. These achievements highlight the strengths of RTT over recombinant protein and gene therapy, where protein half-life¹⁰ and overall duration of protein expression⁶¹, immunogenicity¹¹, patients' safety¹² as well as organ or cell targeting are still challenging.

As shown by other groups^{3,4,8,55,56} and the positive trends observable upon ACE2 treatment in the experimental NASH and IPF models, ACE2 has substantial therapeutic potential for anti-inflammatory and anti-fibrotic treatment. Hence ACE2 transcript therapy should be further optimized to leverage its full potential as well in diseased animal models.

Thinking of next steps, it would be most effective to first clarify the underlying causes of the reduced ACE2 transfection rates and protein expression levels observed in the disease models. For this, it would be easiest and animal resource-saving, to repeat the experiments performed in this thesis either in healthy CBI57/6 or in diseased Balb/c animals. These data can be directly compared to the data in this thesis for the respective healthy or diseased animals and clarify at the same time the question about dependency of the data on genetic differences and/or on disease state. Based on this knowledge, protein expression limitations can be overcome either by increasing the dosing regimen or optimizing the dosing frequency for higher protein expression. However, careful evaluation of the tolerability of this measure has to be taken. If these evaluations do not improve ACE2 protein expression and therapeutic efficacy of ACE2, modifications in the delivery agents should be considered. Once the ideal combination of delivery agent and cmRNA dose is identified, a study evaluating pharmacodynamics and kinetic properties of this formulation mix has to be performed. Based on these findings, the

treatment regimen for a large scale study to evaluate ACE2 therapeutic efficacy needs to be defined.

5 ABBREVIATIONS

ACE	angiotensin converting enzyme
ACE2	angiotensin converting enzyme 2
ACEi	angiotensin converting enzyme inhibitors
ADAM 17	ADAM metallopeptidase domain 17
AEC	alveolar epithelial cell
ALT	alanine aminotransferase
AMP	adenosine 5'-monophosphate
Ang-(1-7)	angiotensin (1-7)
AngI	angiotensin I
AngII	angiotensin II
ARB	angiotensin II receptor blockers
AST	aspartate aminotransferase
AT1R	angiotensin II type 1 receptor
AT2R	angiotensin II type 2 receptor
ATP	adenosine triphosphate
Balb/c	<i>mus musculus</i> laboratory inbred strain
BCA	bicinchoninic assay
BDL	bile duct ligated
brPEI	branched polyethylenimine
CBI57/6	<i>mus musculus</i> laboratory inbred strain
cDNA	complementary DNA
CMP	cytidine 5'-monophosphate
cmRNA	chemically modified RNA
c.o.	codon optimized
CYBA	cytochrome b-245 alpha
Da	dalton
DAPI	4',6-diamidino-2-phenylindole
DMEM	dulbecco's modified essential medium
DMSO	dimethyl sulfoxide
DNA	deoxyribonucleic acid
dNTP	deoxy nucleotide tri phosphate
DTT	1,4-Dithiothreitol
ECM	extracellular matrix
eg.	exempli gratia (for example)
EGTA	egtazic acid
EDTA	edetetic acid
ER	endoplasmic reticulum
FCS	fetal calf serum
FI	fluorescence intensity
g	gram
GAPDH	glyceraldehyd-3-phosphate-dehydrogenase
GLDH	glutamate dehydrogenase
GMP	guanosine 5'-monophosphate
GTP	guanosine triphosphate
h α G	human alpha globin
HSC	hepatic stellate cell

IgG	Immunoglobulin G
IPF	idiopathic pulmonary fibrosis
i.p.	intraperitoneal
i.t.	intratracheal
i.v.	intravenous
IVT	<i>in vitro</i> transcribed
k	kilo
k.o.	knock out
l	liter
LDH	lactate dehydrogenase
LDS	lithium dodecyl sulfate
LED	light emitting diode
μ	micro (10^{-6})
m	milli (10^{-3})
MEM	minimum essential medium
MES	2-(N-morpholino)ethanesulfonic acid
MFI	mean fluorescence intensity
min	minutes
MOPS	3-(N-morpholino)propanesulfonic acid
mRNA	messenger ribonucleic acid
NAFLD	nonalcoholic fatty liver disease
NASH	nonalcoholic steatohepatitis
NEP	neprilysin
n	nano (10^{-9})
ORF	open reading frame
p	pic (10^{-12})
PBS	phosphate-buffered saline
pDNA	plasmid DNA
PEG	polyethylene glycol
PEI	polyethylenimine
poly(A)	poly adenosine
PVDF	polyvinylidene fluoride
qPCR	quantitative polymerase chain reaction
RAS	renin-angiotensin-system
RLU	relative light units
RNA	ribonucleic acid
rpm	rounds per minute
RPMI	roswell park memorial institute
RT	room temperature
RTT	mRNA transcript therapy
SD	standard deviation
SDS	sodium dodecyl sulfate
SEM	standard error or the mean
siRNA	small interfering RNA
TBS	Tris buffered saline
TGFβ	transforming growth factor beta
Tris	tris(hydroxymethyl)aminomethane
U	unit

UMP	uridine 5'-monophosphate
UTR	untranslated region
VLDL	very low density lipoprotein
WFI	water for injection

6 ACKNOWLEDGEMENTS

My name is the only one printed on the cover of this dissertation, but it would not have been completed without the contribution of many people.

The work for this thesis was carried out from April 2014 until March 2017 at Ethris GmbH, Planegg, owned by P.D. Dr. Carsten Rudolph and Prof. Dr. Christian Plank. I want to deeply thank both of them for giving me the opportunity to start my scientific career in the exciting and challenging field of mRNA transcript therapy. I always appreciated their trust, confidence, enthusiasm and scientific support throughout the past years.

I would like to express my special thanks to the whole Ethris team. There was almost every team member involved in this project at a certain point in time and I could not have completed this thesis without their immense contribution and support. In addition, I was always welcome by any Ethris team members regardless of the question I had, which made me learn a lot and solved all problems. Within the Ethris team, I would like to specially thank Dr. Rebekka Kubisch-Dohmen, who always gave me the right support at the right time. Her door was always open for any kind of questions, discussions or just a few motivating words. She was the perfect mentor for critically reviewing results, manuscripts and thesis as well as teaching me the art of replying to reviewers' comments. In addition, I want to thank Dr. Philipp Beck and Dr. Sonja Berchtold who did not only help me with technical issues in the lab but also provided me very helpful scientific input for exam preparation. Last but not least, I wanted to thank Maja Huber, our master student who provided a tremendous contribution with her master thesis data for the progress of this project.

I would also like express my gratitude to Prajakta Oak and Anne Hilgendorff (Comprehensive Pneumology Center, Helmholtz Zentrum Munich) for helping me with the primary lung fibroblasts and Dirk Wohlleber (Institute of Molecular Immunology and Experimental Oncology, TU Munich) for the isolation of primary hepatocytes. In addition, many thanks to our external partners Heinz-Gerd Hoymann and Dirk Schaudien from ITEM (Fraunhofer Institute for Toxicology and Experimental Medicine, Hannover) and the team of Stelic MC, Inc. (Tokyo, Japan) for their great contributions.

I would also like to express my gratitude to the Federal Ministry of Education and Research (BMBF) for financially supporting this project within the Biochance project (031A526).

Finally, none of this would have been possible without the trust, encouragement and love of my family. They gave me the trust, that there will always be a mountain to climb into the sun after each valley within life.

7 ASSOCIATED PUBLICATION AND THESIS

Schrom E., Huber M., Aneja M., Dohmen C., Emrich D., Geiger J., Hasenpusch G., Herrmann-Janson A., Kretzschmann V., Mykhailyk O., Pasewald T., Oak P., Hilgendorff A., Wohlleber D., Hoymann H., Schaudien D., Plank C., Rudolph C., Kubisch-Dohmen R. (2017): Translation of angiotensin converting enzyme 2 (ACE2) upon liver and lung targeted delivery of optimized chemically modified mRNA. *Journal of Molecular Therapy – Nucleic Acids*, accepted 06.04.2017

Huber, M. (2016): Impact of mRNA sequence design on half-life, protein expression and immunogenicity. *Master thesis at the TU Munich, Munich, Germany*

8 REFERENCES

1. Wynn, T. a. Mechanism of fibrosis: therapeutic transplation for fibrotic disease. *Nat. Med.* **18**, 1028–1040 (2013).
2. Clarke, N. E. & Turner, A. J. Angiotensin-converting enzyme 2: the first decade. *Int. J. Hypertens.* **2012**, 307315 (2012).
3. Mak, K. Y. *et al.* ACE2 therapy using adeno-associated viral vector inhibits liver fibrosis in mice. *Mol. Ther.* **23**, 1434–1443 (2015).
4. Osterreicher, C. H. *et al.* Angiotensin-converting-enzyme 2 inhibits liver fibrosis in mice. *Hepatology* **50**, 929–38 (2009).
5. Rey-Parra, G. J. *et al.* Angiotensin converting enzyme 2 abrogates bleomycin-induced lung injury. *J. Mol. Med. (Berl)*. **90**, 637–47 (2012).
6. Li, X. *et al.* Angiotensin converting enzyme-2 is protective but downregulated in human and experimental lung fibrosis. *Am. J. Physiol. Lung Cell. Mol. Physiol.* **295**, L178–85 (2008).
7. Jiang, F. *et al.* Angiotensin-converting enzyme 2 and angiotensin 1-7: novel therapeutic targets. *Nat. Rev. Cardiol.* **11**, 413–26 (2014).
8. Min, F., Gao, F., Li, Q. & Liu, Z. Therapeutic effect of human umbilical cord mesenchymal stem cells modified by angiotensin-converting enzyme 2 gene on bleomycin-induced lung fibrosis injury. *Mol. Med. Rep.* **11.4** 2387–2396 (2014).
9. Shenoy, V. *et al.* Oral delivery of angiotensin-converting enzyme 2 and angiotensin-(1-7) bioencapsulated in plant cells attenuates pulmonary hypertension. *Hypertension* **64**, 1248–59 (2014).
10. Haschke, M. *et al.* Pharmacokinetics and pharmacodynamics of recombinant human angiotensin-converting enzyme 2 in healthy human subjects. *Clin. Pharmacokinet.* **52**, 783–792 (2013).
11. Baker, M. P., Reynolds, H. M., Lumicisi, B. & Bryson, C. J. Immunogenicity of protein therapeutics: The key causes, consequences and challenges. *Self. Nonself.* **1**, 314–322 (2010).
12. Yamamoto, A., Kormann, M., Rosenecker, J. & Rudolph, C. Current prospects for mRNA gene delivery. *Eur. J. Pharm. Biopharm.* **71**, 484–489 (2009).
13. Kaczmarek, J. C. *et al.* Polymer-lipid nanoparticles for systemic delivery of mRNA to the lungs. *Angew. Chem. Int. Ed. Engl.* **55**, 13808–13812 (2016).
14. Jarzębińska, A. *et al.* A single methylene group in oligoalkylamine-based cationic polymers and lipids promotes enhanced mRNA delivery. *Angew. Chemie - Int. Ed.* **55**, 9591–9595 (2016).
15. Fenton, O. S. *et al.* Bioinspired alkenyl amino alcohol ionizable lipid materials for highly potent in vivo mRNA delivery. *Adv. Mater.* **28**, 2939–2943 (2016).
16. Sahin, U., Kariko, K. & Tureci, O. mRNA-based therapeutics - developing a new class of drugs. *Nat. Rev. Drug Discov.* **13**, 759–780 (2014).
17. Vallazza, B. *et al.* Recombinant messenger RNA technology and its application in cancer immunotherapy, transcript replacement therapies, pluripotent stem cell induction, and beyond. *Wiley Interdiscip. Rev. RNA* **6**, 471–499 (2015).
18. Karikó, K., Buckstein, M., Ni, H. & Weissman, D. Suppression of RNA recognition by Toll-like receptors: The impact of nucleoside modification and the evolutionary origin of RNA. *Immunity* **23**, 165–175 (2005).

19. Karikó, K. *et al.* Incorporation of pseudouridine into mRNA yields superior nonimmunogenic vector with increased translational capacity and biological stability. *Mol. Ther.* **16**, 1833–40 (2008).
20. Wynn, T. Cellular and molecular mechanisms of fibrosis. *J. Pathol.* **214**, 199–210 (2008).
21. Almeda-Valdes, P., Aguilar Olivos, N. E., Barranco-Fragoso, B., Uribe, M. & Méndez-Sánchez, N. The role of dendritic cells in fibrosis progression in nonalcoholic fatty liver disease. *Biomed Res. Int.* **2015**, 768071 (2015).
22. Raghu, G. *et al.* An official ATS/ERS/JRS/ALAT statement: Idiopathic pulmonary fibrosis: Evidence-based guidelines for diagnosis and management. *Am. J. Respir. Crit. Care Med.* **183**, 788–824 (2011).
23. Rosenbloom, J., Mendoza, F. a. & Jimenez, S. a. Strategies for anti-fibrotic therapies. *Biochim. Biophys. Acta - Mol. Basis Dis.* **1832**, 1088–1103 (2013).
24. Margaritopoulos, G.A., Vasarmidi, E., Antoniou, K.M. Pirfenidone in the treatment of idiopathic pulmonary fibrosis : an evidence-based review of its place in therapy. *Core Evidence* **11**, 11–22 (2016).
25. Rogliani, P., Calzetta, L., Cavalli, F., Matera, M. G. & Cazzola, M. Pirfenidone, nintedanib and N-acetylcysteine for the treatment of idiopathic pulmonary fibrosis: A systematic review and meta-analysis. *Pulm. Pharmacol. Ther.* (2016).
26. Koyama, Y., Xu, J., Liu, X. & Brenner, D. a. New developments on the treatment of liver fibrosis. *Dig. Dis.* **34**, 589–96 (2016).
27. Ramos-lopez, O. *et al.* Genetic , metabolic and environmental factors involved in the development of liver cirrhosis in Mexico. *World J. Gastroenterol.* **21**, 11552–11566 (2015).
28. Mohamed, J., Nazratun Nafizah, a H., Zariyantey, a H. & Budin, S. B. Mechanisms of diabetes-induced liver damage: The role of oxidative stress and inflammation. *Sultan Qaboos Univ. Med. J.* **16**, e132–41 (2016).
29. Friedman, S. L. Hepatic Stellate Cells: Protean, multifunctional, and enigmatic cells of the liver. *Physiol. Rev.* **88**, 125–172 (2010).
30. Álvarez, D., Levine, M. & Rojas, M. Regenerative medicine in the treatment of idiopathic pulmonary fibrosis : current position. *Stem C. and Clon.: Adv. and Appl.* **8**, 61–65 (2015).
31. Günther, A. *et al.* Unravelling the progressive pathophysiology of idiopathic pulmonary fibrosis. *Eur. Respir. Rev.* **21**, 152–160 (2012).
32. Seibold, M.A. *et al.* A common MUC5B promoter polymorphism and pulmonary fibrosis. *N. Engl. J. Med.* **364-16**, 1503–1512 (2011).
33. Funke, M. & Geiser, T. Idiopathic pulmonary fibrosis: the turning point is now! *Swiss Med. Wkly.* **145**, w14139 (2015).
34. Daccord, C. & Maher, T. M. Recent advances in understanding idiopathic pulmonary fibrosis. *F1000Research* **5**, 1–13 (2016).
35. Wollin, L. *et al.* Mode of action of nintedanib in the treatment of idiopathic pulmonary fibrosis. *Eur. Respir. J.* **45**, 1434–1445 (2015).
36. Bader, M., Santos, R. a, Unger, T. & Steckelings, U. M. New therapeutic pathways in the RAS. *J. Renin. Angiotensin. Aldosterone. Syst.* **13**, 505–8 (2012).
37. Ni, L. *et al.* Angiotensin-(1-7) inhibits the migration and invasion of A549 human lung adenocarcinoma cells through inactivation of the PI3K/Akt and MAPK signaling pathways. *Oncol. Rep.* **27**, 783–90 (2012).
38. Vickers, C. *et al.* Hydrolysis of biological peptides by human angiotensin-converting enzyme-related carboxypeptidase. *J. Biol. Chem.* **277**, 14838–43 (2002).

39. Tipnis, S. R. *et al.* A human homolog of angiotensin-converting enzyme. Cloning and functional expression as a captopril-insensitive carboxypeptidase. *J. Biol. Chem.* **275**, 33238–43 (2000).
40. Lambert, D.W. The cell biology of the SAR coronavirus receptor, angiotensin-converting enzyme in: *Molecular Biology of the SARS-Coronavirus*, Springer Science (2010). <<http://www.springer.com/life+sciences/genetics+&+genomics/book/978-3-642-03682-8>>, accessed 25.04.2017
41. Speth, R., Carrera, E., Jean-Baptiste, M., Joachim, A. & Linares, A. Concentration-dependent effects of zinc on angiotensin-converting enzyme-2 activity. *FASEB J* **28**, 1067.4 (2014).
42. Towler, P. *et al.* ACE2 X-ray structures reveal a large hinge-bending motion important for inhibitor binding and catalysis. *J. Biol. Chem.* **279**, 17996–8007 (2004).
43. De Macêdo, S. M., Guimarães, T. A., Feltenberger, J. D. & Santos, S. H. S. The role of renin-angiotensin system modulation on treatment and prevention of liver diseases. *Peptides* **62**, 189–196 (2014).
44. Moreno, M. *et al.* Reduction of advanced liver fibrosis by short-term targeted delivery of an angiotensin receptor blocker to hepatic stellate cells in rats. *Hepatology* **51**, 942–52 (2010).
45. Corey, K. E. *et al.* The effect of angiotensin-blocking agents on liver fibrosis in patients with hepatitis C. *Liver Int.* **29**, 748–53 (2009).
46. Yi, E.-T., Liu, R.-X., Wen, Y. & Yin, C.-H. Telmisartan attenuates hepatic fibrosis in bile duct-ligated rats. *Acta Pharmacol. Sin.* **33**, 1518–1524 (2012).
47. Paizis, G. *et al.* Chronic liver injury in rats and humans upregulates the novel enzyme angiotensin converting enzyme 2. *Gut* **54**, 1790–6 (2005).
48. Selman, M. *et al.* Gene expression profiles distinguish idiopathic pulmonary fibrosis from hypersensitivity pneumonitis. *Am. J. Respir. Crit. Care Med.* **173**, 188–198 (2006).
49. Marshall, R. P. *et al.* Angiotensin II and the fibroproliferative response to acute lung injury. *Am. J. Physiol. Lung Cell. Mol. Physiol.* **286**, L156–64 (2004).
50. Okada, M. *et al.* Effects of angiotensin on the expression of fibrosis-associated cytokines, growth factors, and matrix proteins in human lung fibroblasts. *J. Clin. Pharm. Ther.* **34**, 289–299 (2009).
51. Uhal, B. D., Dang, M.-T. T., Li, X. & Abdul-Hafez, A. Angiotensinogen gene transcription in pulmonary fibrosis. *Int. J. Pept.* **2012**, 1–8 (2012).
52. Uhal, B. D. *et al.* Cell cycle dependence of ACE-2 explains downregulation in idiopathic pulmonary fibrosis. *Eur. Respir. J.* **42**, 198–210 (2013).
53. Couluris, M. *et al.* Treatment of idiopathic pulmonary fibrosis with losartan: A pilot project. *Lung* **190**, 523–527 (2012).
54. Nadrous, H. F., Olson, E. J., Douglas, W. W., Decker, P. A. & Nadrous, H. J. Idiopathic pulmonary fibrosis: Impact of angiotensin converting enzyme inhibitors and HMG-CoA reductase inhibitors on survival. *Chest* **124**, (2003).
55. Wang, L., Wang, Y., Yang, T., Guo, Y. & Sun, T. Angiotensin-Converting enzyme 2 attenuates bleomycin-induced lung fibrosis in mice. *Cell. Physiol. Biochem.* **36**, 697–711 (2015).
56. Shenoy, V. *et al.* The angiotensin-converting enzyme 2/angiogenesis-(1-7)/Mas axis confers cardiopulmonary protection against lung fibrosis and pulmonary hypertension. *Am. J. Respir. Crit. Care Med.* **182**, 1065–72 (2010).
57. Wikipedia. Messenger RNA. <https://en.wikipedia.org/wiki/Messenger_RNA>, accessed 30.05.2017

58. Voet, D., Voet, J. G. & Pratt, C. W. *Lehrbuch der Biochemie*. (John Wiley & Sons, Inc., 2010).
59. Pesole, G., Grillo, G., Larizza, a & Liuni, S. The untranslated regions of eukaryotic mRNAs: structure, function, evolution and bioinformatic tools for their analysis. *Brief. Bioinform.* **1**, 236–249 (2000).
60. Pestova, T. V., Lorsch, J. R., Hellen, C. U. T. The mechanisms of translation initiation in eukaryotes in *Transl. Control Biol. Med.* 87–128, CSH Monographs (2007).
61. Kotterman, M. a, Chalberg, T. W. & Schaffer, D. V. Viral vectors for gene therapy: translational and clinical outlook. *Annu. Rev. Biomed. Eng* **17**, 63–89 (2015).
62. Tavernier, G. *et al.* mRNA as gene therapeutic: How to control protein expression. *J. Control. Release* **150**, 238–247 (2011).
63. Karikó, K., Kuo, A. & Barnathan, E. Overexpression of urokinase receptor in mammalian cells following administration of the in vitro transcribed encoding mRNA. *Gene Ther.* **6**, 1092–1100 (1999).
64. Sullivan, D. RNAs Reticulocytes. *Blood* **66**, 1149–1154 (1985).
65. Holtkamp, S. *et al.* Modification of antigen encoding RNA increases stability, translational efficacy and T-cell stimulatory capacity of dendritic cells Modification of antigen encoding RNA increases stability, translational efficacy and T-cell stimulatory capacity of dendr. *Blood* **108**, 4009–4018 (2006).
66. Gustafsson, C., Govindarajan, S. & Minshull, J. Codon bias and heterologous protein expression. *Trends Biotechnol.* **22**, 346–353 (2004).
67. Mauro, V. P. & Chappell, S. a. A critical analysis of codon optimization in human therapeutics. *Trends Mol. Med.* **20**, 604–613 (2014).
68. Kauffman, K. J. *et al.* Optimization of lipid nanoparticle formulations for mRNA delivery in vivo with fractional factorial and definitive screening designs. *Nano Lett.* **15**, 7300–7306 (2015).
69. Nguyen, T. H. & Ferry, N. Liver gene therapy: advances and hurdles. *Gene Ther.* **11 Suppl 1**, S76–S84 (2004).
70. Azarmi, S., Roa, W. H. & Löbenberg, R. Targeted delivery of nanoparticles for the treatment of lung diseases. *Adv. Drug Deliv. Rev.* **60**, 863–875 (2008).
71. Lubel, J. S. *et al.* Angiotensin-(1-7), an alternative metabolite of the renin-angiotensin system, is up-regulated in human liver disease and has antifibrotic activity in the bile-duct-ligated rat. *Clin. Sci. (Lond).* **117**, 375–86 (2009).
72. Warner, F. J., Lubel, J. S., McCaughan, G. W. & Angus, P. W. Liver fibrosis: a balance of ACEs? *Clin. Sci. (Lond).* **113**, 109–18 (2007).
73. Apeiron Biologics. Safety and tolerability study of APN01 (recombinant human angiotensin converting enzyme 2). ClinicalTrials.gov identifier *NCT00886353* (2009). <<https://clinicaltrials.gov/ct2/show/study/NCT00886353?term=Apeiron&rank=2>>
74. Huber, M. Impact of mRNA sequence design on half-life, protein expression and immunogenicity. *TU Munich* (2016).
75. Ferizi, M. *et al.* Stability analysis of chemically modified mRNA using micropattern-based single-cell arrays. *Lab Chip* **15**, 3561–3571 (2015).
76. Pfaffl, M. W. Real-time RT-PCR: Neue Ansätze zur exakten mRNA Quantifizierung. *Biospektrum* **10**, 92–95 (2004).
77. Powell, L. D. Inhibition of N-linked glycosylation. *Curr. Protoc. Immunol.* **Chapter 8**, Unit 8.14 (2001).
78. Lambert, D. W. *et al.* Tumor necrosis factor- α convertase (ADAM17) mediates regulated ectodomain shedding of the severe-acute respiratory syndrome-coronavirus (SARS-

- CoV) receptor, angiotensin-converting enzyme-2 (ACE2). *J. Biol. Chem.* **280**, 30113–30119 (2005).
79. UniProtKB. Q9BYF1 (ACE2_HUMAN). <<http://www.uniprot.org/uniprot/Q9BYF1>>
80. Babendure, J. R., Babendure, J. L., Ding, J. & Tsien, R. Y. Control of mammalian translation by mRNA structure near caps. *RNA* **12**, 851–861 (2006).
81. Qadah, T. H. A study of molecular mechanisms regulating human alpha globin production: An in vitro comparative study between normal and α -Thalassemia subtypes. *University of Western Australia*, PhD Thesis (2014).
82. Bataller, R. *et al.* Activated human hepatic stellate cells express the renin-angiotensin system and synthesize angiotensin II. *Gastroenterology* **125**, 117–125 (2003).
83. Huang, Q. *et al.* Expression of angiotensin-converting enzyme 2 in CCL4-induced rat liver fibrosis. *Int. J. Mol. Med.* **23**, 717–723 (2009).
84. Wu, J. & Yan, L. J. Streptozotocin-induced type 1 diabetes in rodents as a model for studying mitochondrial mechanisms of diabetic β cell glucotoxicity. *Diabetes, Metab. Syndr. Obes. Targets Ther.* **8**, 181–188 (2015).
85. Kanuri, G. & Bergheim, I. In vitro and in vivo models of non-alcoholic fatty liver disease (NAFLD). *Int. J. Mol. Sci.* **14**, 11963–80 (2013).
86. Matsumoto, M. *et al.* An improved mouse model that rapidly develops fibrosis in non-alcoholic steatohepatitis. *Int. J. Exp. Pathol.* **94**, 93–103 (2013).
87. Ferrannini, E., Haffner, S. M., Mitchell, B. D. & Stern, M. P. Hyperinsulinaemia: the key feature of a cardiovascular and metabolic syndrome. *Diabetologia* **34**, 416–422 (1991).
88. American Association for Clinical Chemistry. LD. *Lab Tests Online* (2014). <<https://labtestsonline.org/understanding/analytes/ldh/tab/test/>>, accessed 21.04.2017
89. Giannini, E. G., Testa, R. & Savarino, V. Liver enzyme alteration: A guide for clinicians. *Cmaj* **172**, 367–379 (2005).
90. Naik, P. *Essentials of Biochemistry*. Jaypee Brothers Medical Publishers (P) Ltd. (2012).
91. Nelson, D. L. & Cox, M. M. *Lehninger's Principles of Biochemistry*. W. H. Freeman and Company (2005).
92. Standish, R. a. An appraisal of the histopathological assessment of liver fibrosis. *Gut* **55**, 569–578 (2006).
93. Pais, P. & D'Amato, M. In vivo efficacy study of milk thistle extract (ETHIS-094TM) in STAMTM model of nonalcoholic steatohepatitis. *Drugs R D* **14**, 291–299 (2014).
94. Alton, E. W. F. W. *et al.* Repeated nebulisation of non-viral CFTR gene therapy in patients with cystic fibrosis: A randomised, double-blind, placebo-controlled, phase 2b trial. *Lancet Respir. Med.* **3**, 684–691 (2015).
95. Kormann, M. S. D. *et al.* Expression of therapeutic proteins after delivery of chemically modified mRNA in mice. *Nat. Biotechnol.* **29**, 154–157 (2011).
96. Hamming, I. *et al.* Tissue distribution of ACE2 protein, the functional receptor for SARS coronavirus. A first step in understanding SARS pathogenesis. *J. Pathol.* **203**, 631–637 (2004).
97. Limjunyawong, N., Mitzner, W. & Horton, M. R. A mouse model of chronic idiopathic pulmonary fibrosis. *Physiol. Rep.* **2**, e00249 (2014).
98. Peng, R. *et al.* Bleomycin induces molecular changes directly relevant to idiopathic pulmonary fibrosis: a model for 'active' disease. *PLoS One* **8**, e59348 (2013).
99. Huang, Y. *et al.* Pharmacokinetic behaviors of intravenously administered siRNA in glandular tissues. *Theranostics* **6**, 1528–1541 (2016).

100. Wang, J., Lu, Z., Wientjes, M. G. & Au, J. L.-S. Delivery of siRNA therapeutics: Barriers and carriers. *AAPS J.* **12**, 492–503 (2010).
101. Lorenzer, C., Dirin, M., Winkler, A. M., Baumann, V. & Winkler, J. Going beyond the liver: Progress and challenges of targeted delivery of siRNA therapeutics. *J. Control. Release* **203**, 1–15 (2015).
102. Akinc, A. *et al.* Targeted delivery of RNAi therapeutics with endogenous and exogenous ligand-based mechanisms. *Mol. Ther.* **18**, 1357–1364 (2010).
103. Teufel, A. *et al.* Comparison of gene expression patterns between mouse models of nonalcoholic fatty liver disease and liver tissues from patients. *Gastroenterology* (2016).
104. Yoneyama, H. & Fujii, M. Steatohepatitis-liver cancer model animal, WO 2011013247 A1. (2009).
105. Takahashi, Y., Soejima, Y. & Fukusato, T. Animal models of nonalcoholic fatty liver disease. *World J. Gastroenterol.* **18**, 2300–2308 (2012).
106. Kenny, T., Henderson, R., Jackson C. Non-alcoholic fatty liver disease. Patient platform limited (2016) <<http://patient.info/health/non-alcoholic-fatty-liver-disease>>, accessed 01.02.2017
107. Rudolph, C. *et al.* Methodological optimization of polyethylenimine (PEI)-based gene delivery to the lungs of mice via aerosol application. *J. Gene Med.* **7**, 59–66 (2005).
108. Rudolph, C., Lausier, J., Naundorf, S., Müller, R. H. & Rosenecker, J. In vivo gene delivery to the lung using polyethylenimine and fractured polyamidoamine dendrimers. *J. Gene Med.* **2**, 269–78 (2000).
109. Rosenecker, J. *et al.* Interaction of bronchoalveolar lavage fluid with polyplexes and lipoplexes: Analysing the role of proteins and glycoproteins. *J. Gene Med.* **5**, 49–60 (2003).
110. El-Sherbiny, I. M., El-baz, N. M. & Yacoub, M. H. Inhaled nano- and microparticles for drug delivery. *Glob. Cardiol. Sci. Pract.* **2015:2**, 1–14 (2015).
111. Dancer, R. C. a, Wood, a M. & Thickett, D. R. Metalloproteinases in idiopathic pulmonary fibrosis. *Eur. Respir. J.* **38**, 1461–7 (2011).
112. Wang, R., Zagariya, A., Ang, E., Barra-Sunga, O. & Uhal, B. D. Fas-induced apoptosis of alveolar epithelial cells requires ANG II generation and receptor interaction. *Am. J. Physiol.* **277**, L1245–L1250 (1999).
113. Wang, R. *et al.* Angiotensin II induces apoptosis in human and rat alveolar epithelial cells. *Am. J. Physiol.* **276**, L885–L889 (1999).
114. Li, X., Zhang, H., Soledad-Conrad, V., Zhuang, J. & Uhal, B. D. Bleomycin-induced apoptosis of alveolar epithelial cells requires angiotensin synthesis de novo. *Am. J. Physiol. Lung Cell. Mol. Physiol.* **284**, L501–L507 (2003).
115. Cosgrove, G. P. *et al.* Pigment epithelium-derived factor in idiopathic pulmonary fibrosis. *Am. J. Respir. Crit. Care Med.* **170**, 242–251 (2004).
116. Farkas, L., Gauldie, J., Voelkel, N. F. & Kolb, M. Pulmonary hypertension and idiopathic pulmonary fibrosis: A tale of angiogenesis, apoptosis, and growth factors. *Am. J. Respir. Cell Mol. Biol.* **45**, 1–15 (2011).
117. Uyechi, L. S., Gagné, L., Thurston, G. & Szoka, F. C. Mechanism of lipoplex gene delivery in mouse lung: binding and internalization of fluorescent lipid and DNA components. *Gene Ther.* **8**, 828–836 (2001).
118. Wiener, R. S., Cao, Y. X., Hinds, A., Ramirez, M. I. & Williams, M. C. Angiotensin converting enzyme 2 is primarily epithelial and is developmentally regulated in the mouse lung. *J. Cell. Biochem.* **101**, 1278–91 (2007).

119. Ren, X. *et al.* Analysis of ACE2 in polarized epithelial cells: Surface expression and function as receptor for severe acute respiratory syndrome-associated coronavirus. *J. Gen. Virol.* **87**, 1691–1695 (2006).
120. Kedmi, R., Ben-Arie, N. & Peer, D. The systemic toxicity of positively charged lipid nanoparticles and the role of Toll-like receptor 4 in immune activation. *Biomaterials* **31**, 6867–6875 (2010).
121. Liu, Y. *et al.* Strain-based genetic differences regulate the efficiency of systemic gene delivery as well as expression. *J. Biol. Chem.* **277**, 4966–4972 (2002).
122. Dames, P. *et al.* Aerosol gene delivery to the murine lung is mouse strain dependent. *J. Mol. Med.* **85**, 371–378 (2007).
123. Wang, L. *et al.* Angelica sinensis is effective in treating diffuse interstitial pulmonary fibrosis in rats. *Biotechnol. Biotechnol. Equip.* **28**, 923–928 (2014).
124. Cohen, J. C., Horton, J. D., Hobbs, H. H. Human fatty liver disease: Old questions and new insights. *Science (New York, N.Y.)* **332.6037**, 1519–1523 (2011).
125. Wikipedia. Idiopathic pulmonary fibrosis. <https://en.wikipedia.org/wiki/Idiopathic_pulmonary_fibrosis> accessed 20.03.2017
126. Reslova, N., Michna, V., Kasny, M., Mikel, P. & Kralik, P. xMAP Technology: Applications in detection of pathogens. *Front. Microbiol.* **8**, 55 (2017).
127. Fontana, J., Sajdikova, M., Mad'a P. Liver and biotransformation of xenobiotics (2015) <fb.lt.cz/en/skripta/ix-travici-soustava/5-jatra-a-biotransformace-xenobiotik/>, accessed 30.05.2017

9 APPENDIX

9.1 Cell Authentication

Leibniz-Institut
DSMZ-Deutsche Sammlung von
Mikroorganismen und Zellkulturen GmbH



Leibniz-Institut DSMZ GmbH · Inhoffenstraße 7 B · 38124 Braunschweig

Frau Eveline Babel
Ethris GmbH
Target Biology
Sammelweisstraße 3
82152 Planegg

Inhoffenstraße 7 B
38124 Braunschweig
GERMANY

Tel. +49(0)531 26 16-166
Fax: +49(0)531 26 16-150
E-Mail: wdi@dsMZ.de
Internet: www.dsmz.de

Ihr Zeichen/Your ref.

Unser Zeichen/Our ref. wdi

+49(0)531-2616-166

Datum/Date: 22.04.2016

Sehr geehrte Frau Babel,

vielen Dank für Ihren Auftrag zur Identifizierung von Zelllinien. Wir haben von Ihren 18 Proben ein DNA Profil von 8 hoch polymorphen Orten von Short Tandem Repeats (STRs) mit Hilfe einer nonaplex PCR hergestellt. Zusätzlich wurden die humanen Proben auf Anwesenheit von DNA Sequenzen aus Maus, Ratte und Hamster getestet. Für die Identifizierung tierischer Spezies wurde die Probe dem Verfahren des DNA Barcoding (s. Anhang) unterworfen. Der Abgleich der Profile mit der Datenbank brachte folgende Ergebnisse:

#	sample	parental/reference line	comment/match/cross-contamination (CC)
1	A-459	A-549 (DSMZ ACC 107)	full-matching STR reference profile of cell line A-549, authentic
2	CACO-2	Calu-3 (ATCC HTB-055)	full-matching STR reference profile of cell line CACO-2, authentic
6	GripTite 293 MSR	293 (DSMZ ACC 305)	full-matching STR reference profile of cell line 293, authentic*
4	HEK293Nfkb/GFP/Luc	293 (DSMZ ACC 305)	full-matching STR reference profile of cell line 293T, isogenic cross-contamination**
5	HEK293	293 (DSMZ ACC 305)	full-matching STR reference profile of cell line 293, authentic
6	HEPA 1-6	HEPA 1-6 (DSMZ ACC 175)	COI DNA Barcoding analysis reveals <i>Mus musculus</i> species, species-specific
7	HFP-G2	HFP-G2 (DSMZ ACC 180)	full-matching STR reference profile of cell line HFP-G2, authentic
8	HUH7	HuH-7 (JCRB, JCRB 0403)	full-matching STR reference profile of cell line HuH-7, authentic
10	KB	KB (DSMZ ACC 136)	full-matching STR reference profile of cell line HELA, known derivative, authentic
11	MLE-15	MLE 12 (ATCC CRL-2110)	COI DNA Barcoding analysis reveals <i>Mus musculus</i> species, species-specific
12	NIH-3T3	NIH-3T3 (DSMZ ACC 059)	COI DNA Barcoding analysis reveals <i>Mus musculus</i> species, species-specific
13	J774 m. macrophages	J774A.1 (ATCC TIB-67)	COI DNA Barcoding analysis reveals <i>Mus musculus</i> species, species-specific

Die humanen Zellproben sind mit einer Nachweisgrenze von 10^5 frei von Animalzellen aus Maus, Ratte und chinesischem Hamster und entstammen jeweils einer rein humanen Zellkultur.

Mit Ausnahme der murinen Proben zeigen die STR Profile der humanen Proben 1 bis 7 eine Übereinstimmung mit dem STR Profil der parentalen Zelllinien der gemeinsamen STR Referenzdatenbank der Zellbanken ATCC (USA),

Geschäftsführer/
Managing Director:
Prof. Dr. Jörg Overmann
Aufsichtsratsvorsitzender/Head of
Supervisory Board: RD Dr. David Schnieders

Braunschweigische Landessparkasse
(NORD/LB) Kto.-Nr./Account: 2 039 220
BLZ/Bank Code: 250 500 00
IBAN DE22 2505 0000 0002 0392 20
SWIFT (BIC) NOLADE 2 H

Handelsregister/
Commercial Register:
Amtsgericht Braunschweig
HRB 2570
Steuer-Nr. 13/200/24030





JCRB/RIKEN (Japan), KCLB (Korea) und der DSMZ auf. Die Proben A-459, CACO-2, GripTite 293 MSR, HEK293NFkB/GFP/Luc, HEK293, HEP-G2, HUH7 und KB wurden von authentischen Zellkulturen genommen.

*Gekennzeichnete Proben zeigen ein leicht verändertes STR Profil: Der Verlust bzw. das Driften von Allelen ist in der Tabelle 2 grün markiert (Anlage). Das Phänomen der Loss of Heterozygosity (LOH) wird beobachtet, wenn eine Defizienz der DNA Mismatch Reparatur vorliegt und Zellen als Einzelklon oder Sublinien aus einer Hauptpopulation auswachsen können.

**Im Fall der Probe HEK293NFkB/GFP/Luc liegt eine Kreuzkontamination mit der Schwesterzelllinie 293T vor. 293T trägt das Großantigen des SV40 Virus (T-Ag) und zeichnet sich durch höhere Transfektionseffizienz gegenüber 293 aus. Den Nachweis von T-Ag finden Sie im Anhang.

Die Speziesbestimmungen der Proben 6, 10, 11 und 12 von Zellkulturen der Maus zeigen die authentische Spezies *Mus musculus* auf. Eine weiterführende Individualisierung von Mauszelllinien kann auf Grund eines fehlenden STR Systems bzw. auf Grund der Inzuchtproblematik und der daraus mangelnden genetischen Diversität nicht erfolgen.

Auf Grund der Exklusionsrate des genutzten STR Systems mit einer Wahrscheinlichkeit von 1 in 114.000.000 sind die Ergebnisse als sicher zu betrachten. Bitte finden Sie die Dokumentation der Analyse (Elektropherogramme) und eine Tabelle mit der Allelliste im Anhang.

Mit freundlichen Grüßen,

W. Dirks

Geschäftsführer/
Managing Director:
Prof. Dr. Jörg Overmann
Aufsichtsratsvorsitzender/Head of
Supervisory Board: RD Dr. David Schnieders

Braunschweigische Landessparkasse
(NORD/LB) Kto.-Nr./Account: 2 039 220
BLZ/Bank Code: 250 500 00
IBAN DE22 2505 0000 0002 0392 20
SWIFT (BIC) NOLADE 2 H

Handelsregister/
Commercial Register:
Amtsgericht Braunschweig
HRB 2570
Steuer-Nr. 13/200/24030



9.2 Angiotensin Converting Enzyme 2 Open Reading Frames

9.2.1 Open Reading Frame non Codon Optimized

UCAAGCUCUUCUGGCCUUCUCAGCCUUGUUGCUGUAACUGCUGCUCAGUCCACCAUUGAGGAACAGGCCAAGA
CAUUUUUUGGACAAGUUUAACCACGAAGCCGAAGACCUUGUUCUAUCAAGUUCACUUGCUUCUUGGAAUUUAACA
CCAAUUAUJACUGAAGAGAAUGUCCAAAACAUGAAUAAUGCUGGGGACAAAUGGUCUGCCUUUUUAAAGGAACAGU
CCACACUUGCCAAAUGUAUCCACUACAAGAAAUCAGAAUCUCACAGUCAAGCUUCAGCUGCAGGCUCUUCAGCAA
AAUGGGUCUUCAGUGCUCUCAGAAGACAAGAGCAAACGGUUGAACACAAUUCUAAAUAACAUGAGCACCAUCUACA
GUACUGGAAAAGUUUGUAACCCAGAUAAUCCACAAGAAUGCUUAAUUAUUAUGAACCCAGGUUUGAAUGAAAUAUUGG
CAAACAGUUUAGACUACAUGAGAGGCUCUGGGCUUGGGAAAGCUGGAGAUUCUGAGGUCGGCAAGCAGCUGAGGC
CAUUUAUUGAAGAGUAUGUGGUCUUGAAAAUGAGAUGGCAAGAGCAAUCAUUAUGAGGACUAUGGGGAUUUAU
UGGAGAGGAGACUAUGAAGUAAAUGGGGUAGAUGGCUAUGACUACAGCCGCGGCCAGUUGAUUGAAGAUUGGA
ACAUACCUUUGAAGAGAUUAAACCAUUAUUGAACAUCUUCUUGCCUUAUGUGAGGGCAAAGUUGAUGAAUGCCUA
UCCUUCUUAUUCAGUCCAAUUGGAUGCCUCCUGCUCAUUAUGCUUGGUGAUUGUGGGGUAGAUUUUGGACAAA
UCUGUACUCUUCUGACAGUUCUUUGGACAGAAACCAACAUGAUGUUACUGAUGCAAUGGUGGACCAGGCCUG
GGAUGCACAGAGAAUUAUCAAGGAGGCCGAGAAGUUCUUUGUAUCUGUUGGUCUUCUUAUUGACUCAAGGAUU
CUGGGAAAUAUCAUGCUAACGGACCCAGGAAAUGUUCAGAAAGCAGUCUGCCAUCCACAGCUUGGGACCUGGGG
AAGGGCAGCUUCAGGAUCCUUAUGUGCACAAGGUGACAUGGACGACUUCUGACAGCUCUUAUGAGAUUGGGG
CAUAUCCAGUAUGAUUGGCAUUGCUGCACAACCUUUUCUGCUAAGAAAUGGAGCUAAUGAAGGAUUCCAUGAA
GCUGUUGGGGAAAUCAUGUCACUUCUGCAGCCACACCUAAGCAUUUAAAUAUCAUUGGUCUUCUGUCACCCGAUU
UUCAAGAAGACAUGAAACAGAAAUAACUUCUGCUCAACAAGCACUCACGAUUGUUGGGACUCUGCCAUUUAC
UUACAUGUUGAAGAAGUGGAGGUGGAUGGUCUUUAAAAGGGGAAAUAUCCAAAGACCAGUGGAUGAAAAGUGGU
GGGAGAUAGAAGCGAGAGAUAGUUGGGGUGGGAACCUUGGCCCAUGAUGAAACUACUGUGACCCCGCAUCUC
UGUUCUUAUGUUUCAAUGAUUACUUAUUAUUGAUUUAACCAUUCAGUUUCAAAGAAG
CACUUUGUCAAGCAGCUAAACAUGAAGGCCUCUGCACAUAUGGACAUUCUAAACUCUACAGAAGCUGGACAGAA
ACUGUUCAAUAUGCUGAGGCUUGGAAAUAACAACCCUGGACCCUAGCAUUGGAAAUGUUGAAGGAGCAAAGAA
CAUGAAUGUAAGGCCACUGCUCAACUACUUAUGAGCCUUAUUUACCUUGGUCGAAAGACCAGAACAAGAAUUCUUU
GUGGGAUUGGAGUACCGACUGGAGUCCAUUGCAGACCAAAGCAUCAAAGUGAGGAUAAAGCCUAAAUAUCAGCUCU
GGAGAUAAAGCAUUAUGAAUGGAACGACAUAUGAAUUGUACCUUGUCCGAUACUCUGUUGCAUUGCUAUGAGGCAG
UACUUUUUAAAAGUAAAAAUAUGAUGAUUCUUUUGGGGAGGAGGAUGUGCGAGUGGCUAAUUUGAAACCAAG
AAUCUCCUUUAAUUUCUUAUGCACUGCACCUAAAAUUGUGUCUGAUUAUCAUUCUAGAACUGAAGUUGAAAAGGC
CAUCAGGAUGUCCGGAGCCGAUCAUUGAUGCUUUCGUCUGAUAUGACAACAGCCUAGAGUUUCUGGGGAUACA
GCCAACACUUGGACCUCCUAAACAGCCCCUGUUUCAUUAUGGCUGAUUGUUUUGGAGUUGUGAUGGGAGUGAU
AGUGGUUGGCAUUGUCAUCCUGAUCUUCACUGGGAUACAGAGUUCGGAAGAAGAAAAUAAAGCAAGAAUGGAGA
AAAUCCUUAUGCCUCCAUUGAUUAUGCAAAGGAGAAAUAUCCAGGAUUCAAAAACUCUGAUGAUGUUCAGACC
UCCUUUUAG

9.2.2 Open Reading Frame Codon Optimized

AGCAGCAGCUCUUGGCUGCUGCUGAGCCUGGUGGCCGUGACAGCCGCCAGAGCACAAUUGAGGAACAGGCCAAGA
CCUUCUGGACAAGUUAACCACGAGGCCGAGGACCUUGUUCUACCAGAGCAGCCUGGCCAGCUGGAACUACAACACC
AAAUACCCGAAGAGAACGUGCAGAACAUGAAACAACGCCGCGACAAGUGGAGCGCCUUCUGAAAGAGCAGUCCAC
CCUGGCCCAGAUJACCCGUCGAGGAAAUCCAGAACCUGACCGUGAAGCUGCAGCUGCAGGCUCUGCAGCAGAACG
GCAGCAGCGUGCUGAGCGAGGACAAGAGCAAGCGGCUGAACACCAUCCUGAAUACCAUGUCCACCAUCUACAGCAC
GGCAAAGUGUGCAACCCGACAACCCCCAGGAAUGCCUGCUGGAAACCCGGCCUGAACGAGAUCAUGGCUAACAG
CCUGGACUACAACGAGCGGCUUGGGCCUGGGAGUCUUGGAGAAGCGAAGUGGGCAAGCAGCUGCGGCCCCUGUA
CGAGGAUACGUGGUGCUGAAGAACGAGAUGGCCAGAGCCAACCAUACGAGGACUACGGCGACUACUGGCGGGGA
GACUACGAAGUGAAUGGCGUGGACGGCUACGACUACAGCAGAGGCCAGCUGAUCGAGGACGUGGAACACACCUUCG
AGGAAAUAAGCCUCUGUACGAGCAUCUGCACGCCUACGUGCGGGCCAAGCUGAUGAACGCCUACCCAGCUACAUC
AGCCCAUCGGCUGUCUGCCUGCCAUCUGCUGGGCGACAUGUGGGGAGAUUCUGGACCAACCUUGUACAGCCUGA
CAGUGCCCUUCGGCCAGAAACCAACAUCGACGUGACCGACGCCAUGGUGGAUCAGGCCUUGGGACGCCAGCGGAUC
UUCAAAGAGGCCGAGAAGUUCUUCGUGUCCGUGGGCCUGCCAAUUAUGACCCAGGGCUUCUGGGAGAACUCCAUGC
UGACCGACCCCGCAAUGUGCAGAAAGCCGUGUGUACCCCAACCGCCUGGGAUCUGGGCAAGGGCGACUUCGGGAU
CCUGAUGUGCACAAAGUGACCAUGGACGACUUCUGACCGCCACCACGAGAUUGGGCCACAUCAGUACGACAUGG
CCUACGCCGCCAGCCUUCUGCUGAGAAAUGGCGCAACGAGGGCUUCACGAAGCCGUGGGAGAGAUCAUGAGC

CUGAGCGCCGCCACCCCAAGCACCUGAAGUCUAUCGGACUGCUGUCCCCGACUUCCAGGAAGAUAACGAGACAGA
GAUCAACUUUCUGCUGAAGCAGGCCUUGACCAUCGUGGGCACCCUGCCCUUACCCUACAUGCUGGAAAAGUGGCGG
UGGAUGGUGUUUAAGGGCGAGAUCCCAAGGACCAGUGGAUGAAGAAAUGGUGGGGAGAUGAAGCGCGAGAU CGU
GGGCGUGGUGGAACCCGUGCCACACGACGAGACAUACUGCGACCCUGCCAGCCUGUUUCACGUGUCCAACGACUAC
UCCUUAUCCGGUACUACACCCGGACCCUGUACCAGUUCAGUUUCAAGAGGCCUUGGCCAGGCCGCAAGCACGA
AGGACCUCUGCACAAGUGCGACAUCAGCAACAGCACCGAGGCCGGACAGAAACUGUUCAACAUGCUGCGGCUGGGCA
AGUCCGAGCCUUGGACACUGGCCUUGGAAAACGUCGUGGGCGCCAAGAAUAUGAACGUGCGCCCCUGCUGAACUA
CUUCGAGCCCCUGUUCACCCUGGCUGAAGGACCAGAACAAGAACAGCUUCGUGGGCUGGUCCACCGACUGGUCCCCA
UACGCCGACCAGAGCAUCAAGUGCGGAUCAGCCUGAAGUCCGCCUGGGCGAUAAAGCCUACGAGUGGAAACGACA
ACGAGAUGUACCUGUUCGGUCCAGCGUGGCCUAUGCUAUGCGGCAGUACUUUCUGAAAGUGAAGAAUCAGAU GA
UCCUGUUCGGCGAAGAGGAUGUGCGGGUGGCCAACCGAAGCCCCGGAUCAGCUUCAACUUCUUCGUGACCGCCCC
CAAGAACGUGUCCGACAUCAUCCCCGGACCGAGGUGGAAAAGGCCAUCAGAAUGAGCAGAAGCCGGAUCAACGACG
CCUUCGGCGUGAACGACAAUAGCCUGGAAUUCUGGGCAUCCAGCCCACCCUGGGCCCUCCAAAUCAGCCCCUGUG
UCCAUCUGGCUGAUCGUGUUUGGCGUCGUGAUGGGCGUGAUCGUCGUGGGAAUCGUGAUCUGAUCUUCACCGG
CAUCCGGGACCGGAAGAAGAACAAGGCCAGAAGCGGCGAGAACCCUACGCCAGCAUCGACAUCUCAAGGGGG
AGAACAACCCCGGCUUCCAGAACACCGACGACGUGCAGACCAGCUUCUGA